

Decarbonizing the US Power Sector

by

Amanda Farnsworth

B.S. Chemical Engineering
North Carolina State University, 2019

Submitted to the Department of Chemical Engineering in Partial Fulfillment of the Requirements
for the Degree of

Doctor of Philosophy
at the
MASSACHUSETTS INSTITUTE OF TECHNOLOGY

May 2024

© 2024 Amanda Farnsworth. All rights reserved.

The author hereby grants to MIT a nonexclusive, worldwide, irrevocable, royalty-free license to exercise any and all rights under copyright, including to reproduce, preserve, distribute and publicly display copies of the thesis, or release the thesis under an open-access license.

Signature of Author: _____

Department of Chemical Engineering
February 6th, 2024

Certified by: _____

Robert C. Armstrong
Chevron Professor of Chemical Engineering, Emeritus
Thesis Supervisor

Accepted by: _____

Hadley Sikes
Willard Henry Dow Professor of Chemical Engineering
Chair, Department Committee on Graduate Students

Decarbonizing the US Power Sector

by

Amanda Farnsworth

Submitted to the Department of Chemical Engineering
on February 6th, 2024, in partial fulfillment of the requirements for the degree of
Doctor of Philosophy in Chemical Engineering

As the second highest national emitter, the US has the opportunity, and responsibility, to reduce emissions and mitigate the impacts of climate change. The power sector has been identified as the linchpin in our national decarbonization strategy, with high electrification goals for the other sectors. As of 2022, the power sector was responsible for more than a quarter of annual emissions. As electrification increases, the importance of decreasing the emissions and emissions intensity of electricity production grows.

This thesis explores the challenges and opportunities of decarbonizing the US power sector. Two models were built to complete this analysis: Ideal Grid (IG) which is a greenfield capacity expansion and economic dispatch model, and Evolving Grid (EG), which is a brownfield capacity expansion and economic dispatch model. These models are an especially novel addition to the current arsenal of publicly available capacity expansion models because they include embodied emissions, in addition to the industry-standard consideration of power plant tailpipe emissions from fossil fuel combustion. Nine regions of the contiguous US are represented in these models.

First, IG is used to highlight regional decarbonization challenges. Regions with significant land available for variable renewable energy (VRE) buildout and strong wind resources had the cheapest paths to a clean grid. Also, hydropower resources play a significant role. At deep decarbonization levels, the need for long-duration energy storage (like pumped hydropower storage) increases. The role of embodied emissions is explored, showing that as fossil-fuel consumption decreases and VRE penetration increases, they become nonnegligible. To most effectively reduce system emissions, embodied emissions should be accounted for.

Next, fusion is integrated into the model to demonstrate its potential role. Assuming a \$8,500/kW CAPEX, fusion is not economically competitive unless a carbon constraint is applied. But, at deep decarbonization levels, fusion is prominent in all regions. EG shows that intermediary decarbonization goals before 2050 play a pivotal role in determining fusion adoption and overall fleet composition. Lastly, the versatility and value of presented models is demonstrated by outlining other potential applications.

Thesis Supervisor: Robert C. Armstrong

Title: Chevron Professor of Chemical Engineering, Emeritus

Acknowledgements

My PhD journey has challenged me to grow in ways that I had not imagined when I first submitted my MIT application. This experience has developed my technical skills, but also my mental toughness. I am grateful to all the groups of people who helped me reach this opportunity, and succeed.

First, I want to express my gratitude to Dr. Emre Gençer. His direction and input led me to new research areas and elevated my work. I benefited tremendously from our weekly meetings where I was able to develop interesting research questions, review results, and even talk about my larger life goals and career aspirations. I could not have asked for a better mentor.

Also, I sincerely appreciate all guidance from my thesis advisor, Prof. Bob Armstrong. Your vast depths of experience and knowledge were apparent in every interaction we had. Even more importantly, it has always been clear that you have had my best interests in mind.

I have also had the benefit of a thoughtful thesis committee with a diverse background, including Prof. Bill Green and Dr. Sergey Paltsev. Their perspective and insights steered my work to answer more novel and impactful research questions.

Even during my time at NCSU, I benefited from incredible leadership figures who invested their time and energy in my growth and success. I am beyond grateful to Prof. Philip Westmoreland who spent countless hours teaching me complex thermodynamics, and also gave me career and life advice. I also appreciate Prof. Carol Hall, who is an amazing role model for women in chemical engineering. Her teaching style was always tough, but fair. Lastly, I appreciate Prof. Parsons who suggested that I apply to MIT. I had always seen MIT as an unattainable caricature of education, only existent in *Goodwill Hunting*. Now, Matt Damon and I have something in common.

I am also grateful for my cohort, especially its first-year comradery. First-year courses were incredibly challenging. I would not have been successful in them without my office mates, who helped me work through homework problems, study for tests, and just vent. I am especially appreciative of Will Funkenbusch, who acted as my personal 10.34 tutor.

SESAME's group members also provided a strong sense of community which I benefitted from. It always boosted my spirits to see Sydney Johnson and Jim Owen's smiling faces every morning. Jim was especially patient with me, spending hours helping me debug out of the goodness of his heart.

I am incredibly lucky to have gone through this experience with my extended family so close, with relatives only a few hours in each direction. I especially appreciate the Geyers who made my winter into a holiday during this last stretch. I appreciate Pam Maynard for sending me a continuous stream of pictures of dogs to boost my spirits. Also, thank you to the boating community, while not technically family, they treat me as such, and I have benefited from their vibrant zest for life.

I have an amazing set of friends, both in Boston and around the globe. I am lucky to still be in touch with many close friends from high school. College allowed me to broaden my horizons and meet even more people from different backgrounds. And during my time in Boston, I have met impressive people both inside and outside of MIT. I am especially grateful for someone who has been there from beginning, with no change in sight, Kaitlyn Biello.

Lastly, but most importantly, I want to thank my family. You have shaped and molded me into someone that I am proud to be. My father has taught me to always live with adventure and never become complacent. My mother has taught me to always bring energy to a social gathering, and how to talk to anyone or anything with a beating heart. My sister has taught me to be strong-willed, and yet always be considerate and thoughtful to the utmost degree. My partner, Shubhro Saha, has always brought light and

happiness into my life, and bringing out my favorite parts of myself. Although I *could* live life without him, I'm glad that I'll never have to.

I am incredibly proud of what I have accomplished at MIT, but I am even more proud of this long list of people that I have collected in my life.

Table of Contents

<i>Acknowledgements</i>	3
<i>List of Figures</i>	10
<i>List of Tables</i>	13
Chapter 1. Introduction	15
1.1 Motivation	15
1.1.1 Decarbonizing to mitigate climate change.....	15
1.1.2 Focus on the US Power Sector.....	16
1.2 Important models and metrics	18
1.2.1 Current tools	18
1.2.2 Added value of my tools.....	21
Chapter 2. Leveraging IG to highlight regional decarbonization challenges	23
2.1 Overview	23
2.2 Introduction	24
2.2.1 Value of IG in providing bespoke decarbonization solutions	24
2.2.2 Included case study on hydropower.....	26
2.3 Methodology	27
2.3.1 Inputs and outputs.....	27
2.3.2 System assumptions.....	28
2.3.3 Data sources.....	30
2.3.4 Framework and runtime.....	33
2.4 Modeling details	33

2.4.1	Nomenclature.....	33
2.4.2	Selection of parameters based on user inputs	38
2.4.3	Objective function	39
2.4.4	Hourly constraints.....	40
2.4.5	Overall constraints	42
2.5	Results and discussion	43
2.5.1	Each region decarbonizes with different technologies.....	44
2.5.2	Is a carbon tax effective?	47
2.5.3	Why does California’s nuclear ban make decarbonization harder?	50
2.5.4	Including hydro in optimization aids decarbonization.....	52
2.5.5	Value of long-duration energy storage.....	54
2.5.6	Meaning and importance of yearly variation	55
2.6	Conclusions.....	55
2.7	Appendix.....	57
2.7.1	Parameter values independent of user inputs	57
2.7.2	Cost and emissions figures for ten technologies	67
2.7.3	Effectiveness of carbon taxes.....	68
2.7.4	Equations used in pre-processing values	68
2.7.5	PHS CAPEX by region [41]	70
2.7.6	Fuel costs [63].....	70
Chapter 3. The elephant in the room: embodied emissions in our power sector		72
3.1	Overview	72
3.2	Introduction.....	72
3.3	Methods.....	74
3.3.1	Assumptions	74
3.3.2	LCA case study vs. operational emissions case study	75

3.4	Results and discussion	76
3.4.1	LCA case results	76
3.4.2	Ignoring embodied emissions changes generator buildout	78
3.4.3	What amount of emissions are being ignored?	80
3.4.4	Real decarbonization is more expensive	82
3.5	Conclusions.....	83
3.6	Appendix.....	84
3.6.1	Financial values and equations	84
3.6.2	Emissions values.....	86
<i>Chapter 4. Can fusion help decarbonize US power sector?</i>		89
4.1	Overview	89
4.2	Introduction.....	89
4.3	Methodology	92
4.3.1	Fusion and other new technologies.....	92
4.3.2	Considering current infrastructure	93
4.3.3	Technology-specific transmission costs and region-specific distribution costs.....	94
4.3.4	Calculating annualized capital cost with CAPEX.....	96
4.3.5	No embodied emissions	97
4.3.6	Technology-specific regional cost-adjustment factors.....	97
4.4	Results	99
4.4.1	Base case.....	99
4.4.2	The key distinguishing factor: buildout limits	101
4.4.3	Fusion cost sensitivity analysis	103
4.4.4	Allow nuclear buildout	106
4.4.5	Restrict fusion to baseload.....	109

4.4.6	Decarbonization with vs. without fusion	110
4.4.7	Considering current capacities	112
4.5	Conclusions.....	113
4.6	Appendix.....	115
<i>Chapter 5. Fusion Representation in a Transforming Grid.....</i>		<i>118</i>
5.1	Overview	118
5.2	Introduction.....	118
5.2.1	Decarbonization motivation.....	118
5.2.2	Novelty of this EG analysis	119
5.3	Modeling details	119
5.3.1	Nomenclature.....	119
5.3.2	Building the objective function.....	126
5.3.3	Hourly constraints.....	129
5.3.4	Annual constraints	131
5.4	Results	135
5.4.1	Base case analysis.....	135
5.4.2	Varying fusion CAPEX	137
5.4.3	Different learning rates	139
5.4.4	Varying fusion commercialization.....	141
5.4.5	Varying doubling time	142
5.4.6	Varying carbon cap.....	143
5.4.7	Comparison of constraint impacts	145
5.5	Conclusions.....	146
5.6	Appendix.....	147

<i>Chapter 6. Summary of contributions and future directions</i>	<i>154</i>
6.1 Novel and impactful contributions	154
6.2 Enabling electric vehicle-to-grid interactions.....	156
6.2.1 Introduction.....	156
6.2.2 Methodology.....	157
6.2.3 Data sources.....	161
6.2.4 Planned analysis and hypotheses	164
6.3 Subsidy analysis	165
6.3.1 Introduction.....	165
6.3.2 Methodology.....	166
6.3.3 Planned analysis and hypotheses	167
6.4 Connecting back to the big picture.....	167
<i>Chapter 7. References</i>	<i>169</i>

List of Figures

Figure 1-1. Information flow diagram for IG 21

Figure 2-1. (a) US grid represented by nine NERC regions, and (b) generator capacity of each region broken down by energy source. 25

Figure 2-2. GUI with inputs and selected outputs for example case study for IG 28

Figure 2-3. Mapping the cost-emissions space for generators and energy storage technologies..... 30

Figure 2-4. Relative regional capacity limits for hydro technologies 31

Figure 2-5. Regional CFS compared to national average for represented variable renewable generation technologies 33

Figure 2-6. Regional decarbonization strategies at lenient, moderate, and deep decarbonization levels (100, 50, and 25 gCO₂/kWh) 44

Figure 2-7. How a carbon tax affects emissions intensity (a) and system cost (b) in all regions 47

Figure 2-8. Impact of a carbon tax in the Northwest region 48

Figure 2-9. Impact of a carbon tax in the Central region 49

Figure 2-10. California reaching various carbon intensities with and without nuclear 50

Figure 2-11. Fleet comparison for a system with vs. without hydro buildout allowed, at 50 gCO₂/kWh .. 52

Figure 2-12. Impact on generator fleet when PHS is introduced 54

Figure 2-13. Technology specific capital and operational costs 67

Figure 2-14. Technology specific capital and operational emissions 68

Figure 2-15. Impact of carbon tax on emissions intensity, costs, and costs before subsidies..... 68

Figure 2-16. Regional natural gas and coal prices 70

Figure 3-1. LCA emissions vs operational emissions in the cost (2030 projections)-emissions space 73

Figure 3-2. Base case system buildout for nine regions, at decreasing carbon ceilings 77

Figure 3-3. Regional operation of natural gas (solid line is a sum of NGCT and NGCC, and dotted line is NGCCS)..... 78

Figure 3-4. Error introduced in capacity buildout by ignoring embodied emissions.....	79
Figure 3-5. Comparison of emissions from LCA (left bar) vs. when embodied emissions are ignored (right bar, with ignored emissions retroactively added on top and represented with stripes).....	80
Figure 3-6. Added cost of fairly accounting for embodied emissions	82
Figure 4-1. Installations required in 2050 because they are already existent, and their retirement date is after 2050	94
Figure 4-2. Regional distribution costs projections for 2050.....	95
Figure 4-3. Regionally- and technologically- specific interconnection costs	96
Figure 4-4. Technology-specific regional cost-adjustment factors.....	98
Figure 4-5. Fleet composition required to reach decreasing decarbonization targets (in the Southeast, Northwest, and Texas)	99
Figure 4-6. Relative generation from all technologies.....	100
Figure 4-7. Regional fusion integration values, at decreasing carbon caps	101
Figure 4-8. Regional fusion integration: base case (line), and ignore wind limitations (dash).....	103
Figure 4-9. Regional fusion buildout, at varying CAPEX values.....	104
Figure 4-10. Fusion penetration, at varying CAPEX estimates, without an imposed carbon cap	106
Figure 4-11. Fusion penetration base case (line) vs. when nuclear buildout is allowed (dash)	107
Figure 4-12. Base-case fusion buildout compared to nuclear buildout, when allowed.....	108
Figure 4-13. Fusion annual CFs for base-case analysis	109
Figure 4-14. Fusion penetration when operated dispatchably vs. restricted to baseload	110
Figure 4-15. Regional electricity costs with naturally integrated fusion vs. no fusion.....	111
Figure 4-16. Fusion adoption, assuming greenfield vs. considering current infrastructure that will be active in 2050.....	112
Figure 4-17. Fleet capacity and costs breakdown for base case vs. analysis which considers current infrastructure.....	113
Figure 4-18. Fleet buildout with decreasing emissions intensity, for all nine regions.....	117

Figure 5-1. Regional emissions intensities [5].....	134
Figure 5-2. Emissions intensity constraint trend comparison between regions and reduction shapes.....	134
Figure 5-3. National capacities (left) and generation (right), from 2020 to 2050.....	135
Figure 5-4. Regional fusion buildout.....	136
Figure 5-5. National power sector costs and emissions intensity	137
Figure 5-6. Change in capacities, as CAPEX is varied from base case (\$3,000/kW on left, \$6,000/kW on right, and \$12,000/kW on right).....	138
Figure 5-7. Fusion LCOE at each optimized year, depending on learning rate.....	139
Figure 5-8. Fusion penetration, depending on learning rate: 5% left, 10% center left (base case), 20% center right, and 30% right.....	140
Figure 5-9. Maximum regional fusion capacity, based on commercialization date	141
Figure 5-10. Commercialization date's impact on regional maximum fusion buildout	141
Figure 5-11. LCOE and maximum allowed buildout, based on variable doubling time	142
Figure 5-12. Impact of doubling rate on fusion buildout, compared to base case (2.3 years doubling time): 2.7 years on left and 2.0 years on right	143
Figure 5-13. Fusion penetration at varying carbon caps: 2.5 gCO ₂ /kWh (left), 4 gCO ₂ /kWh (base case – center cleft), linear 4 gCO ₂ /kWh (center right), and 15 gCO ₂ /kWh (right)	144
Figure 5-14. System cost, emission intensity, and cumulative emissions given a exponential vs linear decarbonization strategy	145
Figure 5-15. Comparison of parameter impact	145
Figure 5-16. Change in fusion capacity, with varying parameter values (%).....	153
Figure 6-1. Cambium's ,mid-case projected regional capacities in 2035 (left) and 2050 (right).....	162
Figure 6-2. Projections of change of regional annual demand sum, excluding transportation demand ...	163
Figure 6-3. LCOE projections based on enacted subsidies vs. ignoring subsidies	166

List of Tables

Table 1-1. Comparison of current CEMs.....	18
Table 2-1. IG sets.....	33
Table 2-2. Scalar decision variables	34
Table 2-3. Vector decision variables.....	35
Table 2-4. User inputs.....	36
Table 2-5. IG parameters	36
Table 2-6. Regions which hit their hydro capacity limits	53
Table 3-1. Financial values for technologies	84
Table 3-2. Emissions values for all technologies.....	87
Table 4-1. Projected change in interconnection costs, by region.....	96
Table 4-2. Buildout constraints which are active when fusion is first integrated (where yellow indicates buildout limit = 0).....	102
Table 4-3. Regions with most and least fusion penetration, at varying CAPEX	104
Table 4-4. 2050 financial projections	115
Table 4-5. Regional buildout limits	116
Table 4-6. Scaled regional buildout limits	116
Table 5-1. EG sets.....	119
Table 5-2. 2-D scalar decision variables	121
Table 5-3. Binary decision variables.....	121
Table 5-4. Vector decision variables.....	122
Table 5-5. User inputs.....	123
Table 5-6. EG parameters	123
Table 5-7. Tracking dataframe for LIB.....	127
Table 5-8. Tracking dataframe for geo	128

Table 5-9. Years when fusion buildout is limited by learning rate	140
Table 5-10. Scalar financial values for all technologies	147
Table 6-1. Sets specific to V2G analysis	158
Table 6-2. Vector decision variables specific to V2G	158
Table 6-3. User inputs specific to V2G.....	158
Table 6-4. EV parameters	158

Chapter 1. Introduction

1.1 Motivation

1.1.1 Decarbonizing to mitigate climate change

The global atmospheric carbon dioxide concentrations have risen at staggering rates since the start of the industrial revolution, increasing by nearly 50% from 227 parts per million (ppm) in 1750 to 412 ppm in 2020 [1]. More disheartening than the already high levels of carbon dioxide, is the fact that annual global emissions are still on the rise, meaning that this change in atmospheric composition has the potential to get even worse, if significant mitigation measures are not taken soon. In 2022, 37 gigatons of carbon dioxide (GtCO₂) was released into the atmosphere [1].

Global targets have been set to limit the change that we impose on our environment. Climate models have shown that there will be key ecosystem differences in a 1.5C warming scenario vs a 2C scenario vs 2019 warming levels (~1C), including, but not limited to extreme temperatures and precipitation [2].

As of July 2023, countries have revised their Nationally Determined Contributions (NDCs) 2030 targets in the Paris agreement. Advanced and emerging economies' revised goals are both still far short of the necessary overhaul needed to reach Net Zero Emissions (NZE) by 2050. In fact, 2030 emissions from advanced economies must be reduced to ~5 GtCO₂ in 2030, but revised NDCs allow for ~8 GtCO₂ [3]. And even more alarming is the fact that projected emissions from advanced economies based on established and planned policies and regulations allow for greater than 8 GtCO₂ in 2030 [3].

Already, we are seeing the terrifying effects of global warming, foreshadowing the even worse consequences of climate change. Global warming is causing dangerous and alarming weather patterns [4]. An additional 20-36% of the global population may face hunger in 2050 based on high emissions scenarios [5]. Even in low emissions scenarios, an additional 11-33% of the population may face food shortage [5]. Global temperature-related mortality rates are estimated to rise by the end of the century, by up to 17% in places like Ghana [6]. On top of the humanitarian cost of climate change, there is also a significant economic toll. The total cost attributable to climate change of 14 extreme flooding events in New Zealand between 2007 and 2014, sums to ~\$140 million [7]. Global warming is dangerous, unfair, and expensive.

1.1.2 Focus on the US Power Sector

This body of work focuses on just the energy economy of the contiguous states of the US. As the second-highest emitting nation, responsible for ~5 billion tons of CO₂ in 2022, the US has the opportunity, and responsibility, to significantly reduce total global emissions [8].

The power sector is the linchpin of the US's decarbonization goals. In 2022, the US's power sector with an annual load of ~4.1 trillion kilowatt-hours (kWh), was responsible for ~1,500 million metrics tons (MMmt) of carbon dioxide-equivalent (CO₂-e), where CO₂-e indicates the total global warming potential of all greenhouse gases, in terms of equivalent tons of CO₂ released [9].

The power sector is the key to decarbonizing the US's energy economy because it has alternative generation technologies that are already competitive with more traditional power generation, on a levelized cost of electricity (LCOE) basis, or total cost of infrastructure per total kWh of electricity produced. Having said that, not all electrons being injected onto the grid are of equal

value, so LCOE is a metric of limited scope. Regardless, the national decarbonization plan relies on transition to a clean grid combined with electrification of other parts of the economy.

Electrification consists of replacing fossil-fueled processes in the other sectors of the economy to be powered by electricity. Some examples of electrification include replacing natural gas (NG) fired water heaters with electric in the residential and commercial sectors, switching from internal combustion engines to battery electric vehicles in the transportation sector, and converting from blast furnaces to electric arc furnaces in the industrial sector. Electrification relies on decarbonization of the power sector, or else the result is just a shifting of emissions source.

The importance to decarbonize quickly, starting now cannot be overemphasized. In fact, if only current Paris Agreement pledges are met (without further improvement), “researchers find very few (if any) ways to reduce emissions after 2030 to limit warming to 1.5°C [2].” Reaching the US’s goal of 100% clean electricity by 2035 [2] will require immense and unprecedented buildout of renewable technologies, resulting in a total rehaul of our current power sector.

Decarbonizing the power sector has possibilities, but also has daunting challenges. The infamous 2021 Texas blackouts serve as a warning to understand the difficulty and importance of constructing a robust grid by displaying the consequences of power sector failures [10]. In fact, it is estimated that a prolonged collapse of the nation’s electric grid could result in the death of up to 90% of the American population, due to starvation, disease, etc. [11]. We need to decarbonize our power sector quickly, but we need to do it so electricity remains reliable.

1.2 Important models and metrics

1.2.1 Current tools

With the US power sector facing such a daunting evolution in the coming years, many models have been built or tailored to answer specific questions regarding this energy transition. Capacity Expansion Models (CEMs) are the industry standard for mapping out electricity decarbonization pathways. CEMs are models used to simulate and optimize generation and transmission capacity investments, based on model- or user- defined constraints and assumptions.

CEMs are often paired or solved simultaneously with unit commitment and/or economic dispatch models. Unit commitment involves determining the start-up and shut-down schedule of all production units based on technological constraints, including ramping rates, minimum up-times, minimum down-times, etc. Economic dispatch is the optimization of power output from each generating unit based on generator availability and transmission constraints.

Table 1-1 shows a comparison of relevant CEMs which the work from this study can be benchmarked against, where the last two rows indicate the models contributed throughout this thesis. The following section provides clarity on the respective added value of Ideal Grid (IG) and Evolving Grid (EG) to the current arsenal of available CEMs.

Table 1-1. Comparison of current CEMs

	Open source	Online web-based UI	Completes LCA	Language	Built in module(s)

GenX [12]	✓			Julia with JuMP	New England ISO
Switch 2.0 [13]	✓			Python with Pyomo	Hawaii
TIMES/MARKAL [14], [15]	✓		✓	GAMS	
ReEDS [16]	✓	✓		GAMS	Many scenarios for contiguous US
REMIx [17]	✓			GAMS and Python	Morocco and Botswana
RESOLVE [18]				Not available	Hawaii, California, New York, New England
LIMES-EU [19]	✓			GAMS with CPLEX	Europe
DIETERpy [20]	✓	✓		Python and GAMS	Germany, France, Denmark, Belgium, Netherlands, Poland, Czech Republic, Austria, Switzerland, Spain, Italy, Portugal

Ideal Grid [21]	✓	✓	✓	Python with Pyomo	Each NERC region within the US
Evolving Grid	✓		✓	Python with Pyomo	Each NERC region within the US

Also, this body of work leverages and incorporates Life-Cycle Assessment (LCA) and Techno-Economic Analysis (TEA) data available in MIT’s Sustainable Energy System Analysis Modelling Environment (SESAME) [22]. Figure 1-1 shows the connection and information flow between IG and SESAME. Miller’s paper on tracking emissions throughout the solar life-cycle provides a detailed description of the LCA framework [23]. Note that the structure featured in Figure 1-1 is also applicable to EG.

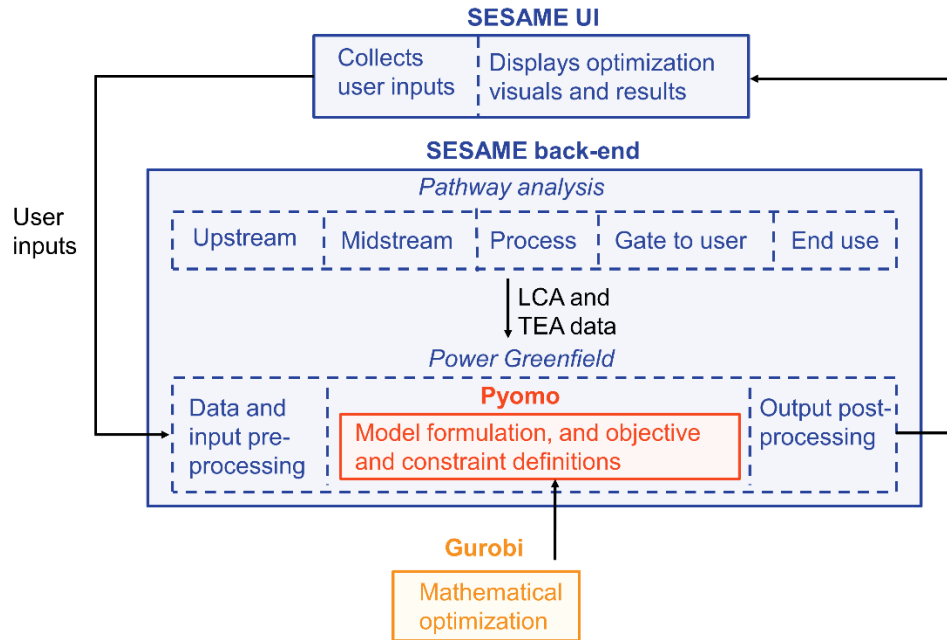


Figure 1-1. Information flow diagram for IG and EG

LCA is the methodical accounting of the resultant global warming potential of each step in the life cycle for a product (e.g. steel) or resource (e.g. electricity) in the energy economy. Similarly, TEA is the bookkeeping of costs resultant from each step in the life cycle for a product or resource in the energy economy. Within the context of electricity generation, the upstream module accounts for extraction and production of fuels for thermal generators, and sourcing materials for and construction of variable renewable generators. The midstream includes transporting and pre-processing fuels. The process module accounts for generator operation. Gate to user is accounting for transmission and distribution of power. Lastly, end use of electricity does not add any system costs or emissions.

1.2.2 Added value of my tools

Chapter 2 and Chapter 4 provide detailed documentation on the methodology, assumptions, and features of Ideal Grid (IG) and Evolving Grid (EG), respectively. But as a basic primer for the

below, IG and EG's added value can be described at a high level as a combination of 3 features, allowing them to provide new and improved insights to the decarbonization landscape.

First, both models are open-source and accessible, meaning that they do not require prohibitively expensive software licenses to run. Next, they both include uniformly preprocessed, regional-specific input data for the North American Electric Reliability Corporation (NERC) regions of the contiguous US states. This means that users can easily and fairly compare decarbonization in each region of the US without the excessive energy barrier of extensive data collection. Lastly, and most importantly, both models utilize LCA to accurately assess the global warming impacts of a variety of decarbonization scenarios, while most CEMs only account for fossil-fuel fired generators' tailpipe emissions. While this is a reasonable approximation for today's grid where the vast majority of emissions are due to natural gas or coal combustion, this will become less and less accurate as we decarbonize. The danger of this commonplace approximation is discussed in detail in Chapter 3.

Chapter 2. Leveraging IG to highlight regional decarbonization challenges

2.1 Overview

This Chapter highlights the importance of regionally tailored decarbonization strategies to reach emissions intensity targets. The presented Ideal Grid model is used to compare and contrast decarbonization strategies for 9 regions of the continental US. For each of these regions, techno-economic analysis (TEA) and life-cycle assessment (LCA) are completed to track emissions intensity and electricity cost based on system installations. Thirteen technologies are included in this analysis: nuclear, wind, solar, natural gas (3 types), coal (3 types), lithium-ion batteries (LIB), conventional hydro, run-of-river (RoR) hydro, and pumped hydro storage. Leveraging only the first ten listed technologies, the impact of carbon emissions intensity constraint and carbon taxes are explored. It is shown that a carbon tax can linearly incentivize decarbonization in certain regions and exponentially incentivize decarbonization in other regions. It is shown that wind capacity factors can be used to indicate decarbonization strategies due to a strong correlation that is explored. At deep decarbonization levels (25 gCO₂/kWh), regions have a varying reliance on nuclear. Regions source anywhere from 27-72% of their electricity from nuclear, with electricity costs ranging from \$112/MWh to \$137/MWh. At lenient decarbonization targets (100 gCO₂/kWh), electricity costs range from \$93/MWh to \$112/MWh. An additional case study on the potential role of hydro technologies (conventional, run-of-river, and pumped hydro storage) shows that hydro can reduce system cost by up to 8%. Also, since hydro technologies provide load-shifting and dispatchable capabilities, the penetration of other

low-carbon firm and dispatchable technologies (such as nuclear and natural gas with carbon capture) decreases.

2.2 Introduction

2.2.1 Value of IG in providing bespoke decarbonization solutions

Each region within the US has unique characteristics. For example, Texas has the highest energy demand, 13,000 Trillion Btu annually, which is about double the demand of the next highest energy intensive state, California [24]. Not only does demand vary greatly from state to state, but current infrastructure also varies significantly from region to region. For example, New Hampshire currently generates 59% of its electricity from nuclear, which can be contrasted with Delaware which generates 92% of its electricity via natural gas. These regional differences make designing decarbonization strategies more complex and more important.

Clearly, transformation of electricity grids requires bespoke solutions as renewable resources, available infrastructure, and projected demand profiles vary regionally. IG provides a platform which can be used to compare the decarbonization difficulty of regions within the US. Figure 2-1 shows the nine regions which are represented in this model and their current generation fleet. The regions are divided along North American Electric Reliability Corporation (NERC) boundaries. We can see that current power sector designs vary significantly from region to region due to the distinctiveness of each region. There is clear variability from region to region in magnitude and composition of generator fleets, such as a relatively high reliance on hydropower in the Northwest, and a comparatively small generator fleet in the Southwest.

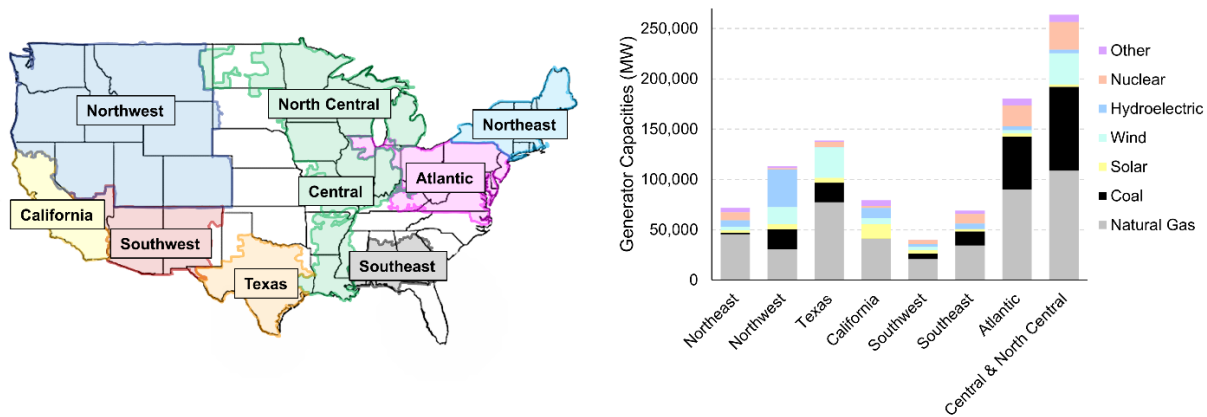


Figure 2-1. (a) US grid represented by nine NERC regions, and (b) generator capacity of each region broken down by energy source.

This Chapter compares decarbonization strategies of different regions which highlights that decarbonization is harder in some regions than others due to available renewable resources. This is invaluable insight as we look to plan an energy transition that is feasible and robust for each region. Since the same tool and assumptions are used for analyzing all regions which make the highlighted similarities and differences in decarbonization more traceable.

Most similar to our manuscript, are a group of studies contrasting the regional challenges of the continental US. Mallapragada, et. al. compared the role of battery energy storage in Texas to New England, but with a greater focus on VRE penetration rather than emissions reduction [25]. A different study contrasts decarbonization in California with decarbonization in New England, but did so with two separate regional models, operating under different assumptions [27]. Bistline and Blanford discuss how the cost of decarbonization will vary regionally, but do not cite the technologies that will be installed in these regions nor do they include their operational patterns [28]. Another manuscript quantifies the impact of state-level policy on carbon mitigation in Utah and Arizona, but does not capture regional variation as these are two bordering states [29]. Ueckerdt, et al. contrasts regional decarbonization strategies on a global level, but does not

examine variation within the US [30]. Each of these studies provides insight in decarbonizing the USA, but none compares each region of the United States to highlight the causes and impacts of differences in demand and renewable resources.

2.2.2 Included case study on hydropower

In 2019, US hydropower capacity is 80.25 GW, outputting 274 TWh of energy annually [31]. This contribution accounts for 6.7% of generation capacity, and 6.6% overall power production and 38% of renewable power production [31]. Around this technology, there is a heated debate regarding its value and impacts. It has been shown that hydropower can be leveraged to lower the cost of decarbonization, where hydro integration provides increasing value to the system as decarbonization targets become more stringent [32], [33]. Conversely, another fraction of researchers emphasizes that hydro can damage the social and ecological ecosystems of a region, and that these impacts are not accurately captured in power system expansion and planning [34], [35]. This study contains a case study aimed to fairly assess the value of hydro while penalizing it appropriately for its direct and indirect emissions.

The term “hydro” primarily refers to a conventional dammed river because the vast majority of hydro resources are this type. However, hydropower technologies can fit into 3 main categories. Dammed hydro will hereafter be referred to as “conventional.” Run-of-river hydro (RoR) does not incorporate any water storage, so power generation is intermittent and non-dispatchable as it depends solely on river flowrate. Pumped hydro storage (PHS) requires two nearby reservoirs at varying heights. Water is pumped up or drained down to the respective higher or lower reservoir to convert electricity to and from gravitational potential energy. IG’s built-in LCA provides invaluable insight into the current debate around hydro.

2.3 Methodology

2.3.1 Inputs and outputs

Ideal Grid, like most CEMs, optimizes the system via minimization of total system cost.

Capacity installations are not limited only based on geography of each region, giving the model the freedom to explore a wide range of decarbonization strategies. Operation of the infrastructure is constricted based on current technological parameters and constraints with technology-specific details included in Section 1.4. Using the graphical user interface (GUI) pictured in Figure 2-2, the user can seamlessly explore the impact of changes in: costs from current values, imposed emissions ceilings and taxes, and regional and yearly variation. All necessary system parameters are pre-existing in the model, allowing users of all levels of expertise to explore scenarios and find impactful insights. More details on the technology-specific characteristics are provided in the following sections.

This optimization provides the user with capacity buildout and unit-operations optimizations for all technologies. Information is provided on cost and emissions for each technology as well.

Emissions and cost values are provided from each technology so that the user can understand the system's response to case-study adjustments. This model provides statistics on technology curtailment, fractional energy losses due to transmission and distribution, and other valuable metrics. Lastly, the economic dispatch data provided at an hourly resolution helps ground the user identify predictable trends (such as solar only producing power in the mid-day hours), and less intuitive trends (such as the complimentary characteristic of solar and wind because wind power output tends to increase in the nighttime hours). All this information allows the user to fully understand the system and specific impact of each technology.

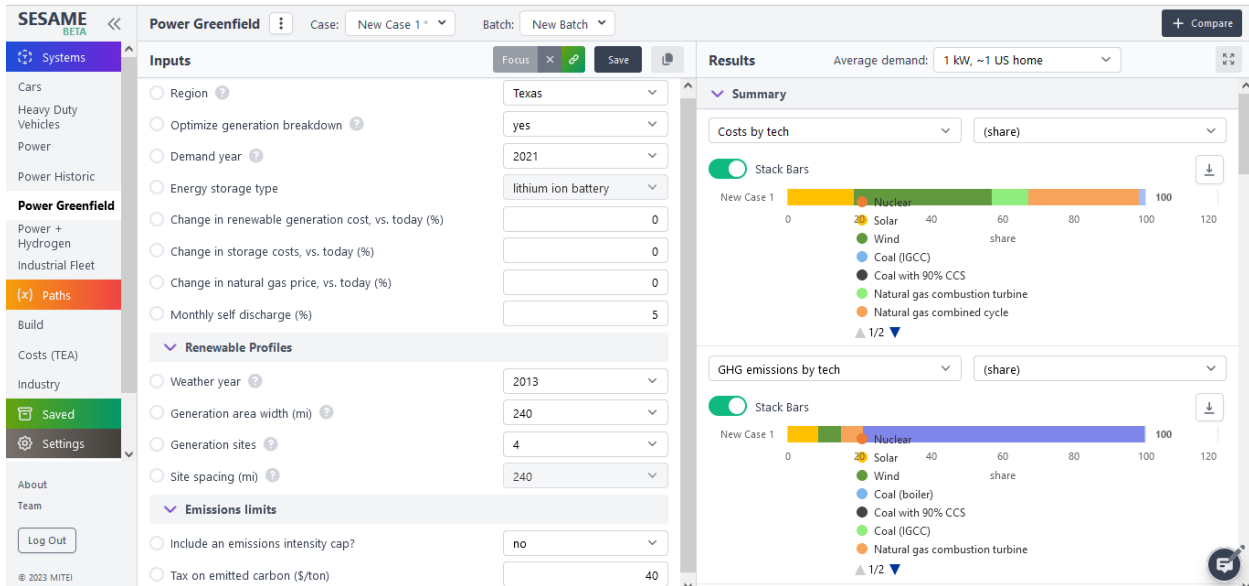


Figure 2-2. GUI with inputs and selected outputs for example case study for IG

2.3.2 System assumptions

Ideal Grid operates under a series of simplistic assumptions. Each NERC region is analyzed as a single-nodal system with an assumed transmission and distribution (TD) efficiency loss of 4.7%, tax of 6.35%, and TD cost of \$47/kWh consistent across all regions. As the name suggests, this is a greenfield model, meaning that the model does not consider the current generator fleet of each region. Lastly, IG is deterministic, and so operates under an assumption of perfect foresight in demand and VRE profile predictions.

Currently, Ideal Grid includes sixteen technologies: three types of lithium ion batteries (4-, 2-, and 8-hour duration), utility-scale single crystal silicon solar panels with an inverter loading ratio of 1.3, 2.8 MW nameplate-rated land-based wind turbines with 90.2 m hub height, fixed-bottom offshore wind, RoR hydro, conventional hydro, PHS, combustion turbine natural gas plants (CT), combined cycle natural gas plants (CC), combined cycle carbon capture and storage (CCS), coal boiler, geothermal, fusion, and nuclear fission plants. Throughout this thesis,

different combinations of technologies are assumed to be available, to explore a variety of potential futures.

Figure 2-1 shows that these technologies represent the vast majority of current grid installations. Hydroelectric is only considered in some of the below findings because of the aforementioned debate outlined in Section 1.2.2. Biomass is not currently considered because it is highly land- and water-intensive which brings up debate regarding environmental disruption and habitat destruction. Geothermal (geo) is present in Chapters 4-6. Lastly, the potential role of fusion is explored in depth in Chapter 4.

Figure 2-3 shows the respective costs and emissions values for all generating technologies. Note that transmission costs, distribution costs, and taxes are not included. These values are just approximations used to orient the reader and are not used in the model. Note that LCOE and emissions intensity for VREs vary based on installation location and LCOE and emissions intensity for all generators vary based on usage. All greenhouse gas emissions are converted to CO₂ equivalent for easy combination and comparison. CO₂ equivalent is hereafter referred to as CO₂-e. Exact values and more detailed explanations are included in the Supplementary Information.

For the technologies that include carbon capture technology, the operating costs of the generator include carbon compression. Natural gas is assumed to capture 267 gCO₂-e per kWh electricity produced, and coal is assumed to capture 553 gCO₂-e/kWh [22]. A transportation and storage fee of \$20/t CO₂-e is assumed for all regions [36].

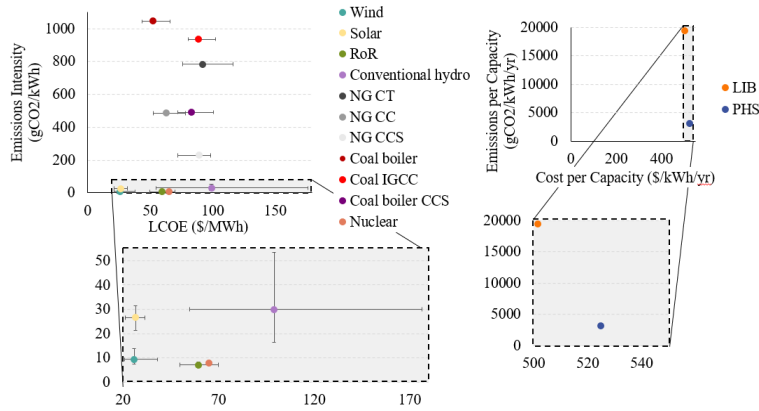


Figure 2-3. Mapping the cost-emissions space for generators and energy storage technologies

2.3.3 Data sources

Cost and emissions data of each technology type come from model interconnections shown in Figure 1-1. Data collection and preprocessing was required for all other model inputs.

Demand profiles were sourced from the NREL’s 2022 *Cambium* data set [37]. NREL provides hourly demand data within NERC boundaries. Some of the smaller NERC regions are aggregated to represent the regions shown in Figure 2-1. It should be noted that results are shown in a relative format to allow for inter-regional comparisons. Demand is scaled down by a different factor in each region so that average hourly demand is equal. This format measures installations in “capacity over average demand” units, where installations totaling 1 implies that all resources were operating at 100% capacity factor.

All three types of hydro resources (conventional, RoR, and PHS) have capacity limits in each region. Conventional hydro is limited based on estimates from *Electric Power Annual*, *Hydropower Vision*, and *An Assessment of Energy Potential at Non-Powered Dams in the US* [38]–[40]. RoR capacity limits are sourced from the *New Stream Reach Development* [41]. PHS capacity limits are obtained from NREL’s *Closed-Loop Pumped Storage Hydropower Resource*

Assessment for the US [42]. More details around these limitations can be found in *Accurately Modeling Hydropower in the US* [43].

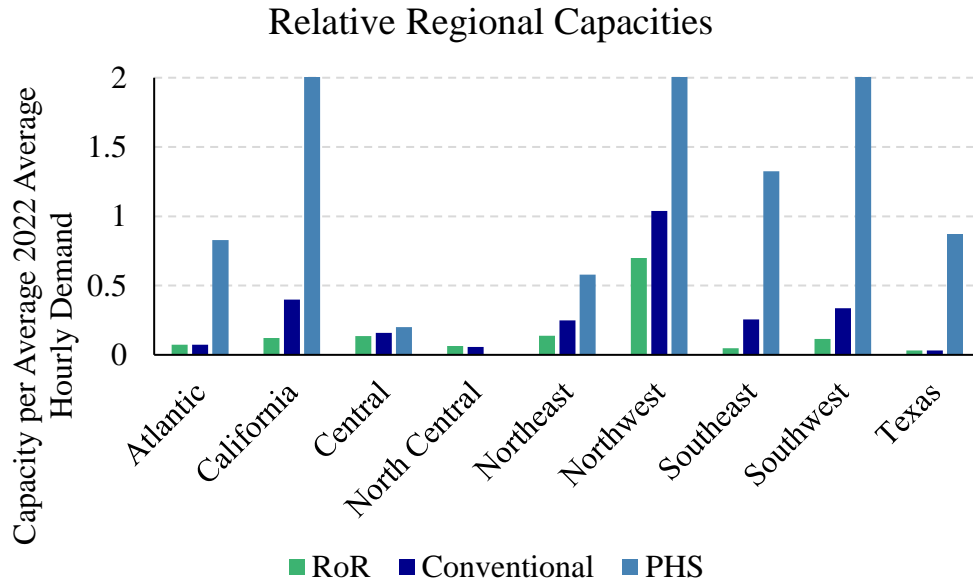


Figure 2-4. Relative regional capacity limits for hydro technologies

Wind and solar hourly availabilities are compiled from data pulled from the Zero-emissions Electricity system Planning with Hourly operational Resolution (ZEPHYR) [44]. For each region, hourly capacity factor (CF) vectors are sourced for 169 equidistant sites within the boundary, each 30 miles apart. Capacity factor is average power output per nameplate capacity. These 169 CF curves are then aggregated to create a profile that is representative of the region. Wind CF values are calculated based on NREL’s Wind Integration National Dataset (WIND) Toolkit, assuming a 100m hub height [45]. Solar CF values are calculated based on NREL’s National Solar Radiation Database (NSRDB), assuming single-crystalline modules with single-axis tracking systems and 1.3 DC-to-AC inverter ratios [46].

RoR hourly availabilities are calculated based on the United State Geological Survey (USGS) daily flowrate data. This source provides flowrate data on over 1.9 million water-resources within the US. River resources were sorted into their appropriate regions based on latitude and longitude coordinates. These data are only available at a daily timestep, so the corresponding CF values are assumed for all 24 hours of the day. Daily flowrates were summed together and then used to calculate power output using:

$$CF_d = \begin{cases} \frac{Q_d}{Q_{max}} * \eta_{turb} & \text{for } Q_d \leq Q_{max} \\ \eta_{turb} & \text{for } Q_d > Q_{max} \end{cases}$$

where Q_d is hourly flowrate, Q_{max} is the flowrate which 30% of the hours exceed, and turbine efficiency, η_{turb} , is 85%. The values calculated with this method match the estimated values published in the New Stream-reach Development assessment with less than 15% discrepancy. Also, conventional hydropower CFs are constrained at monthly checkpoints to account for reservoir volume limitations. Within each month, the hourly CF is allowed to ramp without restriction.

For wind and solar resources, a collection of representative capacity factor curves was manually sourced for each region, at a range of years (2007-2013), at a variety of geographical coordinates distributed within each region. Regarding weather data, the user can select year of weather data, number of generation curves that are aggregated to represent the overall regional VRE power output, and distance between selected sites. In all selection options, the collection of capacity factor curves that are aggregated form an equidistant grid. Figure 2-5 compares the average CF for each variable generation technology in each region, across the aforementioned timeline, in comparison to the national average.

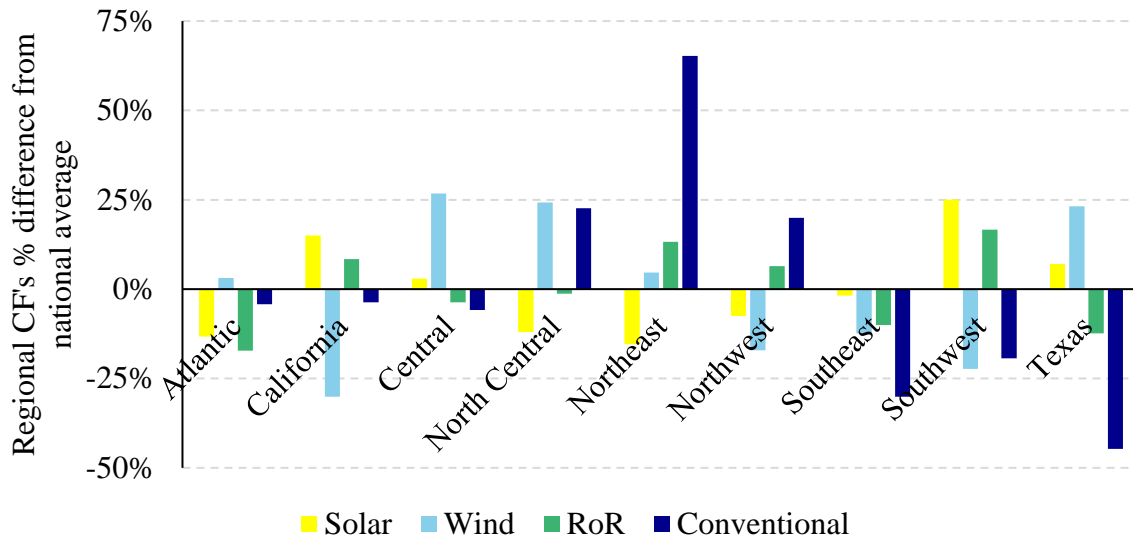


Figure 2-5. Regional CFs compared to national average for represented variable renewable generation technologies

2.3.4 Framework and runtime

IG is formulated in Python with Pyomo and solved with Gurobi. An academic license is used to access Gurobi version 9. Because of the modular flexibility of Pyomo, other open-source solvers can easily be substituted for Gurobi. IG runs on Amazon’s EC2 t2.medium instance with 2 cores, and 4gb ram. With these parameters, the model completes optimizations and displays results in ~45 seconds when run for 1 year of optimization with 10 available technologies.

2.4 Modeling details

2.4.1 Nomenclature

Table 2-1. IG sets

Notation	Description	Unit
----------	-------------	------

$hour$	Incremental integer vector from 0 to 8759 with a step size of 1 that monitors the number of hours into the selected year	hour
Ψ	All generator types and energy storage types: solar, wind, RoR, conventional, nuclear, natural gas (3 types), coal, LIB, and PHS	-
Φ	All generator types: solar, wind, RoR, conventional, nuclear, natural gas (3 types), and coal	-
Υ	Non-dispatchable generating types: solar, wind, RoR, and nuclear	-
υ	Dispatchable generating types: conventional, natural gas (3 types), and coal	-
Ω	Thermal generating types: nuclear, natural gas (3 types), and coal	-
Θ	VRE generating types: solar, wind, and RoR	-
ω	Generators using carbon capture technology: CC natural gas with 95% CCS	-
ζ	Generators technologies eligible for early retirement: coal	-
τ	Energy storage types: LIB, and PHS	-
β	LIB types: 4-hour duration	-

Table 2-2. Scalar decision variables

Notation	Description	Unit
-----------------	--------------------	-------------

$GCopt_{\phi}$	Generating capacity for each generator type	kW
$GCES_t$	Generating capacity for each energy storage type	kWh

Table 2-3. Vector decision variables

Notation	Description	Unit
$G2LIB_{hour}$	Dispatchable generated energy sent to batteries at every time step $hour$	kWh
$G2PHS_{hour}$	Dispatchable generated energy sent to PHS at every time step $hour$	kWh
$G2D_{hour}$	Dispatchable generated energy sent to demand at every time step $hour$	kWh
$VRE2LIB_{hour}$	VRE generated energy sent to batteries at every time step $hour$	kWh
$VRE2PHS_{hour}$	VRE generated energy sent to PHS at every time step $hour$	kWh
$VRE2D_{hour}$	VRE generated energy sent to demand at every time step $hour$	kWh
$VRE2C_{hour}$	VRE generated energy curtailed at every time step $hour$	kWh
$LIB2D_{hour}$	Energy leaving batteries at every time step $hour$	kWh
$PHS2D_{hour}$	Energy leaving PHS at every time step $hour$	kWh
$LIBlevel_{hour}$	Batteries energy level at every time step $hour$	kWh
$PHSlevel_{hour}$	PHS energy level at every time step $hour$	kWh

Table 2-4. User inputs

Notation	Description	Unit
<i>region</i>	NERC region	-
d_{cG}	Decrease in renewable generator costs compared to today's values	%
d_{cS}	Decrease in storage costs compared to today's values	%
$d_{cdispatchablefuel}$	Decrease in storage costs compared to today's values	%
<i>M</i>	Monthly self-discharge of batteries	%
<i>Dyear*</i>	Year of demand profile shape	-
<i>year*</i>	Year of hourly weather used to estimate solar and wind generation	-
<i>sites*</i>	Number of VRE generation sites aggregated to represent solar and wind CF curves	sites
$area_{width}^*$	Height and width of area used to approximate VRE CF curves	mi
e_{tax}	Emissions tax	\$/gCO ₂ -e
e_{cap}	Emissions intensity cap	gCO ₂ -e /kWh

* parameters adjustable in the user interface, but not explored in this analysis. Instead, the most robust selections are chosen for each of the above options, as described below.

Table 2-5. IG parameters

Notation	Description	Unit
-----------------	--------------------	-------------

$CF_{Y,hour}$	VRE CF at every time step <i>hour</i>	1
<i>Dunderlined</i>	Demand at every time step <i>hour</i>	kW
$TDlosses$	Fraction of generated electricity that is lost due to transmission and distribution inefficiencies	1
OCC_Y	Annualized capital cost for each technology	\$/kW
FOM_Y	Fixed operating cost for each technology	\$/kWh/year
VOM_Y	Variable operating cost for each technology	\$/kWh
$fuelcost_Y$	Fuel cost for each technology	\$/MMBtu
$heatrate_Y$	Heat rate for each technology	MMBtu/kWh
eGC_Y	Emissions per capacity for each technology	gCO ₂ -e/kW
$egen_Y$	Emissions per electricity generated for each technology	gCO ₂ -e/kWh
e_t	Emissions per electricity sent to storage for each energy storage type	gCO ₂ -e/kWh
η_t	Efficiency of charging and discharging energy for each energy storage type	1
η_{hourly_t}	Hourly efficiency for each energy storage type	1
L_Y	Lifetime of each technology	Years
$cCCS$	Cost of transporting and storing captured carbon	\$/gCO ₂ -e
$ecaptured_w$	Captured emissions per electricity generated for each energy storage type using carbon capture technology	gCO ₂ -e/kWh

CPC_t	Charging and discharging capacity for each energy storage type, per energy capacity	kW/kWh
---------	---	--------

2.4.2 Selection of parameters based on user inputs

As mentioned in the above section, the parameters used in this linear optimization vary based on input selections. The user's selected *region* and *Dyear* are used to select the appropriate *Dunderlined* vector from an internal data library. Cost of natural gas and coal is dependent on region selected. Values input for d_{cG} , d_{cS} , and $d_{cdispatchablefuel}$ are used to scale the SESAME-sourced TEA values based on the input percent. The raw cost and emissions values used in this model can be seen in the Supplementary Information.

VRE profiles are selected from the extensive data library aggregated based on selected values for *region*, *year*, $area_{width}$, and *sites*. The latter two inputs refer to the model's aggregation level of weather trends. Site number refers to the number of locations that renewable trends are gathered from, before being aggregated into a single profile. Area refers to the distance between the aggregated sites. There are many studies which show that the more generator profiles you aggregate together, and the farther apart they are, the less variability you will see with VRE output profiles. Bera et al. show that aggregation of geographically diverse wind can reduce its intermittency [47]. Ellis et al. show that solar power output variability decreases as the number of systems grows, with diminishing returns [48]. Another study address the issue that cost-optimal VRE deployment can lead to inequitable power systems [49]. All other inputs (self-discharge, carbon tax, carbon ceiling, and renewable breakdown) are set to a scalar value by the user.

Note that many of the parameters described in this section are only relevant to the GUI shown in Figure 2-2, and are not explored in this body of work. Costs and emissions in this Chapter are based on 2022 estimates ($d_{cG} = d_{cS} = d_{c_{dispatchablefuel}} = 0$), although Chapters 3 and 4 explore at projected values. Similarly, the demand curve for this analysis is real data for 2022 ($D_{year} = 2022$), but Chapters 3 and 4 explore projections out to 2050. For all analysis in this thesis, all equidistant CF profiles available in a region are aggregated together to provide the most accurate regional representation ($area_{width} = 360$ square miles, and $sites = 169$) for all available years, ($year = 2007 - 2013$) as described above.

2.4.3 Objective function

The objective function, Equation 2.1, minimizes costs from 4 major components.

$$yearlycost = \min \left\{ \begin{array}{l} \sum_{i \in \psi} GC_i * (capital_i + FOM_i) + \\ \sum_{i \in \psi} (VOM_i + fuel\ cost_i * heatrate_i) * total_i + \\ \sum_{i \in \psi} e_{tax} * (eGC_i * GC_i + e_i * total_i) + \\ \sum_{i \in \omega} ecaptured_i * cCCS \end{array} \right\} \quad (2.1)$$

The first component minimizes fixed yearly cost of all generator and storage types. These values are a combination of capital costs and fixed operation and maintenance costs, after tax credits, depreciation, interest rate, inflation, and more have been accounted for. The second component minimizes variable costs. These values are a combination of variable operational and maintenance costs, and fuel costs. The third component captures the cost of taxed emissions. Emissions from installed capacities, and fuel sourcing and usage are all taxed. This term is trivial when e_{tax} is input as \$/gCO₂-e. The fourth and last term accounts for the cost of transporting and storing captured carbon from generators with carbon capture technology. The linear

combination of costs can be understood as a weighted optimization of technology installation and technology use.

2.4.4 Hourly constraints

Technologies are sized based on a consideration of their CF limits and their maximum hourly usage. Below, Equations 2.2 through 2.7 are used to size and track energy storage parameters. It is clear from these equations that all energy storage technologies are assumed to be symmetric in terms of their charging and discharging capabilities.

$$G2LIB_j + VRE2LIB_j \leq \sum_{i \in \beta} GC_i \quad \forall j \in hour \quad (2.2)$$

$$LIB2D_j \leq \sum_{i \in \beta} GC_i \quad \forall j \in hour \quad (2.3)$$

$$G2PHS_j + VRE2PHS_j \leq GC_{PHS} \quad \forall j \in hour \quad (2.4)$$

$$PHS2D_j \leq GC_{PHS} \quad \forall j \in hour \quad (2.5)$$

$$EClevel_{LIB} \leq \sum_{i \in \beta} GC_i * CPC_i \quad \forall j \in hour \quad (2.6)$$

$$EClevel_{PHS} \leq GC_{PHS} * CPC_{PHS} \quad \forall j \in hour \quad (2.7)$$

Equations 2.2 and 2.3 ensure that the batteries are operating within their respective charging and discharging limits. These limits are imposed before the consideration of charging and discharging inefficiencies, but that the electricity that is delivered to the battery, or to the demand is reduced by the charging and discharging efficiencies cited above in the nomenclature.

Equations 2.4 and 2.5 apply the same constraints to PHS. Equations 2.6 and 2.7 determine the energy capacities of each type of storage needed based on the highest energy inventory

throughout the optimization. Similarly, Equations 2.8, and 2.9 size $GC_{dispatchables}$, and $GC_{nuclear}$ based on maximum power output throughout the optimization.

$$output_{i,j} \leq GC_i \quad \forall j \in hour \wedge i \in u \quad (2.8)$$

$$output_{nuclear,j} = GC_{nuclear} * CF_{nuclear} \quad \forall j \in hour \quad (2.9)$$

The capacity factors of thermal units are followed at an hourly basis, as can be seen in Equation 2.10. At this point, it is significant to note the absolute lack of ramping allowed by nuclear generators in contrast with the complete freedom of natural gas, fusion, geo, conventional hydro, and coal generators to ramp at unrestricted rates. While this is not the actual technology limitations, these approximations represent current operation of these units [50].

$$CF_{i,j} = \frac{output_{i,j}}{GC_i} \quad \forall j \in hour \wedge i \in u \quad (2.10)$$

The flow of electricity can be tracked with the below equations. Equation 2.11 calculates the hourly thermal electricity generated by summing output from each thermal generator and tracking its flow. It can be noted from Equation 2.11 that thermally generated electricity is prevented from being curtailed, as is the convention with current CEMs [12]. Equation 2.12 shows that at every hour, electricity generated from VREs can be sent to storage or demand, or be curtailed. Transmission and distribution losses are considered in this stage for simplicity because the same fractional loss is considered regardless of energy pathway. This simple balance can be monitored and post-processed to show the usage efficiency of generated electricity. Equation 2.13 ensures that demand is satisfied either directly by generation, or indirectly through energy storage.

$$G2D_j + G2LIB_j + G2PHS_j = \sum_{i \in \Omega} GC_i * CF_{i,j} * (1 - TDlosses) \quad \forall j \in hour \quad (2.11)$$

$$VRE2D_j + VRE2LIB_j + VRE2PHS_j + VRE2C_j = \sum_{i \in \Theta} GC_i * CF_{i,j} * (1 - TDlosses) \quad \forall j \in hour \quad (2.12)$$

$$G2D_j + VRE2D_j + LIB2D_j * \eta_{LIB} + PHS2D_j * \eta_{PHS} = \underline{Dunderlined}_j \quad \forall j \in hour \quad (2.13)$$

The hourly energy levels for both types of energy storage are calculated in Equations 2.14 and 2.15 through a simple balance tracking electricity charged and discharged. It can also be noted that parasitic losses are imposed on electricity being stored in LIB. These constraints are not applied to the first hour of the analysis.

$$LIBlevel_j = LIBlevel_{j-1} * \eta_{hourly_{LIB}} + (G2LIB_j + VRE2LIB_j) * \eta_{LIB} - LIB2D_j \quad \forall j \in hour / 0 \quad (2.14)$$

$$PHSlevel_j = PHSlevel_{j-1} + (G2PHS_j + VRE2PHS_j) * \eta_{PHS} - PHS2D_j \quad \forall j \in hour / 0 \quad (2.15)$$

2.4.5 Overall constraints

Equation 2.16 links the energy level in storage at the first hour of the year with that of the last hour of the year. This is necessary to ensure that this optimized year is not used as an energy source or sink.

$$Elevel_0 = Elevel_{j[-1]} \quad (2.16)$$

Equation 2.17 shows the simple relationship used to convert user-input monthly battery efficiency to hourly battery efficiency.

$$\eta_{LIB} = e^{\frac{-M}{780}} \quad (2.17)$$

When an e_{cap} is nonzero, the Equation 2.18 is introduced to limit the overall emissions intensity where total emissions are normalized by total demand. Since Ideal Grid considers emissions from all life-stages, there is a limit on carbon intensities that are achievable. Because of this, the current minimum e_{cap} allowed in the GUI is 25 gCO₂-e/kWh.

$$\sum_{j=0}^{j[-1]} \underline{Dunderlined}_j * e_{cap} = \sum_{i \in \mathcal{I}} \{eGC_i * GC_i + e_i * total_i\} \quad (2.18)$$

2.5 Results and discussion

The added value of Ideal Grid is captured in the high diversity and large span of cases that are presented below. The specific focus of these studies is highlighting the unique regional challenges of decarbonizing the US power sector. First, analysis without hydro is presented, then Sections 6.2.4 and 6.2.5 explore hydro's impact on decarbonization.

2.5.1 Each region decarbonizes with different technologies

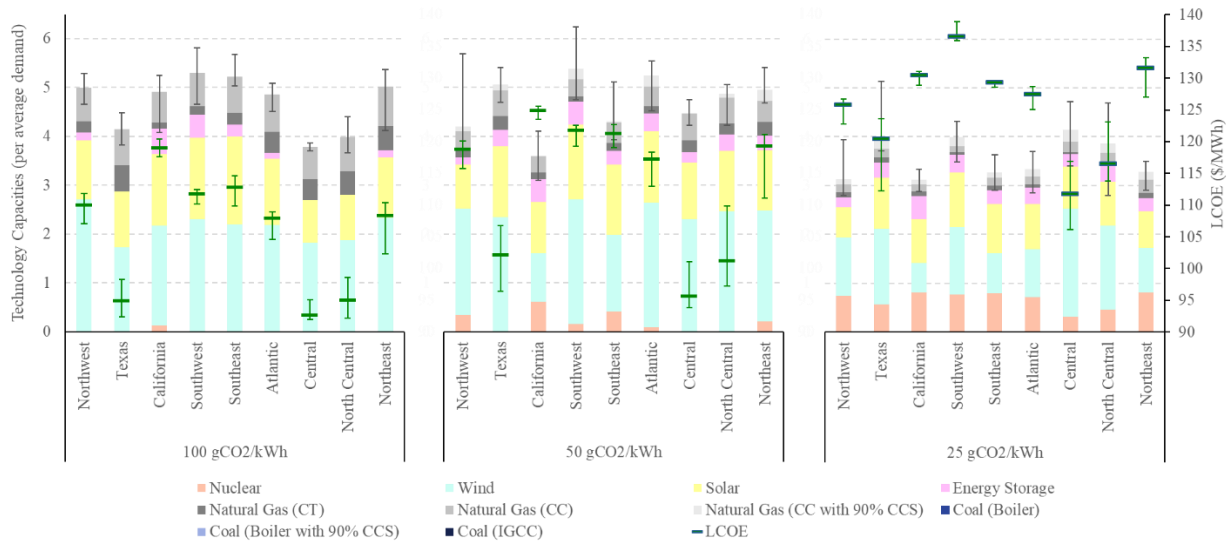


Figure 2-6. Regional decarbonization strategies at lenient, moderate, and deep decarbonization levels (100, 50, and 25 gCO₂/kWh)

Figure 2-6 shows an optimized grid in each region of the US at three different decarbonization levels: 100 gCO₂/kWh, 50 gCO₂/kWh, and 25 gCO₂/kWh. This optimization is completed 7 times using weather data from seven years (2007 to 2013). The mean values are presented in, Figure 2-6 with error bars representing yearly variation in cost and total capacity installed. Demand year was chosen to be 2021 because it is the most recent available.

In the lenient decarbonization case, over 50% of technology installations are VREs, which are supported with natural gas technologies and energy storage. The total generation capacity is over two times greater than average hourly power demand, as is consistent with other decarbonization reports [51]. Figure 2-13 shows that combustion turbine generators are cheaper to build, and combined cycle generators are cheaper to operate. Because of this, combined cycle generators operate at a higher capacity factor (23%), compared to combustion turbine (0.8%). Also, there is a higher reliance on wind over solar, but still has a large variability in range which matches the

patterns that we can be seen in other papers. A Chinese study shows that system stability maximizes when there is more wind installed than solar [52]. A study of the Pennsylvania-New Jersey-Maryland Interconnection showed that wind installations were favored over solar at all VRE penetration levels [51]. The most notable regional variation is that certain regions have a high need for energy storage (2.1 power capacity per average demand in California and 1.9 power capacity per average demand in Southwest), in sharp contrast with regions that require zero energy storage (Central, North Central, and Texas). Regions with the lowest wind CFs require the most energy storage, and regions with high wind CFs require the least amounts of energy storage, as seen in Figure 2-5. This is due to the high reliance on wind. California has the second highest solar CF, but this does not offset the need for storage because of the long and consistent nightly periods of solar unproductivity. This regional discrepancy correlates with cost ranking. Central, North Central, and Texas have the lowest regional costs (92.5, 94.9, 94.9 \$/MWh, respectively), in contrast with California and Southwest which have the highest and third highest regional costs (118.9, 111.6 \$/MWh, respectively). This is because energy storage adds a capital cost of balancing demand and supply, on top of the cost of generating the electricity. In conclusion, wind CF is the most influential regional factor when determining the level of energy storage, and consequently the regional system cost of lenient decarbonization. Note that this analysis only represents 4-hour duration energy storage, but analyses in later chapters introduce 2-hour and 10-hour duration energy storage. Lastly, it should be noted that California is already relying on 0.13 power capacity per average demand installation of nuclear, which contributes 11% of non-curtailed system electricity.

Moderate decarbonization prompts all regions to adopt substantial amounts of energy storage.

The most notable discrepancy between regions is the introduction of nuclear or not. Like above,

certain regions rely heavily on this introduced technology (0.61 power capacity per average demand in California, 0.40 power capacity per average demand in Southeast). This means ~17 GW of nuclear in California and ~10 GW in the Southeast. Other regions do not install any nuclear generation (Central, North Central, and Texas). Again, a low wind CF is correlated with regions that rely on supporting technologies, in this case, nuclear. Because nuclear is more expensive than wind and solar, regions that rely on nuclear have higher costs. Lastly, it is noted that certain regions are relying on natural gas with carbon capture (0.21 power capacity per average demand in Southwest, 0.22 power capacity per average demand in Atlantic, and 0.23 power capacity per average demand in the Northeast), while others do not (California and Central). The cause of this cannot be easily isolated. Natural gas with carbon capture operated at a higher CF (24%) than without (10% CF) because it has 29% higher operational costs but has 53% lower operational emissions. The reduction in operational emissions from carbon capture technologies is ~ 54%. This assumes that the amine regeneration technology that is used in carbon capture requires natural gas heating and 0% carbon capture is assumed for the fueling of this process. Also, the introduction of carbon capture technology increases the natural gas heat rate (and therefore reduces fuel efficiency) by 13%. And, upstream emissions attributed to methane leakage are not reduced. Note that carbon capture technologies present an interesting tradeoff where larger and larger fractions of carbon can be captured, but at increasing costs. The carbon capture technology represented in this analysis is only a conservative approximation of what capabilities and technologies may be commercialized in 2050.

Deep decarbonization is attained by an increased reliance on nuclear in all regions. Most regions have most of their non-curtailed electricity generated from nuclear (72% in California, 72% in Northeast, etc.). Central and North Central regions have the lowest dependencies on nuclear

(27% and 40% of non-curtailed electricity). Again, the highest uses of nuclear are correlated to a low wind CF. It should be noted that this high reliance on nuclear is occurring under the constraint of zero ramping. As this limitation is loosened and ramping is introduced into the model, the reliance on nuclear will increase even farther.

2.5.2 Is a carbon tax effective?

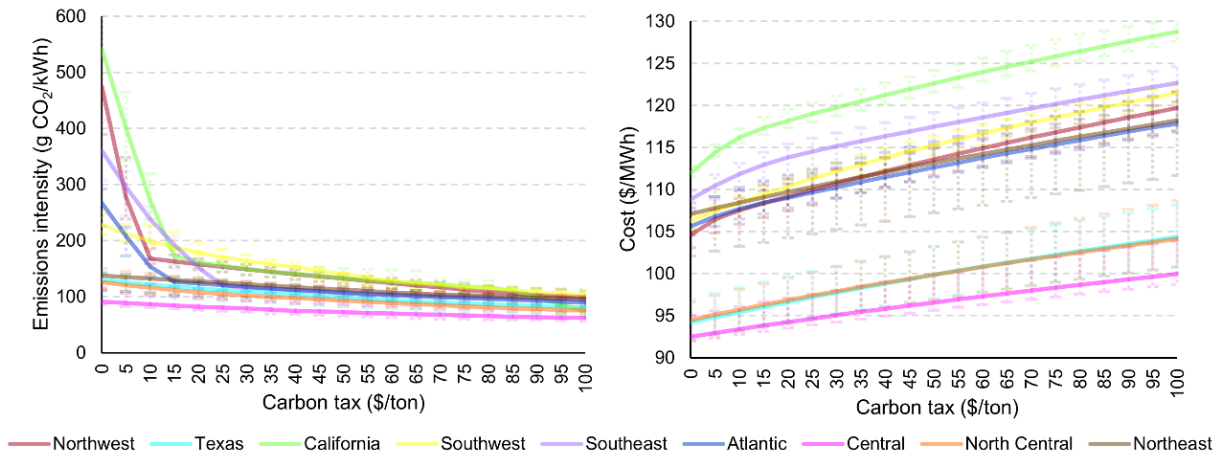


Figure 2-7. How a carbon tax affects emissions intensity (a) and system cost (b) in all regions

One strategy to meet potential decarbonization goals is to impose a carbon tax. Current carbon taxes that are suggested roughly range from \$0 – 100/t [53]. Figure 2-7 shows how an increasing tax rate affects emissions intensity and system cost. Ideally, a tax would prompt a significant reduction in emissions, while only negligibly increasing electricity cost. Figure 2-7 shows that without a tax incentive to decarbonize, the cheapest power system composition varies greatly from region to region. Emissions intensities vary from 540 gCO₂/kWh in California to 90 gCO₂/kWh in the Central region. Similarly, costs range from \$112/MWh in California to \$92/MWh in the Central region. In all regions, an increasing carbon tax monotonically decreases emissions intensity, and monotonically increases system cost. Below, two regions are analyzed more closely to highlight the varying impact of a carbon tax from region to region.

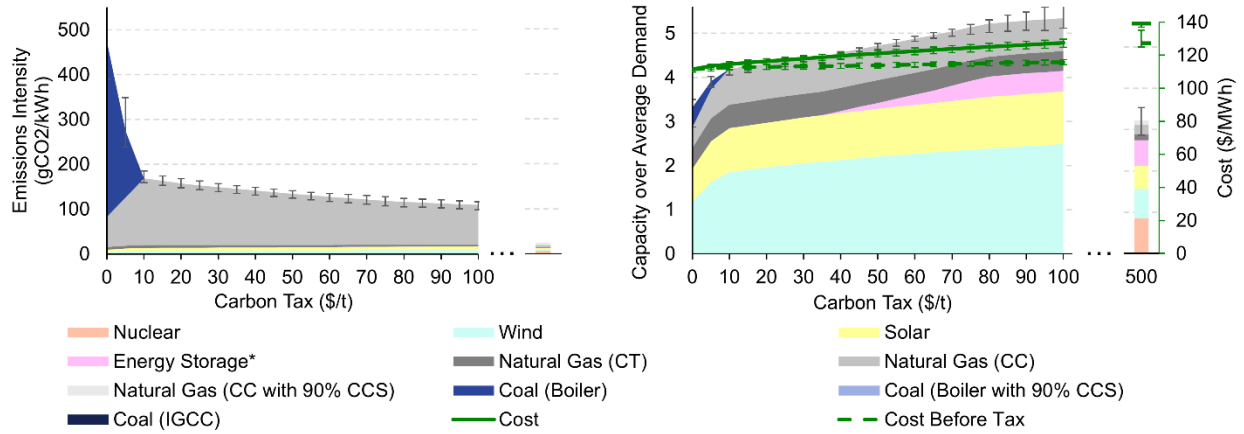


Figure 2-8. Impact of a carbon tax in the Northwest region

Figure 2-8 shows that in the Northwest region, a low carbon tax (\$10/t) is effective in significantly decreasing system emissions (65%) while only slightly increasing system cost (2.8%). The vast majority of these offset emissions are from a coal (boiler) power plant (392 gCO₂/kWh to 0 gCO₂/kWh). Coal is offset by combined cycle natural gas, which is cheaper to install, but more expensive to operate, as seen in Figure 2-13. This tax-motivated reduction in coal is similar to what is seen in an analysis of decarbonizing the Chinese power sector [54]. As discussed above, combined cycle operates at a higher CF than combustion turbine because it has lower operational costs. An increased carbon tax past \$10/t linearly decarbonizes the system at a rate of -0.71 gCO₂/kWh per \$/t carbon tax with an R² value of 0.989, while increasing system cost at a rate of \$0.13/MWh per \$/t carbon tax with an R² value of 0.997. This decarbonization comes from a 50% reduction of combined cycle natural gas operation. Instead, electricity demand is satisfied with VREs. Batteries are introduced to support the VREs at a carbon tax of \$35/ton. It is notable that nuclear does not become economically competitive until high carbon taxes, above \$100/t.

Note that the impact of a carbon tax is lessened when other low-carbon generation technologies are introduced into the system, such as hydro. The value and impact of hydro on regional behavior is discussed in the following sections.

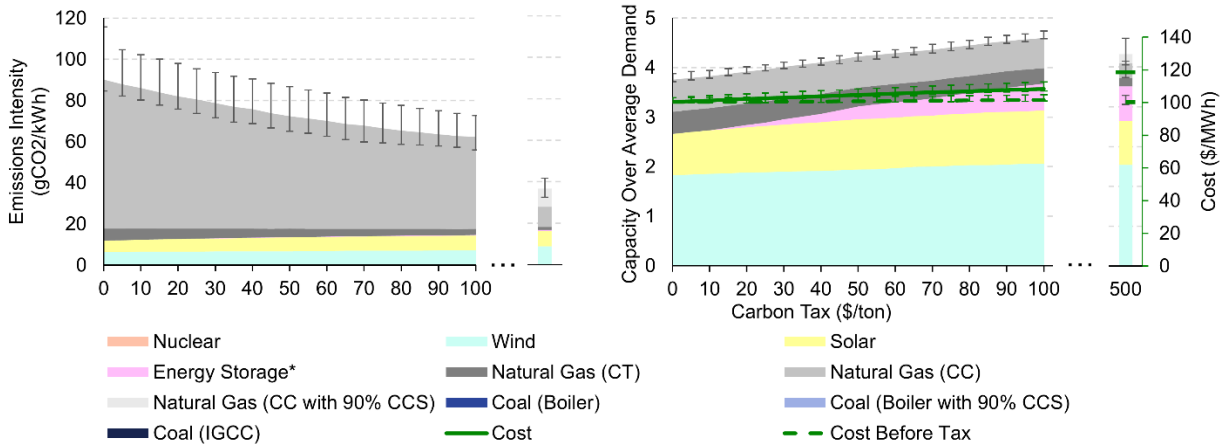


Figure 2-9. Impact of a carbon tax in the Central region

In contrast, Figure 2-9 shows that a tax on the Central region causes a linear decrease in emissions for all tax values. 0.28 gCO₂/kWh emissions are prevented for every dollar of carbon tax with a R² value of 0.976, while increasing system price at a rate of \$0.074/kWh with an R² value of 0.998. This shallower decarbonization rate in comparison to the Northwest is due to the already low emissions intensity (90 gCO₂/kWh without a carbon tax, and 62 gCO₂/kWh with a \$100/t carbon tax), and the fact that a zero emissions intensity is impossible to reach. In fact, the Central region without a carbon tax has a lower emissions intensity than the Northwest region with a \$100/t tax (110 gCO₂/kWh). Like the Northwest region, emissions reduction comes mainly from a reduced reliance on natural gas (40% reduction in combined cycle operation) and increased reliance on VREs (18% capacity increase). At high carbon taxes (\$500/t), no nuclear is installed, and there is a higher reliance on natural gas with carbon capture than was seen in the Northwest. This trend is consistent across regions where a higher reliance on nuclear means a lower reliance on carbon capture. Lastly, system cost before tax is included in figures within this section to track tax revenue.

2.5.3 Why does California’s nuclear ban make decarbonization harder?

Currently, California is facing the retirement of its last remaining nuclear power plants and cannot replace these resources due to a 1976 law banning new nuclear power plant construction [55]. Figure 2-10 illustrates the impact of this legislation. At a less restrictive emissions intensity target (200 gCO₂/kWh), nuclear is not incorporated into the system because of its relatively high electricity cost in comparison to other low-carbon generator options, as seen in Figure 2-3. As the emissions cap tightens to 50 gCO₂/kWh, nuclear technology becomes economically competitive. Because nuclear operates at a high and consistent capacity factor of 93.7%, in contrast to wind and solar which operate with seasonal and hourly variability at lower capacity factors (~25% and ~29% in California), both overall generator fleet and energy storage decrease in size (by 45% and 47%) when nuclear is incorporated. This larger generator fleet without nuclear results in a 7% increase in price. This price and system size increase matches the trends seen in Carrara’s publication [56]. Lastly, it is important to examine the error bars representing yearly variation. Yearly variation increases as the emissions cap tightens because a system more highly reliant on VREs is less stable due to its decreased dispatchability.

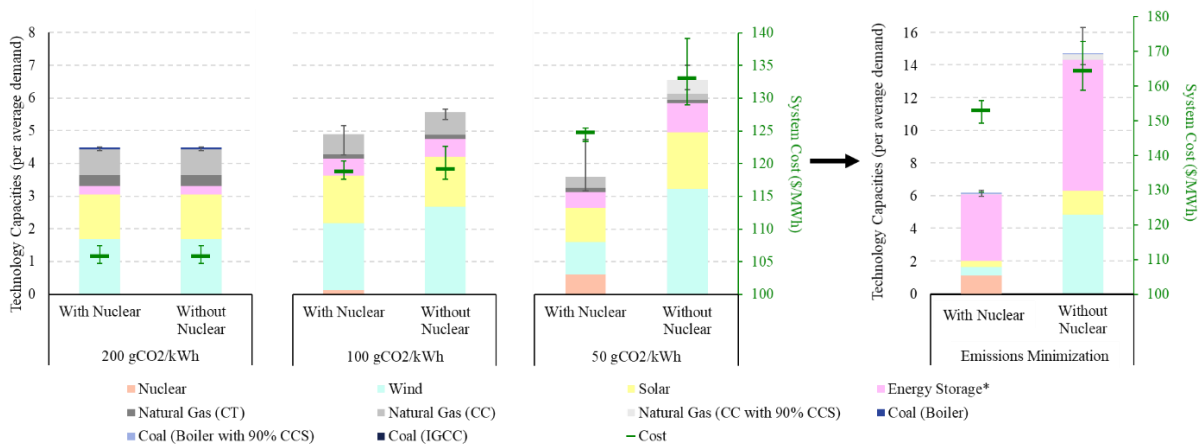


Figure 2-10. California reaching various carbon intensities with and without nuclear

As an extreme case, emissions intensity can be minimized, regardless of system cost. This analysis highlights the value of complete LCA by showing decarbonization limits. The low emissions intensity of nuclear power (8.0 gCO₂/kWh), as seen in Figure 2-3, allows California to reach a low of 16 gCO₂/kWh with nuclear, versus a low of 40 gCO₂/kWh without nuclear. Solar and wind have relatively low emissions intensities (23 gCO₂/kWh and 14 gCO₂/kWh) when operating at their above capacity factors, but in extreme cases where much of their generated electricity is lost (curtailed, lost in TD, or lost in battery operation), their effective CF drops and consequently their emissions intensity increases. In the case where nuclear is restricted, the collective CF of VREs drops to 16%, causing their emissions intensity to rise to 27 gCO₂/kWh. Lastly, there is a very slight reliance on a coal boiler with carbon capture which substitutes natural gas because its lower operational cost offsets its higher capital investment, as seen in Figure 2-13.

2.5.4 Including hydro in optimization aids decarbonization

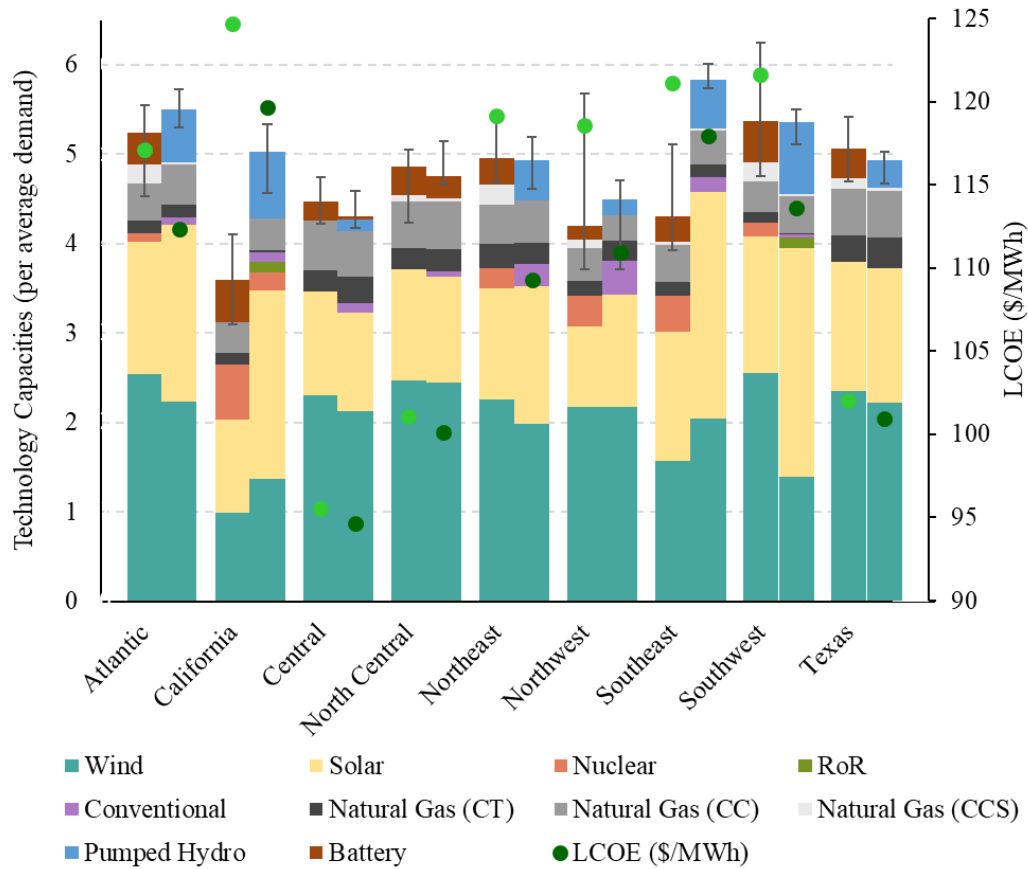


Figure 2-11. Fleet comparison for a system with vs. without hydro buildout allowed, at 50 gCO_2/kWh

First, it is clear from Figure 2-11 that some form hydro is adopted in all regions, when allowed by the model, even considering respective embodied emissions, that some groups cite as a reason to avoid hydro, as mentioned in section 1.2.2. Note that the social consequences of hydro are not considered in this analysis and should still be considered before any new hydro construction.

Easiest to spot is the replacement of LIB with PHS. More analysis on this trend is provided in the following section. Nuclear penetration and natural gas with carbon capture is decreased because

hydro technologies directly compete with low-carbon firm and dispatchable technologies. It's interesting to note that conventional hydro is cheaper than nuclear if both are compared at low CFs. For example, at a CF of 36%, (about the national average for conventional hydro) nuclear LCOE is about \$150/MWh, which is higher than most conventional hydro installation options, as shown in Figure 2-3. The impact of hydro on solar and wind resources is not homogeneous across all regions. In most locations (Atlantic, California, North Central, Northeast, and Southwest), solar capacity is increased and wind capacity is decreased, albeit to varying degrees. Other regions (Central and Texas) require less solar and wind buildout, but only to a slight degree because these regions are mostly flat, with limited hydro resources. The characteristics motivating these discrepancies is a complex combination of many factors. Lastly, and most importantly, there is a system cost reduction ranging from 2-8% when hydro is allowed.

Also worth noting is the importance of including capacity limits on hydro. In this analysis, hydro capacity limits were hit in six out of the nine analyzed regions, in one hydro technology or another. Table 2-6 shows which regions hit capacity limits at the 50 gCO₂/kWh carbon ceiling.

Table 2-6. Regions which hit their hydro capacity limits

	Using LCA Techniques								
	Atlantic	California	Central	North Central	Northeast	Northwest	Southeast	Southwest	Texas
Conventional	X		X	X	X				
RoR		X						X	
PHS			X	-					

2.5.5 Value of long-duration energy storage

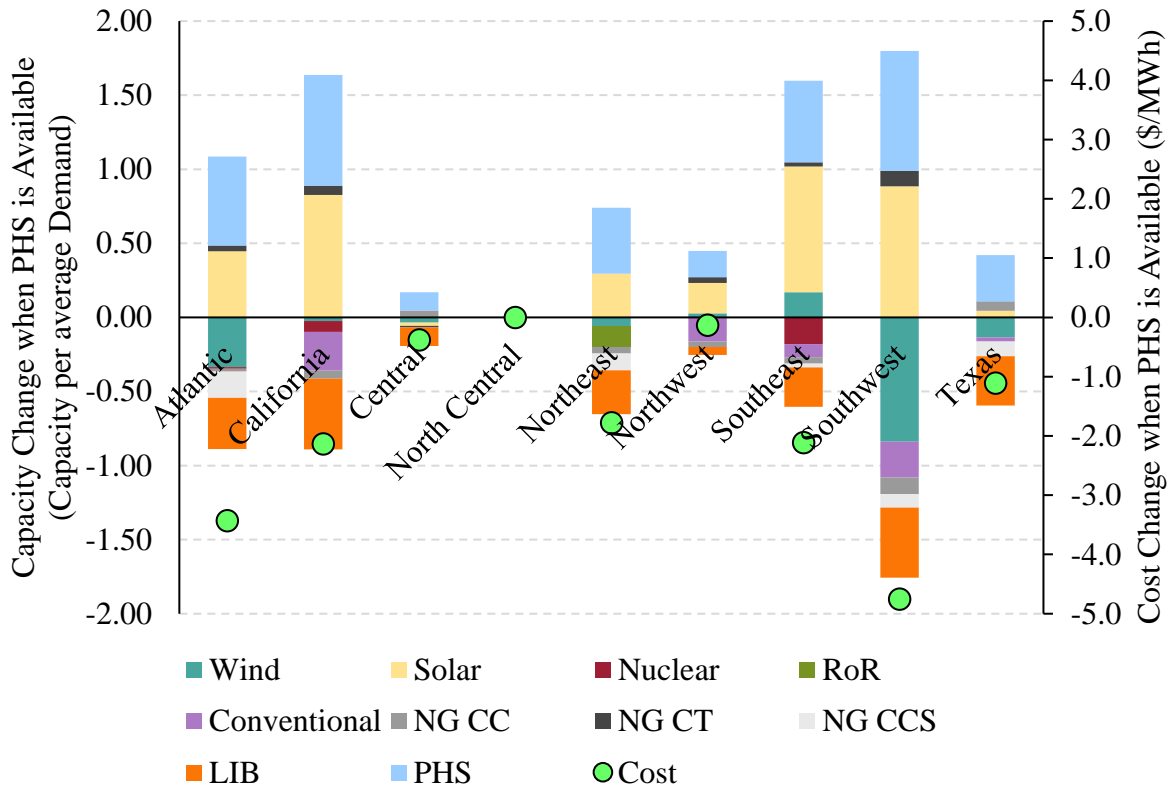


Figure 2-12. Impact on generator fleet when PHS is introduced

The role of PHS – or more generally, long-duration energy storage – is shown in Figure 2-12.

Leveraging this technology allows for up to 4% system cost saving, depending on region. More interestingly, it changes least-cost fleet breakdown. Obviously, a more diverse arsenal of energy storage technologies increases the reliance on storage. Reliance on solar also increases because of its extreme oscillation, which pairs well with storage. In contrast, PHS decreases system reliance on nuclear, conventional, hydro, and natural gas with carbon capture. This is because PHS gives the system a load-shifting ability, meaning that dispatchable, and firm generation technologies are needed less. Dirty natural gas (CT) reliance increases because there is more space in the carbon budget as the other technologies are phased out. Lastly, Central and Texas

regions see a minuscule decrease in energy storage capacity as PHS replaces LIB, but that overall storage energy capacity still increases.

2.5.6 Meaning and importance of yearly variation

Error bars are present in all results graphs to show yearly variation in optimization. This variation is caused by diversity in VRE output trends, which causes the optimum generation fleet to vary from year to year. Regardless of this variation, the proposed system must guarantee robust output to satisfy the electricity demand. System robustness can be increased in several ways, including load-shifting, utilizing battery electric vehicles as energy storage, targeted load shedding, etc.

2.6 Conclusions

This report describes the novel and impactful nature of Ideal Grid, most notably its ability to execute numerous and diverse analyses without requiring any data collection or pre-processing. This allows users to explore the power sector landscape without the entry-barrier which limits the potential users of many other tools. Within Ideal Grid, LCA and TEA results can be produced for a massive number of case studies.

In this paper, there is a focus on identifying regional discrepancies in decarbonization schemes to highlight regional challenges. Lenient, moderate, and deep decarbonization targets are imposed on all regions. At all three decarbonization levels, the wind capacity factor directly corresponds to technologies used and resultant costs. In lenient decarbonization, regions with high wind CFs do not require energy storage. In contrast, regions with low wind CFs require large amounts of energy storage. California even requires 11% electricity generation from nuclear, resulting in the highest cost at this decarbonization target, \$118.9/MWh. At deeper decarbonization levels, all

regions rely more heavily on nuclear generation. California and New England rely most heavily on nuclear, generating 72% of their electricity in each region.

California's relatively high reliance on nuclear draws additional attention to its current ban of new nuclear installations. Without nuclear, California's minimum carbon intensity that can be reached is 40 gCO₂/kWh, while allowing for nuclear extends the decarbonization potential to 16 gCO₂/kWh. To reach moderate decarbonization levels without nuclear, the power system must increase in size by 45%, and correspondingly increase electricity cost by 7%.

A carbon tax is imposed on all regions to test and quantify its effectiveness. A low carbon tax (\$10/t) is effective in drastically reducing emissions by phasing out all coal generation. After coal has been phased out of all regions, a carbon tax linearly decreases carbon emissions and linearly increases price. In the Northwest region, an increasing carbon tax reduces emissions at a rate of 0.71 gCO₂/kWh per \$/t tax and increases cost at a rate of \$0.13/MWh per \$/t tax. In the Central region, a carbon tax is less effective, where 0.28 gCO₂/kWh emissions are prevented for every \$/t tax, at the cost of \$0.074/MWh per \$/t tax.

Lastly, a wide range of sources are used to comprehensively evaluate hydro resources across the USA. Regional capacity limits and performance profiles are identified for conventional, RoR, and PHS resources. LCA is used to show that the optimal decarbonization strategy for every region involves the leveraging of at least one hydro resource. Hydro provides valuable load-shifting and dispatchable capabilities, which leads to an overall decrease in system cost by up to 8%. National reliance on solar is increased because it pairs well with load-shifting and highly dispatchable technologies. Also, the need to firm and/or dispatchable, low-carbon generation technologies is lessened as hydro technologies compete for that role. Consequently, introducing hydro to the system reduces nuclear and natural gas with carbon capture penetration.

2.7 Appendix

2.7.1 Parameter values independent of user inputs

	Value	Unit	Source
TD_{losses}	0.047	-	[57]
$capital_{LIB}$	22.8	\$/kW/year	[58] Utility-Scale Battery Storage; 4hr battery storage – moderate case; 2022 CAPEX, normalized by lifetime; **reduction by a factor of 4 to convert from power capacity to energy capacity
FOM_{LIB}	8.5	\$/kW/year	[58] Utility-Scale Battery Storage; 4hr battery storage – moderate case; 2022 Fixed Operation and Maintenance Expenses; **reduction by a factor of 4 to convert from power capacity to energy capacity
VOM_{LIB}	0	\$/kWh	[58] Utility-Scale Battery Storage; 4hr battery storage – moderate case; 2022 Fixed Operation and Maintenance Expenses
$fuelcost_{LIB}$	0	\$/MMBtu	-
$heatrate_{LIB}$	0	MMBtu/kWh	-
$capital_{wind}$	59.72	\$/kW/year	[58] Land-Based Wind; Moderate case; 2022 annualized CAPEX multiplied by calculated

			FRC, considering tax credits, depreciation, etc.;; exact equations included below
FOM_{wind}	42	\$/kW/year	[58] Land-Based Wind; Moderate case; 2022 Fixed Operation and Maintenance Expenses
VOM_{wind}	0	\$/kWh	[58] Land-Based Wind; Moderate case; 2022 Variable Operation and Maintenance Expenses
$fuelcost_{wind}$	0	\$/MMBtu	-
$heatrate_{wind}$	0	MMBtu/kWh	-
$capital_{solar}$	38.71	\$/kW/year	[58] Solar – Utility PV; Moderate case; 2022 annualized CAPEX multiplied by calculated FRC, considering tax credits, depreciation, etc.;; exact equations included below
FOM_{solar}	20	\$/kW/year	[58] Solar – Utility PV; Moderate case; 2022 Fixed Operation and Maintenance Expenses
VOM_{solar}	0	\$/kWh	[58] Solar – Utility PV; Moderate case; 2022 Variable Operation and Maintenance Expenses
$fuelcost_{solar}$	0	\$/MMBtu	-
$heatrate_{solar}$	0	MMBtu/kWh	-
$capital_{nuclear}$	309.80	\$/kW/year	[58] Nuclear; Moderate case; annualized CAPEX multiplied by calculated FRC, considering interest rates, depreciation, etc.;; exact equations included below

$FOM_{nuclear}$	146	\$/kW/year	[58] Nuclear; Moderate case; 2022 Fixed Operation and Maintenance Expenses
$VOM_{nuclear}$	0.003	\$/kWh	[58] Nuclear; Moderate case; 2022 Variable Operation and Maintenance Expenses
$fuelcost_{nuclear}$	0.68	\$/MMBtu	[58] Nuclear; Moderate case; 2022 Fuels Costs
$heatrate_{nuclear}$	0.01044	MMBtu/kWh	[58] Nuclear; Moderate case; 2022 Heat Rate
$capital_{ngct}$	40.58	\$/kW/year	[58] Natural Gases – CT; Moderate case; annualized CAPEX multiplied by calculated FRC, considering interest rates, depreciation, etc.; exact equations included below
FOM_{ngct}	21	\$/kW/year	[58] Natural Gas_FE – CT; Moderate case; 2022 Fixed Operation and Maintenance Expenses
VOM_{ngct}	0.005	\$/kWh	[58] Natural Gas_FE – CT; Moderate case; 2022 Variable Operation and Maintenance Expenses
$fuelcost_{ngct}$	-	\$/MMBtu	Dependent on input-selected region; exact values included below
$heatrate_{ngct}$	0.00972	MMBtu/kWh	[58] Natural Gas_FE – CT; Moderate case; 2022 Heat Rate
$capital_{ngcc}$	45.64	\$/kW/year	[58] Natural Gas_FE – CC; Moderate case; annualized CAPEX multiplied by calculated FRC, considering interest rates, depreciation, etc.; exact equations included below

FOM_{ngcc}	28	\$/kW/year	[58] Natural Gas_FE – CC; Moderate case; 2022 Fixed Operation and Maintenance Expenses
VOM_{ngcc}	0.002	\$/kWh	[58] Natural Gas_FE – CC; Moderate case; 2022 Variable Operation and Maintenance Expenses
$fuelcost_{ngcc}$	-	\$/MMBtu	Dependent on input-selected region; exact values included below
$heatrate_{ngcc}$	0.00636	MMBtu/kWh	[58] Natural Gas_FE – CC; Moderate case; 2022 Heat Rate
$capital_{ngccs}$	105.03	\$/kW/year	[58] Natural Gas_FE – CC – CCS; Moderate case; annualized CAPEX multiplied by calculated FRC, considering interest rates, depreciation, etc.; exact equations included below
FOM_{ngccs}	63	\$/kW/year	[58] Natural Gas_FE – CC – CCS; Moderate case; 2022 Fixed Operation and Maintenance Expenses
VOM_{ngccs}	0.006	\$/kWh	[58] Natural Gas_FE – CC – CCS; Moderate case; 2022 Variable Operation and Maintenance Expenses
$fuelcost_{ngccs}$	-	\$/MMBtu	Dependent on input-selected region; exact values included below
$heatrate_{ngccs}$	0.00717	MMBtu/kWh	[58] Natural Gas_FE – CC – CCS; Moderate case; 2022 Heat Rate

$capital_{coalboiler}$	136.42	\$/kW/year	[58] Coal_FE – new; Moderate case; annualized CAPEX multiplied by calculated FRC, considering interest rates, depreciation, etc.; exact equations included below
$FOM_{coalboiler}$	74	\$/kW/year	[58] Coal_FE – new; Moderate case; 2022 Fixed Operation and Maintenance Expenses
$VOM_{coalboiler}$	0.008	\$/kWh	[58] Coal_FE – new; Moderate case; 2022 Variable Operation and Maintenance Expenses
$fuelcost_{coalboiler}$	-	\$/MMBtu	Dependent on input-selected region; exact values included below
$heatrate_{coalboiler}$	0.00849	MMBtu/kWh	[58] Coal_FE – new; Moderate case; 2022 Heat Rate
$capital_{coalboiler90}$	245.85	\$/kW/year	[58] Coal_FE – CCS – 90%; Moderate case; annualized CAPEX multiplied by calculated FRC, considering interest rates, depreciation, etc.; exact equations included below
$FOM_{coalboiler90}$	125	\$/kW/year	[58] Coal_FE – CCS – 90%; Moderate case; 2022 Fixed Operation and Maintenance Expenses
$VOM_{coalboiler90}$	0.015	\$/kWh	[58] Coal_FE – CCS – 90%; Moderate case; 2022 Variable Operation and Maintenance Expenses
$fuelcost_{coalboiler90}$	-	\$/MMBtu	Dependent on input-selected region; exact values included below

$heatrate_{coalboiler90}$	0.01078	MMBtu/kWh	[58] Coal_FE – CCS – 90%; Moderate case; 2022 Heat Rate
$capital_{coalIGCC}$	389.81	\$/kW/year	[58] Coal_FE – IGCC; Moderate case; annualized CAPEX multiplied by calculated FRC, considering interest rates, depreciation, etc.; exact equations included below
$FOM_{coalIGCC}$	141	\$/kW/year	[58] Coal_FE – IGCC; Moderate case; 2022 Fixed Operation and Maintenance Expenses
$VOM_{coalIGCC}$	0.014	\$/kWh	[58] Coal_FE – IGCC; Moderate case; 2022 Variable Operation and Maintenance Expenses
$fuelcost_{coalIGCC}$	-	\$/MMBtu	Dependent on input-selected region; exact values included below
$heatrate_{coalIGCC}$	0.00849	MMBtu/kWh	[58] Coal_FE – IGCC; Moderate case; 2022 Heat Rate
$capital_{conventional}$	243.56	\$/kW/year	[58] Hydropower; Averaged value for moderate case for NSD 2; 2022 annualized CAPEX multiplied by calculated FRC, considering tax credits, depreciation, etc.; exact equations included below
$FOM_{conventional}$	45	\$/kW/year	[58] Hydropower; Averaged value for moderate case for NSD 2; Fixed Operation and Maintenance Expenses

$VOM_{conventional}$	0	\$/kWh/year	[58] Hydropower; Averaged value for moderate case for NSD 2; Variable Operation and Maintenance Expenses
$fuelcost_{conventional}$	0	\$/MMBtu	-
$heatrate_{conventional}$	0	MMBtu/kWh	-
$capital_{RoR}$	240.53	\$/kW/year	[58] Hydropower; Averaged value for moderate case for NSD 1-4; 2022 annualized CAPEX multiplied by calculated FRC, considering tax credits, depreciation, etc.; exact equations included below
FOM_{RoR}	86	\$/kW/year	[58] Hydropower; Averaged value for moderate case for NSD 1-4; Fixed Operation and Maintenance Expenses
VOM_{RoR}	0	\$/kWh/year	[58] Hydropower; Averaged value for moderate case for NSD 1-4; Variable Operation and Maintenance Expenses
$fuelcost_{RoR}$	0	\$/MMBtu	-
$heatrate_{RoR}$	0	MMBtu/kWh	-
$capital_{PHS}$	-	\$/kW/year	Dependent on input-selected region; exact values included below
FOM_{PHS}	17.8	\$/kW/year	[58] Pumped Storage Hydropower; Moderate case; 2022 FOM

VOM_{PHS}	0.00051	\$/kWh	[58] Pumped Storage Hydropower; Moderate case; 2022 FOM
$fuelcost_{PHS}$	0	\$/MMBtu	-
$heatrate_{PHS}$	0	MMBtu/kWh	-
$e_{GC_{LIB}}$	72,900	gCO ₂ /kWh	[59] Build a Pathway; Other Technology *
$e_{GC_{solar}}$	58,580	gCO ₂ /kW	[59] Build a Pathway; utility, fixed tilt; all other inputs are default *
$e_{GC_{wind}}$	30,660	gCO ₂ /kW	[59] Build a Pathway; all inputs are default *
$e_{GC_{nuclear}}$	3,283	gCO ₂ /kW	[59] Build a Pathway; HTGR reactor; all inputs are default; does not include decommission emissions *
$e_{GC_{ngct}}$	35,485	gCO ₂ /kW	[59] Build a Pathway; Gas Turbine *
$e_{GC_{ngcc}}$	39,900	gCO ₂ /kW	[59] Build a Pathway; Combined Cycle *
$e_{GC_{ngccs}}$	48,768	gCO ₂ /kW	[59] Build a Pathway; Combined Cycle with Use CCS on; 90% captured from plant; 0% captured from Amine Regeneration; all other inputs default *
$e_{GC_{coalboiler}}$	3,044	gCO ₂ /kW	[59] Build a Pathway; all inputs are default *
$e_{GC_{coalboiler90}}$	3,044	gCO ₂ /kW	[59] Build a Pathway; all inputs are default *
$e_{GC_{coalIGCC}}$	3,402	gCO ₂ /kW	[59] Build a Pathway; IGCC type; all other inputs are default *
$e_{GC_{conventional}}$	87,540	gCO ₂ /kW	[60]

$e_{GC_{RoR}}$	45235	gCO ₂ /kW	[60]
$e_{GC_{PHS}}$	3150	gCO ₂ /kW	[61]
e_{wind}	0	gCO ₂ /kWh	-
e_{solar}	0	gCO ₂ /kWh	-
$e_{nuclear}$	7.6	gCO ₂ /kWh	[59] Build a Pathway; HTGR reactor; all other inputs are default; emissions are only from methane leaking
e_{ngct}	780	gCO ₂ /kWh	[59] Build a Pathway; Gas Turbine
e_{ngcc}	481	gCO ₂ /kWh	[59] Build a Pathway; Combined Cycle
e_{ngccs}	223	gCO ₂ /kWh	[59] Build a Pathway; Combined Cycle with Use CCS on; 90% captured from plant; 0% captured from Amine Regeneration; all other inputs default
$e_{coalboiler}$	1,044	gCO ₂ /kWh	[59] Build a Pathway; all inputs are default
$e_{coalboiler90}$	491	gCO ₂ /kWh	[59] Build a Pathway; all inputs are default
$e_{coalIGCC}$	935	gCO ₂ /kWh	[59] Build a Pathway; IGCC type; all other inputs are default
e_{LIB}	0	gCO ₂ /kWh	-
$e_{conventional}$	0	gCO ₂ /kWh	-
e_{RoR}	0	gCO ₂ /kWh	-
e_{PHS}	0	gCO ₂ /kWh	-

η_{LIB}	0.92	-	[58] Assuming equal charging and discharging efficiencies
$\eta_{hourly_{LIB}}$	0.9999315	-	[62] Converted from $M = 5\%$ based on the below equation
η_{PHS}	0.8944272	-	[58] Assuming equal charging and discharging efficiencies
$\eta_{hourly_{PHS}}$	1	-	
$CF_{nuclear}$	0.937	-	[58] Nuclear; Moderate case; 2022 net CF
L_{wind}	30	years	[58] Financial and CRP inputs tab; Land-based wind
L_{solar}	30	years	[58] Financial and CRP inputs tab; Solar – Utility PV
$L_{nuclear}$	60	years	[58] Financial and CRP inputs tab; Nuclear
L_{ngct}	55	years	[63] Natural Gas; Technology Life
L_{ngcc}	55	years	[63] Natural Gas; Technology Life
L_{ngccs}	55	years	[63] Natural Gas; Technology Life
$L_{coalboiler}$	75	years	[63] Coal; Technology Life
$L_{coalboiler90}$	75	years	[63] Coal; Technology Life
$L_{coalIGCC}$	75	years	[63] Coal; Technology Life
L_{EC}	15	years	[58] Utility-Scale Battery Storage; Technology Life
$L_{conventional}$	100	years	[58] Hydropower; Technology Life

L_{RoR}	100	years	[58] Hydropower; Technology Life
L_{PHS}	100	years	[58] Pumped Storage Hydropower; Technology Life
c_{CCS}	0.00002	\$/gCO ₂	[36] Cost of transportation and storage of carbon; assuming 8\$/ton for storage and 0.05 \$/ton/mile with an average transportation distance of 240 miles
$e_{captured_{ngccs}}$	267	gCO ₂ /kWh	[59]
$e_{captured_{coalboiler90}}$	553	gCO ₂ /kWh	[59]

*Note: Sparse data on these values because emissions analyses usually focus on operational emissions

**explanations for chosen assumptions

2.7.2 Cost and emissions figures for ten technologies

Figure 2-13 and Figure 2-14 can be used to directly compare costs and emissions values for all ten technologies. Costs and emissions values are broken up into their capacity-related and operation-related components.

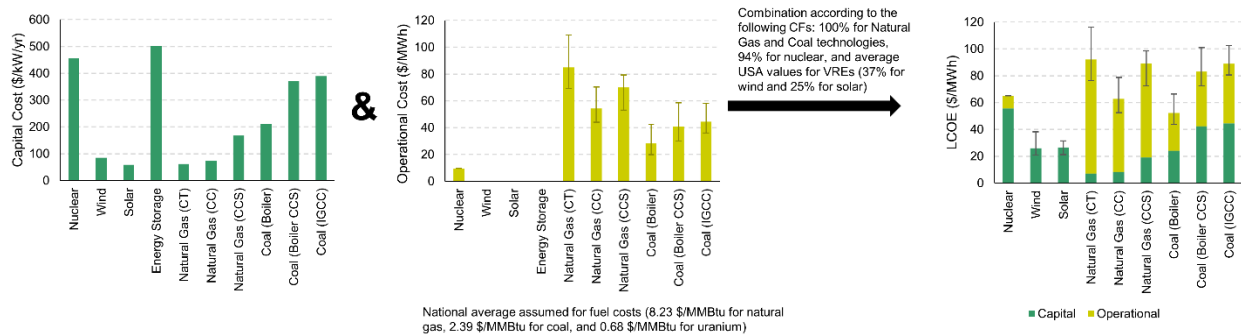


Figure 2-13. Technology specific capital and operational costs

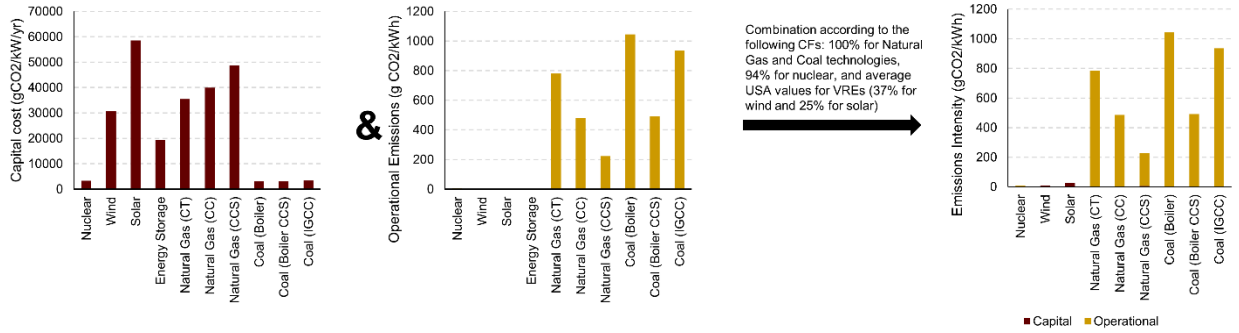


Figure 2-14. Technology specific capital and operational emissions

2.7.3 Effectiveness of carbon taxes

Figure 2-15 shows the impact of a carbon tax on emissions intensity (a), cost (b), and cost before tax (c). This allows the user to understand what portion of electricity price increase is due to switching to more expensive technologies vs. paying taxes.

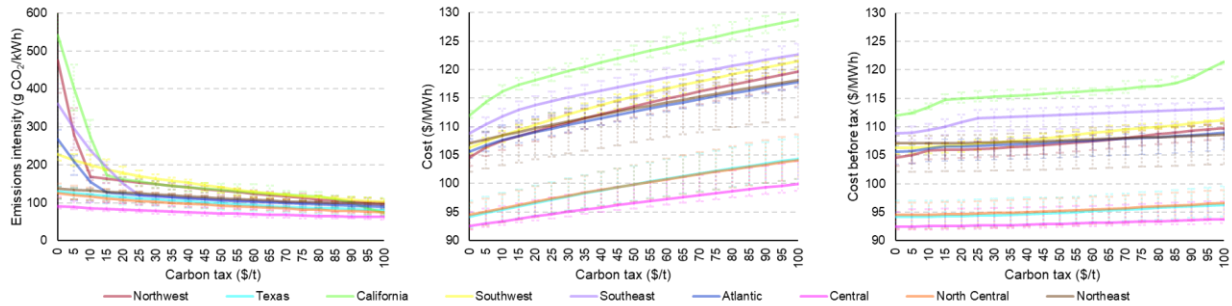


Figure 2-15. Impact of carbon tax on emissions intensity, costs, and costs before subsidies

2.7.4 Equations used in pre-processing values

Equation 2.19 used to convert monthly to hourly LIB efficiency losses [62]:

$$\eta_{EC} = e^{-M/730} \quad (2.19)$$

Equations 2.20 through 2.26 are used to convert CAPEX to capital for all generators (Φ) [58]:

$$WACC_{nominal} = DF * IR * (1 - TR) + (1 - DF) * RROE \quad (2.20)$$

$$WACC = \frac{1 + WACC_{nominal}}{1 + i} - 1 \quad (2.21)$$

$$CRF = \frac{WACC}{1 - \frac{1}{(1 + WACC)^L}} \quad (2.22)$$

$$PVD = \sum_{i=1}^{i=length(FD)} FD_i * f_i \quad (2.23)$$

$$PFF = \frac{1 - TR * PVD * \left(1 - \frac{ITC}{2}\right) - ITC}{1 - TR} \quad (2.24)$$

$$FCR = CRF * PFF \quad (2.25)$$

$$capital = CAPEX * FCR * CFF - PTC * CF * \frac{8760}{1000} \quad (2.26)$$

Where:

DF is debt fraction and = 67% for nuclear, 55% for natural gas and 55% for coal,

IR is nominal interest rate and = 5%,

TR is federal and state tax rate and = 25.7%,

RROE is rate of return on equity and = 10%,

i is inflation rate and = 2.5%,

ITC is investment tax credit and = 0% for all thermal and wind generators and 30% for solar,

PTC is production tax credit and = 0\$/MWh for all thermal and solar generators and 14.4 \$/MW for wind,

CF is annual capacity factor,

WACC is weighted average cost of capital,

CRF is capital recovery factor,

PVD is present value of depreciation,

PPF is project finance factor,

and FCR is fixed charge rate.

2.7.5 PHS CAPEX by region [42]

	California	Southwest	Southeast	Texas	Northeast	Atlantic	Northwest	North	Central	Central
CAPEX (\$/kW)	3221	3417	3846	3910	3481	3458	3312	-	-	3767

2.7.6 Fuel costs [64]

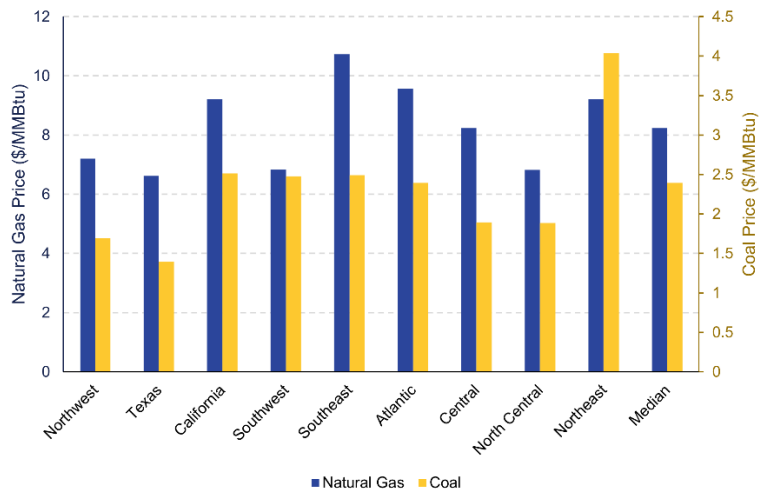


Figure 2-16. Regional natural gas and coal prices

For Natural Gas:

For the selected region, hourly state prices are scaled by hourly percent consumption and summed together to calculate hourly regional values. The median value from the 2019 price vector is selected to reflect pre-pandemic and pre-Russo-Ukrainian War trends.

For Coal:

For the selected region, annual state prices are scaled by annual percent consumption and summed together. 2019 regional values are used to reflect pre-pandemic and pre-Russo-Ukrainian War trends.

Chapter 3. The elephant in the room: embodied emissions in our power sector

3.1 Overview

Inaccurate accounting of greenhouse gas emissions will have detrimental consequences for our planet. Specifically, this Chapter shows that: 1) ignoring embodied emissions in policy and planning will mean never actually reaching carbon neutrality, 2) carbon negative technologies are needed to actually reach net-zero, 3) fair and accurate decarbonization is even harder and more expensive than we are currently estimating. Ignoring embodied emissions is not only neglectful, but also leads to a suboptimal design of a decarbonized power sector. At deep levels of decarbonization, 20 gCO₂-e/kWh, embodied emissions are over 50% of total system emissions. As our grid becomes cleaner, further reducing power sector emissions becomes even more challenging and expensive.

3.2 Introduction

Although the necessary grid transformation is daunting, we have a unique opportunity to build it right. Early and targeted analysis can provide a detailed roadmap to ensure economic viability and system reliability throughout the transition. The importance of comprehensive and accurate grid analysis on all levels cannot be overemphasized.

Currently, the standard, both in modeling and policy, is to only account for operational emissions, and therefore ignore embodied emissions associated with mining materials, manufacturing, transportation of infrastructure, etc. For example, Biden’s existing goal is to achieve a “carbon pollution-free” power sector by 2035 [65]. “Carbon pollution-free” can be translated to mean “without burning fossil fuels.” Figure 3-1 which is an adjusted version of Figure 2-3 built with 2030 cost projections – shows that significant emissions are produced

during infrastructure creation and decommissioning, or outside of operations, for all technologies. While it is clear that solar, wind, hydro, and nuclear are leaps-and-bounds cleaner than fossil-fuel fired generators, this study focuses on the fact that their embodied emissions are nonzero. At deep decarbonization levels, with significant VRE penetration and reduction of fossil fuel consumption, embodied emissions will become the dominant greenhouse gas contributor.

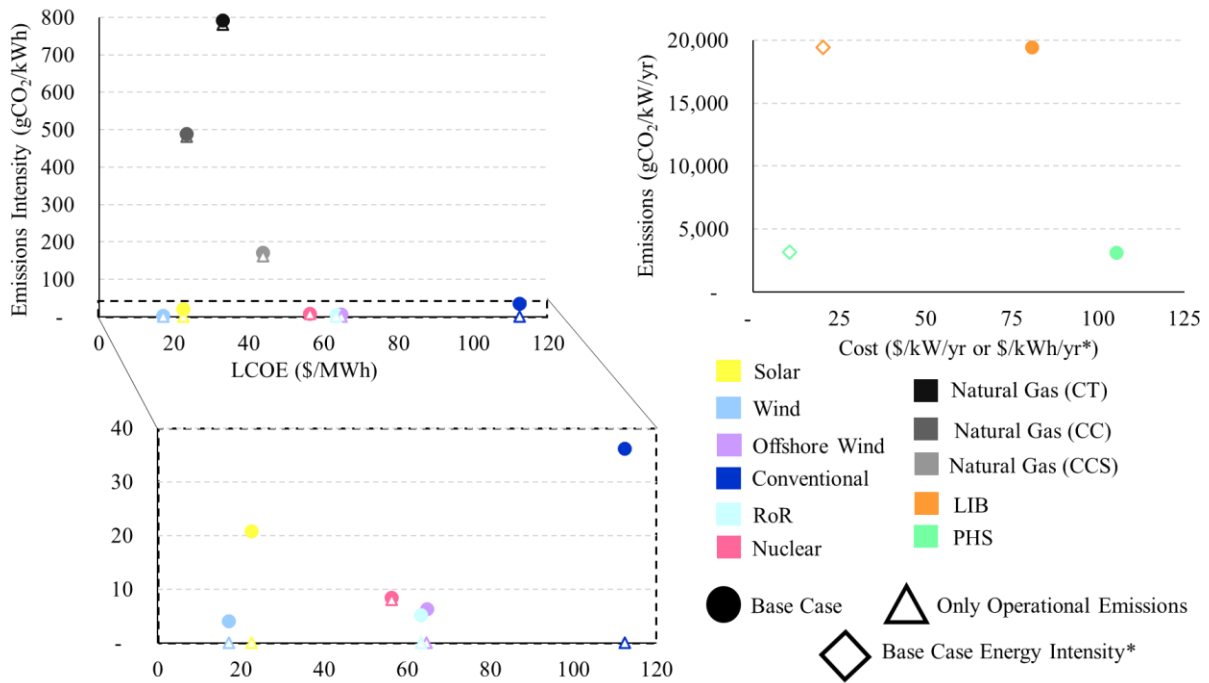


Figure 3-1. LCA emissions vs operational emissions in the cost (2030 projections)-emissions space

Since policy ignores embodied emissions, most grid decarbonization planning tools/analysis do as well, as shown in Table 1-1. Embodied emissions deserve heightened attention to track electricity emissions intensity more accurately, and to achieve the highest reduction of emissions,

from all stages of the life cycle. Ignoring embodied emissions can lead to designing suboptimal decarbonization schemes.

Previous studies have already highlighted a need for more comprehensive emissions tracking in CEM. Byles and Mohagheghi emphasize the added value of holistic emissions analysis to better inform policy [66]. Rauner and Buzinski note the importance of balancing direct (or operational) with indirect (or embodied) emissions [67]. Van De Ven et al. demonstrate that at 80% solar penetration, indirect emissions can reach up to 50 gCO₂-e/kWh [68]. Indirect emissions become comparable with direct at deep decarbonization levels [69]. Accounting for embodied emissions leads to a more accurate and effective decarbonization strategy, but to what degree?

Life-cycle assessment (LCA) is a commonly used method of tracking emissions for a variety of difference current and emerging technologies which allows fair benchmarking and comparisons [70]. This study leverages MIT's Ideal Grid to demonstrate the importance of integrating LCA into CEM [21]. This body of work marks the first of its kind to focus on the importance of incorporating LCA into CEM.

3.3 Methods

3.3.1 Assumptions

Most of the assumptions described in Chapter 2 remain, with only a few adjustments. Most notably, in this analysis, cost values are sourced from the 2023 Annual Technology Baseline, using values projected for 2030 [71]. Similarly, projected 2030 electricity demand was sourced from NREL's Cambium data set [37]. Hourly demand data is available in the North American Electric Reliability Cooperation (NERC) regions, which can be easily aggregated into the regions shown in Figure 2-1. The optimization is conducted for seven consecutive years (2007-

2013). This seven-year timeline is chosen because weather data vary from year to year, and it is important to design a robust system that will satisfy demand for a variety of scenarios. The optimized fleet must satisfy demand during all seven years.

Solar, land-based wind, and offshore wind have capacity limits in each region. NREL’s *Assessment of Offshore Wind Energy Resources for the United States* provides estimates for offshore wind capacity limits [72]. Solar and land-based wind restrictions were obtained from NREL’s *US Renewable Energy Technical Potentials* [73].

The calculations conducted in this experiment were run on MIT’s SuperCloud [74], where each case ran in ~2 minutes.

3.3.2 LCA case study vs. operational emissions case study

As described above, this Chapter explores the differences in optimization between two distinct case studies. The first, more accurate set of case studies conducted consider emissions from all stages of the life cycle, using the below Equation 3.1 to impose a carbon ceiling. This case study is referred to as “LCA,” or “base-case.”

$$\sum_{j=0}^{61,320} \{ \underline{Dunderlined}_j * CAP \} \geq \sum \{ eGC_i * GC_i + e_i * \sum_{j=0}^{61,320} (CF_{j,i} * GC_i) \}, i \in Y \quad (3.1)$$

Note that Equation 3.1 is a slightly more explicit variation of Equation 2.18. Exact emissions values are available in Table 3-2 of the Appendix.

The second, more common set of case studies conducted only consider emissions from the operational phase. In this case, the first term on the right side of Equation 3.1 is set to zero. This is referred to hereafter as “only operational emissions,” or “ignoring embodied emissions.”

3.4 Results and discussion

3.4.1 LCA case results

As is shown in Chapter 2, the US regions require bespoke decarbonization strategies. Figure 3-2 shows the least-cost fleet of generators and energy storage technologies that are required at decreasing carbon ceilings. The diversity of profiles in Figure 3-2 motivates the multi-regional element of this analysis. All systems install large amounts of VRE capacity, but at varying ratios. The Southeast installs over 25 times more solar than wind while the Northwest installs over 3 times more wind than solar. These results are impacted by a variety of characteristics and constraints, such as capacity buildout limitations based on geography and land availability. A comprehensive understanding and investigation of these results provides clarity to the future sections of this Chapter. This is the base-case that “operational emissions only” analyses will be compared to.

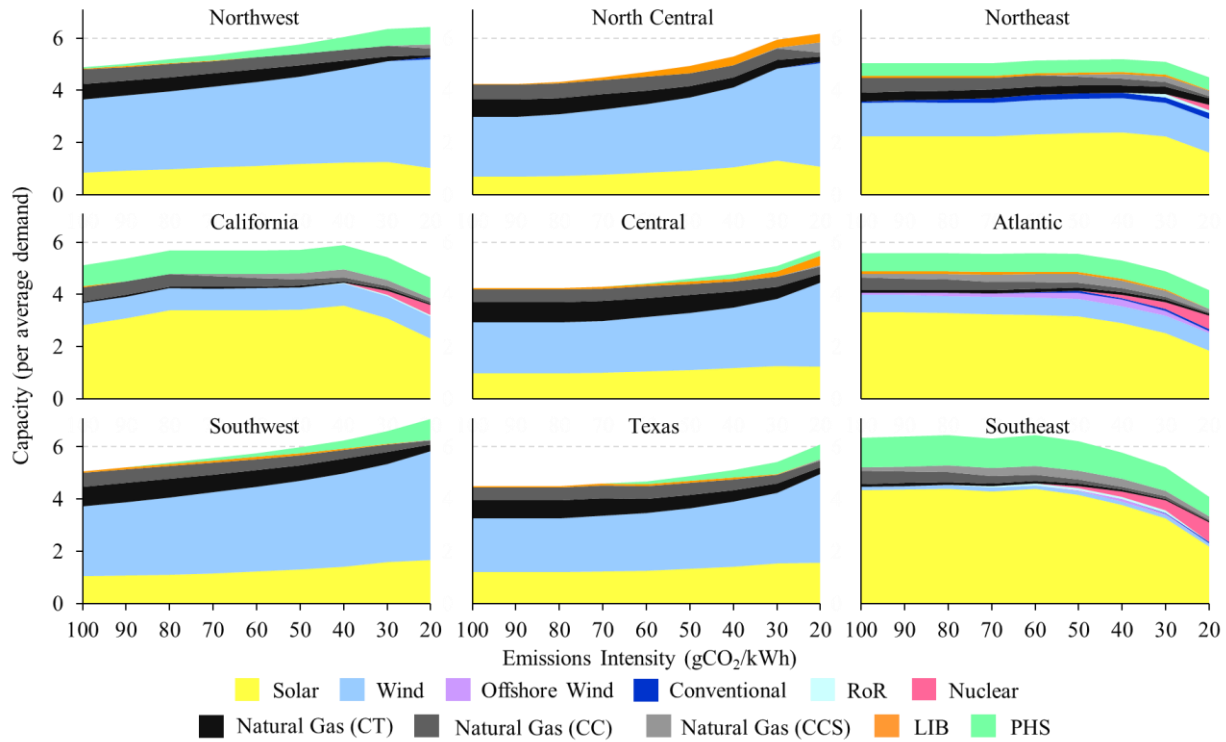


Figure 3-2. Base case system buildout for nine regions, at decreasing carbon ceilings

PHS is the primary energy storage technology because of its lower emissions intensity, as shown in Figure 3-1. In fact, LIBs are only installed in the above results when PHS has reached its regional capacity limit. Atlantic, California, Northeast, and Southeast see a decrease in total system capacity after nuclear is installed, beginning anywhere from 60 to 30 gCO₂-e/kWh, depending on the region. These four regions which rely on nuclear have all reached their land-based wind capacity. Without this constraint, regions rely on nuclear less heavily, proving the importance of accurate capacity limits. All these observations are consistent with Chapter 2’s conclusions.

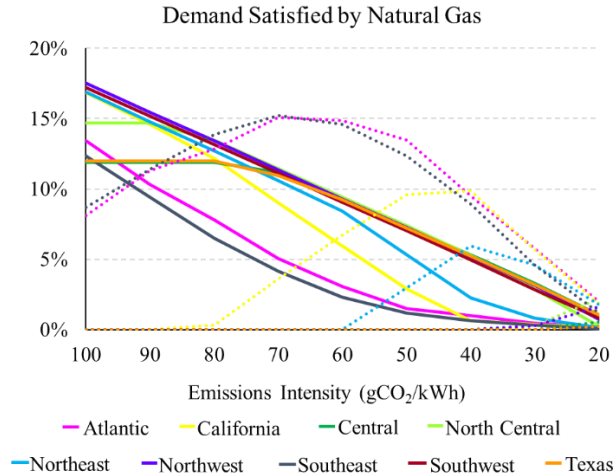


Figure 3-3. Regional operation of natural gas (solid line is a sum of NGCT and NGCC, and dotted line is NGCCS)

Operation of natural gas is a more illuminating trend than installed capacity. Figure 3-3 shows that operation of natural gas without carbon capture (NGCT and NGCC) decreases steadily and monotonically. In contrast, natural gas with carbon capture peaks as an intermediary decarbonization steppingstone, with maximum operation occurring at 50 gCO₂-e/kWh. This is due to the emissions intensity of NGCCS being almost 200 gCO₂-e/kWh.

3.4.2 Ignoring embodied emissions changes generator buildout

As mentioned above, the same analysis is conducted with the common, but inaccurate approximation of ignoring embodied emissions. This is the type of analysis that current policies and decarbonization strategies are based on. Figure 3-4 shows the difference in buildout for three regions: Southeast, Central, and California. Area above the horizontal axis indicates an increase in installed capacity when embodied emissions are ignored, and the opposite is true for area below the horizontal axis. This area shows the error introduced by only accounting for operational emissions. More accurate bookkeeping of emissions leads to different recommended generator buildouts.

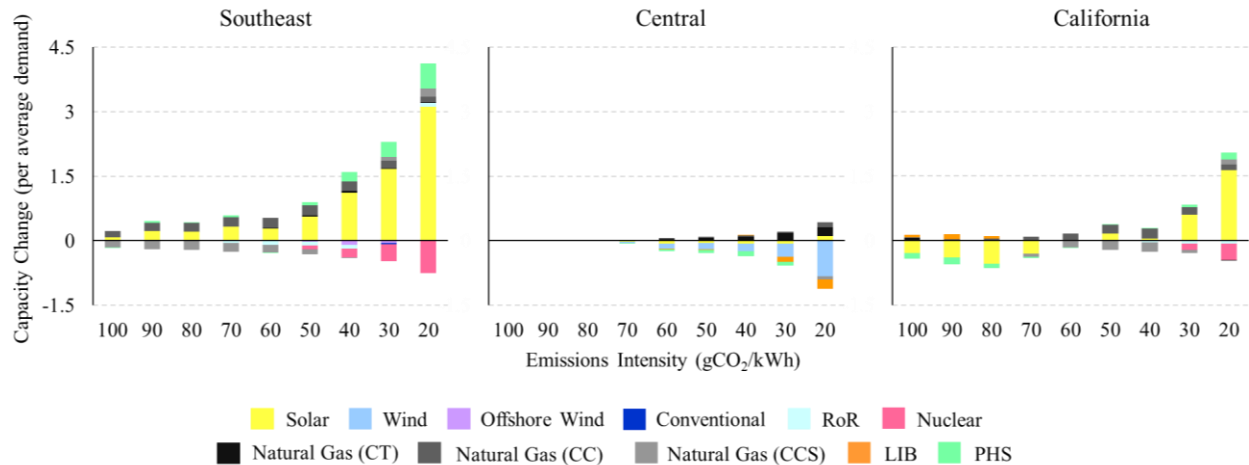


Figure 3-4. Error introduced in capacity buildout by ignoring embodied emissions

Ignoring embodied emissions causes a technological bias of nonuniform magnitude. In general, we observe wider deployment of more emission intensive solar, and less wind and nuclear, albeit to varying degrees, depending on the region. Solar displaces wind because it's ~3 times higher embodied emissions are ignored. Nuclear is reduced because there is more room in the carbon budget for increased renewables and natural gas operation.

The largest magnitude changes in capacity occur in the Southeast. In fact, the solar increase is >50% at 30 and 20 gCO₂-e/kWh emissions intensity. This is a staggering value. Ignoring embodied emissions leads to a doubling of recommended solar installations. These two grid decarbonization strategies are different. Therefore, ignoring embodied emissions leads to a suboptimal grid design.

Conversely, the Central region sees the smallest changes. At 30 and 20 gCO₂-e/kWh, the wind decrease is 12, then 26%, respectively. While these values are smaller in magnitude than the Southeast's, they remain nonnegligible. At high carbon ceilings, there is no difference between the LCA and only operational emissions optimizations. This is because the least-cost system has a lower emissions intensity than the applied constraint. Lastly, it should be noted that some

regions see an unintuitive polytonic change in capacity, such as California’s solar response. Even in systems which are more resilient against introduced error, the changes in decarbonization strategy are too large to be ignored.

Policy makers, companies, and the general public are basing their decisions off inaccurate assumptions. Integrating LCA into CEM changes grid decarbonization optimization. Therefore, to enact the best policies and make the best choices, these groups must stop ignoring embodied emissions.

3.4.3 What amount of emissions are being ignored?

Figure 3-5 shows the comparison of emissions in the base-case vs. when embodied emissions are ignored. When LCA techniques are used, the sum of total system emissions remains below the imposed carbon ceiling. When embodied emissions are ignored, operational emissions grow until they are restricted by the carbon cap, meaning that embodied emissions cause system emissions to exceed the intended target.

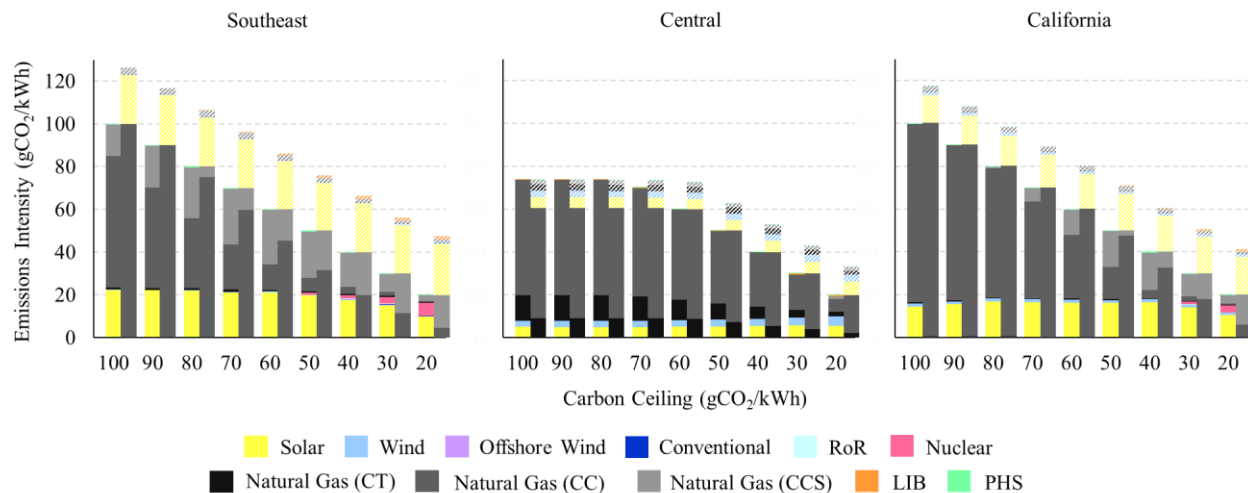


Figure 3-5. Comparison of emissions from LCA (left bar) vs. when embodied emissions are ignored (right bar, with ignored emissions retroactively added on top and represented with stripes)

The fraction of ignored emissions increases as emissions ceiling lowers because 1) VRE penetration increases, and 2) total system emissions decreases. Unaccounted for emissions are highest in the Southeast, starting at 21% and reaching 58% as the carbon ceiling drops from 100 to 20 gCO₂-e/kWh. Conversely, ignored emissions are lowest in the Central region, ranging from 18% to 40% of total. These comparatively lower values are due to the smaller change in capacities and greater reliance on wind, which is less emissions intensive. The total system emissions are equal for the Central region at 100, 90, and 80 gCO₂-e/kWh (after embodied emissions are accounted for) because the least-cost optimization has a lower emissions intensity than the imposed carbon ceiling. Figure 3-5 shows how current accounting methods underestimate the difficulty of decarbonizing.

In fact, the national sum of neglected emissions at 20 gCO₂-e/kWh, add up to 61 MMmt of CO₂ per year, meaning that actual emissions intensity is ~38 gCO₂-e/kWh. This is roughly equivalent to the yearly emissions of more than 13 million cars on the road [75]! Reaching decarbonization targets based on LCA or only operational emissions would be a massive improvement compared to the US's current carbon intensity of ~370 gCO₂-e/kWh. But, since massive reform is required, we are presented with the unique opportunity and responsibility to transform our grid in the most sustainable way possible. Also, it would be harmful and misleading to ignore embodied emissions which comprise almost 50% of power-sector emissions in this particular scenario.

Another important conclusion is that net-zero electricity cannot be reached without significant contribution from negative emission technologies. The two most promising technologies are direct-air capture and bioenergy with carbon capture and storage (BECCS) [76]. There is a wide range of estimated DAC costs, from \$180-1,000/ton-of-CO₂ captured [77]. Also, it has been shown that up to 200 MMmt of CO₂ can be captured via BECCS in Europe [78].

3.4.4 Real decarbonization is more expensive

Since considering all emissions leads to a different, cleaner optimization, the cost must increase, but to what degree?

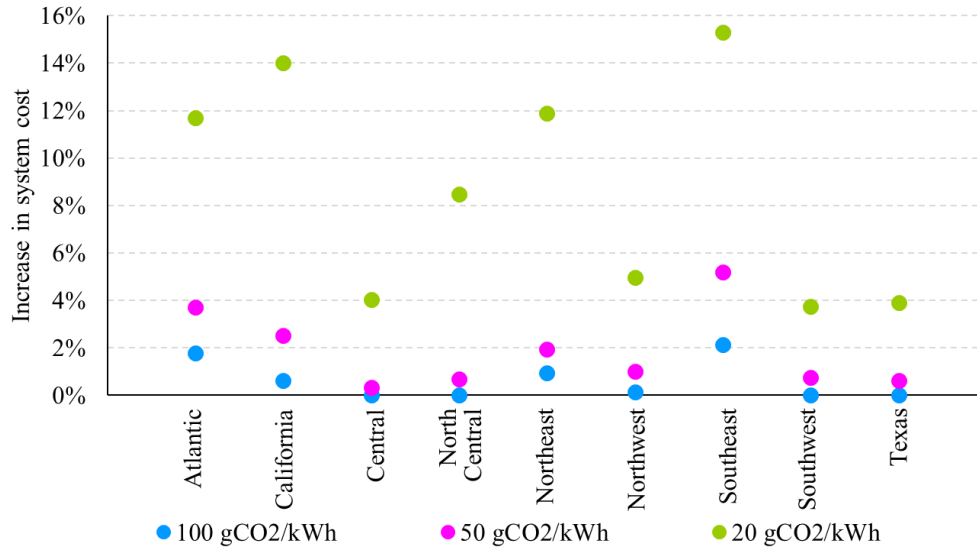


Figure 3-6. Added cost of fairly accounting for embodied emissions

Figure 3-6 shows the increase in cost to reduce all emissions, rather than just operational. As the carbon ceiling tightens, the cost hike increases, which agrees with the trends seen in the above sections because embodied emissions become a larger fraction of total system emissions. The national average cost increases from 0.1 to 0.8 to 7.4 \$/kWh, or a 0.1% to 1% to 8% difference as the carbon ceiling drops from 100 to 50 to 20 gCO₂-e/kWh. At deeper decarbonization levels, marginal carbon abatement costs increase.

The Southeast sees the largest impact on price, reaching a 15% difference at 20 gCO₂-e/kWh. Conversely, Central sees the smallest impact on price, reaching a 4% difference at 20 gCO₂-e/kWh. The bottom line is: it costs more to decarbonize than we are currently predicting.

3.5 Conclusions

Global warming does not distinguish emissions sources. We have a limited carbon budget and the damage of not being honest about emissions will have irreversible consequences. This study marks the first of its kind to highlight the importance of considering embodied emissions. A comprehensive investigation was conducted across nine regions of the US power sector, at a range of carbon ceilings, to understand the impact of this commonplace neglect. First and foremost, it is important to start being precise with our societal terminology. Is our goal to eliminate operational emissions or all emissions from the power sector? To accurately plan for our goals, they need to be understood and defined with accuracy.

Ignoring embodied emissions produced staggeringly different decarbonization strategies, meaning that if we base our policies and decisions off this assumption, we will be evolving our grid to a suboptimal decarbonized design. Ignoring embodied emissions increases reliance on solar because solar has a higher emissions intensity than other low-carbon options. Also, nuclear penetration is decreased, and natural gas adoption is increased. This is because when embodied emissions are ignored, there is more space in the carbon budget for burning fossil fuels. At deeper decarbonization levels, the error introduced increases. This means, as our grid begins to transition, an understanding of the importance of embodied emissions only increases.

Ignoring embodied emissions in policy and planning is counterproductive against reach net-neutrality. Embodied emissions are real with a nonnegligible impact on the system. In fact, in regions that highly favor solar, neglected emissions can reach up to 58% of total system emissions at a carbon ceiling of 20 gCO₂-e/kWh. In regions that highly favor wind, neglected emissions can reach up to 40%. In fact, the national sum of embodied emissions is 61 MMmt CO₂-e annually. At higher carbon ceilings, with lesser VRE penetration, ignored emissions

account for ~20% of total. To be serious about decarbonization targets, these nonnegligible embodied emissions must be accounted for. And, to reach actual carbon neutrality, carbon-negative technologies must be leveraged.

The costs required to decrease all emissions are higher than those required to just decrease operational emissions. In most cases, the more decarbonized our grid becomes, the more difficult and expensive it is to further reduce emissions.

3.6 Appendix

3.6.1 Financial values and equations

Financial values included below are sourced from NREL’ ATB [71].

Table 3-1. Financial values for technologies

	CAPEX (\$/kW)	Fixed Operation Cost (\$/kW/yr)	Variable Operational Cost (\$/MWh)	Fuel cost (\$/MMBtu)	Heat Rate (MMBtu/MWh)	Lifetime (yr)	Interest Rate (%)	Rate of Return on Equity (%)	Debt Fraction (%)	Investment Tax Credit (%)	Production Tax Credit (\$/MWh)	Construction Finance Factor
Abbreviation	OCC	FO M	VO M			L	IR	RRO E	DF	ITC	PTC	CFF
Solar	1,00 2	18	0	0	0	30	7	8.8	45.5	0	25.4 6	1.04
Wind	1,08 3	27	0	0	0	30	7	10	33	0	25.4 6	1.06

Offshore Wind	2,58 1	90	0	0	0	30	7	11	50.7	30	0	1.11
Convention al Hydro	7,32 8	36	0	0	0	100	7	11	48.7	30	0	1.07
RoR Hydro	7,08 2	47	0	0	0	100	7	11	48.7	30	0	1.07
Nuclear	6,11 5	152	2.5	0.65 8	10.4 5	60	8	11	48.9	30	0	1.26
Natural Gas (CT)	939	23	6.4	3.99	9.72	55	8	11	55	0	0	1.12
Natural Gas (CC)	1,03 9	29	1.8	3.99	6.24	55	8	11	55	0	0	1.12
Natural Gas (CCS)	2,01 8	54	4.1	3.99	6.99	55	8	11	55	0	0	1.12
PHS	3,16 6	18.7	0.54	0	0	100	7	11	69.5	30	0	1.07
LIB	1,20 4	30	0	0	0	15	7	8.8	45.5	30	0	1.04

Depreciation Values:

$f_{t,y}$ = depreciation factor for technology, t, in year, y

$FD_{t,y}$ = fraction of capital depreciated for technology, t, in year, y

$f_{solar,y} = [0.9421, 0.8876, 0.8363, 0.7879, 0.7423, 0.6993]$

$FD_{solar,y} = [0.2, 0.32, 0.192, 0.1152, 0.1152, 0.0576]$

$f_{wind,y} = [0.9224, 0.8508, 0.7848, 0.7239, 0.6677, 0.6158]$

$FD_{wind,y} = [0.2, 0.32, 0.192, 0.1152, 0.1152, 0.0576]$

$f_{offw,y} = [0.9363, 0.8766, 0.8208, 0.7685, 0.7195, 0.6736]$

$FD_{offw,y} = [0.2, 0.32, 0.192, 0.1152, 0.1152, 0.0576]$

$f_{conventional,y} = [0.9244, 0.8546, 0.79, 0.7303, 0.6751, 0.6241]$

$FD_{conventional,y} = [0.2, 0.32, 0.192, 0.1152, 0.1152, 0.0576]$

$$f_{RoR,y} = [0.9244, 0.8546, 0.79, 0.7303, 0.6751, 0.6241]$$

$$FD_{RoR,y} = [0.2, 0.32, 0.192, 0.1152, 0.1152, 0.0576]$$

$$f_{NGCT,y} = [0.9499, 0.9023, 0.8571, 0.8142, 0.7734, 0.7346, 0.6978, 0.6629, 0.6297, 0.5981, 0.5682, 0.5397, 0.5127, 0.487, 0.4626, 0.4394]$$

$$FD_{NGCT,y} = [0.05, 0.095, 0.0855, 0.077, 0.0693, 0.0623, 0.059, 0.059, 0.0591, 0.059, 0.0591, 0.059, 0.0591, 0.0295]$$

$$f_{NGCC,y} = [0.9499, 0.9023, 0.8571, 0.8142, 0.7734, 0.7346, 0.6978, 0.6629, 0.6297, 0.5981, 0.5682, 0.5397, 0.5127, 0.487, 0.4626, 0.4394]$$

$$FD_{NGCC,y} = [0.05, 0.095, 0.0855, 0.077, 0.0693, 0.0623, 0.059, 0.059, 0.0591, 0.059, 0.0591, 0.059, 0.0591, 0.0295]$$

$$f_{NGCCS,y} = [0.9499, 0.9023, 0.8571, 0.8142, 0.7734, 0.7346, 0.6978, 0.6629, 0.6297, 0.5981, 0.5682, 0.5397, 0.5127, 0.487, 0.4626, 0.4394]$$

$$FD_{NGCCS,y} = [0.05, 0.095, 0.0855, 0.077, 0.0693, 0.0623, 0.059, 0.059, 0.0591, 0.059, 0.0591, 0.059, 0.0591, 0.0295]$$

$$f_{PHS,y} = [0.9244, 0.8546, 0.79, 0.7303, 0.6751, 0.6241]$$

$$FD_{PHS,y} = [0.2, 0.32, 0.192, 0.1152, 0.1152, 0.0576]$$

$$f_{LIB,y} = [0.9421, 0.8876, 0.8363, 0.7879, 0.7423, 0.6993]$$

$$FD_{LIB,y} = [0.2, 0.32, 0.192, 0.1152, 0.1152, 0.0576]$$

Converting OCC to capital:

Tax rate = 25.7% (TR)

Inflation = 2.5% (i)

Capacity Factor is dependent on region and technology (CF)

$$WACC_{nominal,t} = DF_t * IR_t * (1 - TR_t) + (1 - DF_t) * RROE_t$$

$$WACC_t = (1 + WACC_{nominal,t}) / (1 + i_t) - 1$$

$$CRF_t = WACC_t / (1 - (1 / (1 + WACC_t))^{L_t})$$

$$PVD_t = \text{sum}(FD_{t,i} * f_{t,i}) \text{ for all } i$$

$$PFF_t = (1 - TR_t * PVD_t * (1 - ITC_t / 2) - ITC_t) / (1 - TR_t)$$

$$FCR_t = CRF_t * PFF_t$$

$$CRF_{10yr,t} = WACC_t / (1 - (1 / (1 + WACC_t))^{10})$$

$$PTC_discount_t = PTC_t / (1 - TR_t) * CRF_t / CRF_{10yr,t}$$

$$\text{capital} = OCC_t * FCR_t * CFF_t - PTC_discount_t * CF_t * 8760 / 1000 \text{ [$/kW/yr]}$$

LCOE calculation:

LCOE is not used anywhere in this study, except in Figure 3-1, to orient the reader of the general emissions-cost space.

$$LCOE_t = (\text{capital}_t + FOM_t) * 1000 / 8760 / CF_t + VOM_t + \text{fuelcost}_t * \text{heatrate}_t \text{ [$/MWh]}$$

3.6.2 Emissions values

Emissions values below are sourced from MIT's pathway analysis tool [59].

Table 3-2. Emissions values for all technologies

	Embodied Emissions (gCO ₂ /kW)									Operational Emissions (gCO ₂ /kWh)	
	100	90	80	70	60	50	40	30	20		
Grid Emissions Intensity (gCO ₂ /kWh)											all
Abbreviation	eGC									eOP	
Solar	45,096	44,413	43,730	43,047	42,193	41,509	40,826	40,143	39,459	0	
Wind	13,374	13,238	13,102	12,966	12,830	12,695	12,559	12,423	12,287	0	
Offshore Wind	22,269	22,016	21,763	21,509	21,256	21,003	20,749	20,496	20,243	0	
Conventional Hydro	110,376									0	
RoR Hydro	28,330									0	
Nuclear	3,735									8	
Natural Gas (CT)	32,755									781	
Natural Gas (CC)	39,901									481	
Natural Gas (CCS)	44,334									162	
PHS	3,150									0	
LIB	19,440									0	

LCA calculation:

This LCA calculation is not used anywhere in this study, except in Figure 3-1, to orient the reader of the general emissions-cost space.

$$LCA_t = \text{Embodied_emissions}_t / 8760 / CF_t + \text{operational_emissions}_t$$

Chapter 4. Can fusion help decarbonize US power sector?

4.1 Overview

This chapter examines the potential role of fusion in decarbonizing the U.S. power sector. Fusion penetration is explored under a variety of assumptions in every region in the US to identify specific fusion adoption trends and regional characteristics that dictate these trends. Geothermal and onshore wind capacity limits are the most important factors affecting fusion penetration at an assumed CAPEX of \$8,500/kW. As the assumed fusion CAPEX is lowered, fusion integration is dictated more so by annual wind and solar CFs. This is because at \$3,000-4,000/kW CAPEX, fusion is competitive with VREs even without carbon ceilings. This analysis assumes that nuclear buildout is not allowed. Fusion has a role in the decarbonized US power sector, but to significantly varying degrees depending on region of analysis. Some regions see up to 18% system cost increase when fusion is unavailable, whereas other regions can reach the same decarbonization targets at almost the same price with and without fusion.

4.2 Introduction

Current electricity decarbonization technology options are progressing in promising directions, but still leave important gaps to fill. Solar and wind generation technologies are economically competitive on a levelized cost of electricity basis, but their intrinsic intermittency means that they must be augmented to continuously match supply and demand in the electricity system. This can be accomplished in many ways including storage, transmission, or firm generation resources such as nuclear and hydropower. These add additional costs to the system and can come with siting and permitting issues. Currently, nuclear has a negative public perception as being disproportionately dangerous in comparison to other generator options. Hydropower is dispatchable but is limited based on geography [43]. Carbon capture technologies have the

potential to greatly reduce emissions of natural gas-powered generators, but costs rise with percent of carbon captured, and complete capture is not feasible. Even with all these technological options, there remains a need for a firm, low-carbon electricity source [79]. DAC technologies are still under development, with a lot of uncertainty around commercialized cost [77].

Fusion is a promising, rapidly developing technology which has the potential to fill this firm, low-carbon generation need. Many approaches being pursued today use magnetic or inertial forces to compress fuels into a plasma. In the plasma, two light atomic nuclei react to form a heavier one and release energy. This particular analysis considers the fusing of deuterium and tritium to produce helium, a neutron, and release energy (-17.6 MeV) via magnetic confinement. This particular reaction is chosen because it is the most common fuel-confinement combination. The energy of these neutrons can be converted to heat, which can in turn be converted to electricity via standard thermal power conversion cycles. This power generation technology is carbon neutral with readily available fuel sources. Fusion is also a naturally self-quenching reaction, meaning that there is no risk of uncontrolled reactions [80]. While fusion generator technologies remain under development, there is a significant push towards commercialization within the next 5-10 years. In fact, \$4.8 billion in funding was raised in 2022 by fusion startups [81]. This combination of promising potential and momentum prompts the following investigation of the potential impact of fusion in the power sector.

Since fusion technology is still developing, there have been a limited number of studies investigating fusion's potential for impact on the power sector. Most similar to this study is Schwartz et al.'s article on the value of fusion in the US power sector at net-zero emissions intensity [82]. This research expands on that work as it conducts many more case studies. A 2020

paper shows that fusion is most competitive in countries which do not have alternative renewable energy options, such as Japan, Korea, or Turkey [83]. Nicholas et al. provide a high-level discussion on how fusion fundamentally complements renewables because it provides firm potential [84]. An investigation by the International Atomic Energy Agency shows that fusion will contribute significantly to the world energy market, if successfully introduced [85]. Lastly, Sepulveda et al.'s paper highlights the importance of firm, low-carbon power sources in decreasing electricity price at deep decarbonization levels [86]. Although this analysis is based on nuclear fission, geothermal, and biofuels, the conclusions can also be related to fusion, as it is expected to have similar benefits to the electricity system if successfully commercialized.

Fusion's cost is important to its potential for widespread integration into the power sector. Bustreo et al. analyze fusion's potential in decarbonizing the European power sector, with a focus on identifying capital cost ceilings that fusion must stay below to remain commercially viable in each region [87]. Also, it is shown that fusion can play a big role in the energy transition, but that capital cost and date of commercialization can play a big role in penetration levels [88]. Other research suggests that fusion developers should target markets with high-priced electricity to better compete against renewables [89].

This study is novel and impactful for its focus on understanding regional characteristics that make fusion economically viable or not. This involves comparing a diverse set of case studies conducted on each region to pinpoint key regional factors which determine fusion adoption. Note that all case studies are conducted in the year 2050, well as after expected fusion commercialization.

4.3 Methodology

This section of work builds on what is presented in Chapters 2 and 3, with the below adjustments. The most important assumptions of this Chapter are: 1) neglect of embodied emissions, 2) consideration of current infrastructure, 3) successful introduction of fusion, 4) adjusted calculation of annualized capital costs to reflect regional discrepancies, primarily in land and labor costs, 5) approximation of transmission costs for each technology and distribution costs are approximated for each region, and 6) application of technology-specific regional cost-adjustment factors. Each of these is described and defended below.

4.3.1 Fusion and other new technologies

First and foremost, fusion is a new technology. Since it is still developing, there are a lot of assumptions made about its characteristics. First, its CAPEX is assumed to be \$8,500, as this is roughly a 20% increase from NREL's ATB 2050 nuclear CAPEX projection [71]. This 20% increase is to account for the increased complexity fusion relative to fission at this stage of development. Fusion's FOM is assumed to be 15% of its annualized cost, which comes out to \$94.9/kW/year. Fusion's VOM is calculated to be \$12.2/MWh, assuming \$2/MWh traditional variable costs, and \$10.2/MWh assigned to replacement costs. CF is limited to 85%, but infinite ramping is allowed within hours. The benefits of this ability from pulsed fusion operation is explored by Guazzotto and Freidberg [90].

Geothermal generation and two additional LIB durations (2-hour and 8-hour) are introduced. Costs values are sourced from NREL's 2023 ATB, and capacity restrictions were sourced from NREL's *US Renewable Energy Technical Potentials* [73].

4.3.2 Considering current infrastructure

Based on the installation date and lifetime of current infrastructure, current units which will not have retired in 2050 can be incorporated into the model. Note that these technologies can be retired early to reduce system FOM costs, as shown in the below in Equations 4.1 and 4.2.

$$GCreq_{tech} \leq GC_{tech} \quad \forall tech \in Y \quad (4.1)$$

$$yearlycost = \min \left\{ \begin{array}{l} \sum_{i \in \psi} GC_i * (capital_i + transmission_i) + \\ \sum_{i \in \psi} (GC_i - earlyretires_i) * FOM_i + \\ \sum_{i \in \psi} (VOM_i + fuel\ cost_i * heatrate_i) * total_i + \\ \sum_{i \in \psi} e_{tax} * (eGC_i * GC_i + e_i * total_i) + \\ \sum_{i \in \omega} ecaptured_i * cCCS \end{array} \right\} \quad (4.2)$$

The required installations, $GCreq_{tech}$, relevant to Equation 4.1 are shown in Figure 4-1. Equation 3.3 shows how transmission costs are made to be technology-specific and how early retirements, $earlyretires_{tech}$, can reduce system cost. The values are calculated from data sourced from the EPA's eGRID [91]. Lastly, note that only coal, NGCT, and NGCC are eligible for early retirement.

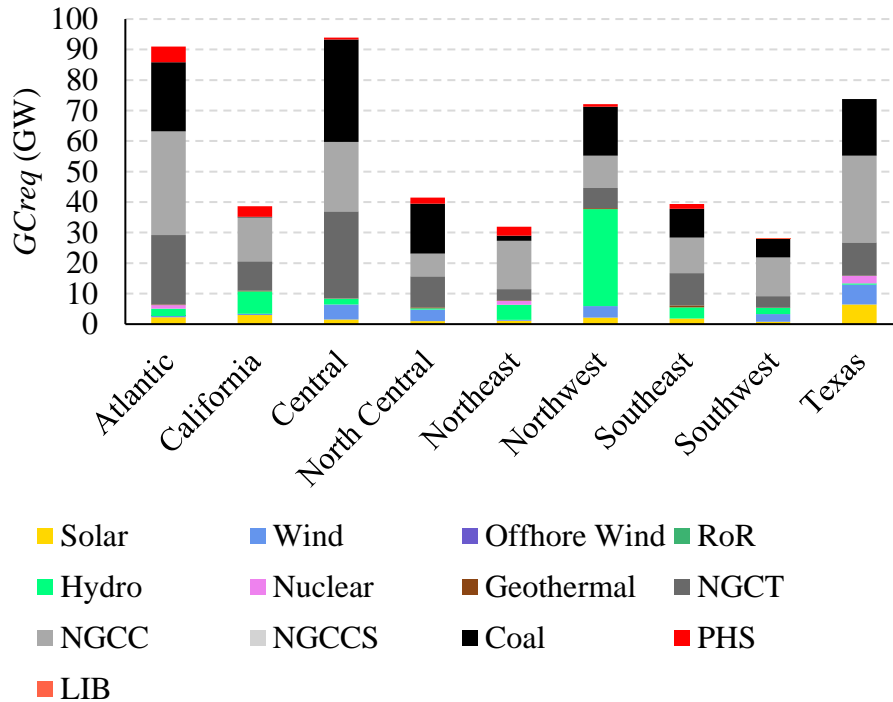


Figure 4-1. Installations required in 2050 because they are already existent, and their retirement dates are after 2050

Current infrastructure is only considered in one case study in this section, while the base-case and majority of results assume greenfield buildout.

4.3.3 Technology-specific transmission costs and region-specific distribution costs

Distribution costs are estimated and projected out in Tables 54.1-54.25 of the EIA's *Annual Energy Outlook 2023* [9]. Distribution costs are provided for regions separated along the NERC boundaries, which coincide conveniently with IG's nine regions of analysis, allowing for easy aggregation of the 2050 projected values. Resultant values are shown in Figure 4-2. Note that distribution costs in the Northeast are over double the cost of any other region.

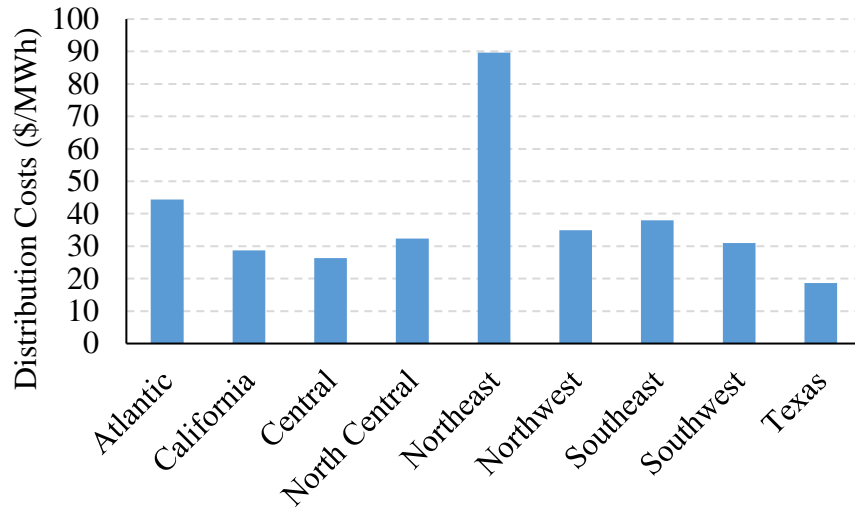


Figure 4-2. Regional distribution costs projections for 2050

Transmission costs are calculated based on a series of publications from Berkley Labs. A series of analyses have been conducted to gain clarity on the interconnection costs of different technologies, in different regions. A study was done in the following territories: New England’s ISO [92], the Southwest Power Pool [93], New York [94], Pennsylvania-New Jersey-Maryland [95], and the Midcontinent Independent System Operator [96]. These reports show that there is significant regional- and technological-variability in interconnection costs. Since this analysis was only conducted for a collection of regions, the other areas are assumed to have costs equal to the national average. Also, no data were available on the cost of offshore wind installations in the Central and North Central regions, so again, the national average is assumed. Note that wind turbine installations in the Great Lakes is also considered to be “offshore.” The resultant values are shown in Figure 4-3.

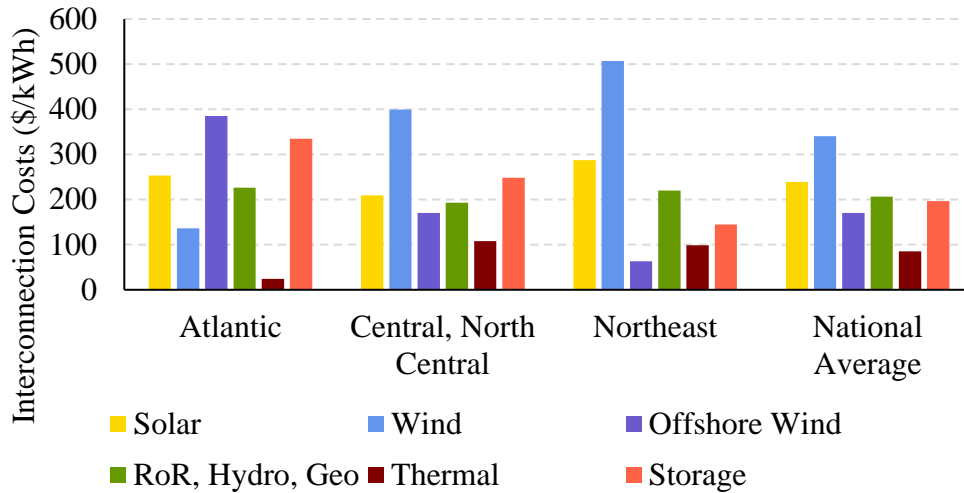


Figure 4-3. Regionally- and technologically- specific interconnection costs

Figure 4-3 shows current interconnection values, but these values are expected to increase by 2050. The EIA’s *Annual Energy Outlook 2023* contains regional estimates for transmissions costs increases. These values are collected and aggregated in the same way that distribution costs were. Note that calculated % increases are applied equally to all technologies. Below, Table 4-1 shows the % price increase of each region by 2050, reaching up to 100% in some regions.

Table 4-1. Projected change in interconnection costs, by region

	Atlantic	California	Central	North Central	Northeast	Northwest	Southeast	Southwest	Texas
2050 interconnection cost increases relative to 2022	30%	103%	52%	50%	75%	105%	64%	27%	93%

4.3.4 Calculating annualized capital cost with CAPEX

All financial values in this chapter are 2050 projections from NREL’s 2023 ATB publication.

Exact values are available in the appendix. Annualized capital costs are calculated with CAPEX,

rather than OCC (as seen in the above Chapters 2 and 3). Equations 4.4 and 4.5 show the exact calculations performed.

$$CRC_{tech} = \frac{df}{1 - (1 + df)^{-L_{tech}}} \quad (4.3)$$

$$capital_{tech} = CRC_{tech} * CAPEX_{tech} \quad (4.4)$$

$$transmission_{tech} = CRC_{tech} * transmissionCAPEX_{tech} \quad (4.5)$$

$$\forall tech \in Y$$

where df is discount factor, assumed to be 0.06 for all technologies. Also, note that the same multiplication is applied to transmission investment values, as shown in Equation 3.6.

4.3.5 No embodied emissions

This Chapter ignores all embodied emissions. This is done to allow for comparison of results from this analysis to similar studies. Note that natural gas combined cycle and combustion turbine are both assumed to emit 352 gCO₂/kWh, natural gas with 95% carbon capture is assumed to emit 38 gCO₂/kWh, and coal is assumed to emit 781 gCO₂/kWh. These are the only considered sources of emissions.

4.3.6 Technology-specific regional cost-adjustment factors

National cost projections that are presented in Table 4-4 are adjusted based on the regional of installation, with values shown in Figure 4-4. Values for all technologies, except PHS are sourced from EIA's Capital Cost and Performance Characteristic Estimates for Utility Scale Electric Power Generating Technologies [97]. These locational adjustments are calculated based on differences in wages, environmental factors (to account for design choices affected by wind,

seismic, snow, and tsunami effects), water availability, and wastewater discharge requirements, among other considerations. These adjustments are applied to the CAPEX, before annualized capital cost is calculated.

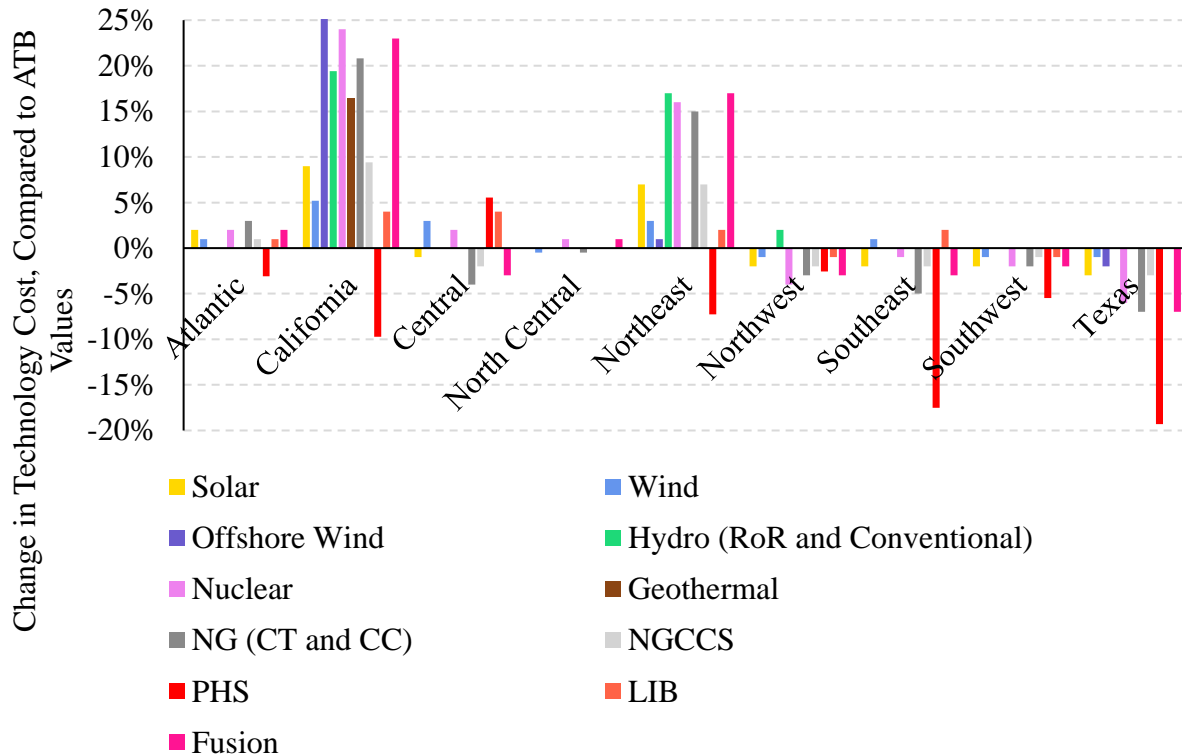


Figure 4-4. Technology-specific regional cost-adjustment factors

PHS values shown in Figure 4-4 are sourced from NREL’s *Closed-Loop Pumped Storage Hydropower Resources Assessment for the US* [42]. This analysis conducted individual assessment of ~15,000 sites for PHS within the US and estimated normalized capital costs at each site. The values shown in Figure 4-4 are a simple percent difference from the national average.

4.4 Results

4.4.1 Base case

First, analysis is conducted with the above base-case assumptions. A range of carbon intensity ceilings (from 20 gCO₂/kWh to 1 gCO₂/kWh) is applied in order lower to evaluate what the decarbonization target must be to incentivize fusion in each region. Figure 4-5 shows that decarbonization schemes vary significantly from region to region. There are many dimensions of variation, but the Southeast and Texas represent extremes in terms of fusion deployment. The Southeast leverages fusion even at the most lenient carbon ceiling (20 gCO₂/kWh) whereas Texas does not integrate fusion until the tightest carbon ceiling (1 gCO₂/kWh). The Northwest is moderate, with fusion integration beginning at ~7 gCO₂/kWh. Note that a version of this figure incorporating all regions is available in the appendix.

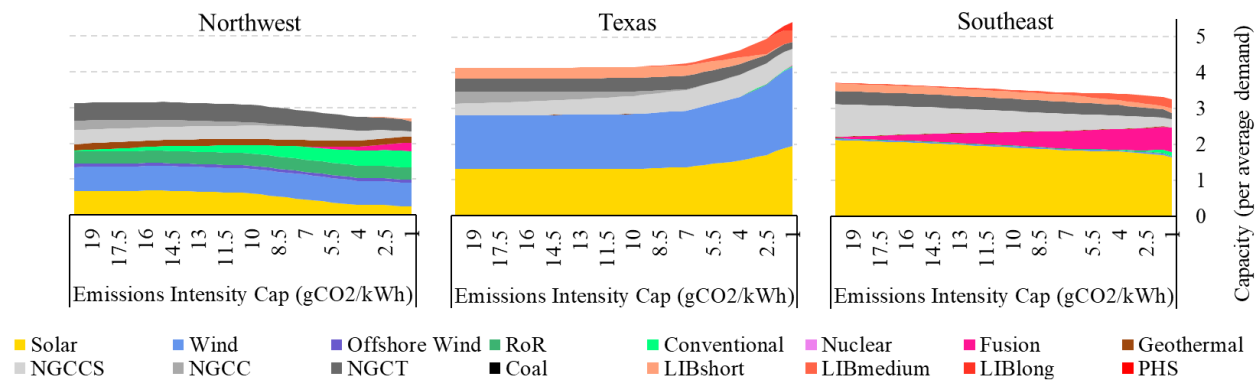


Figure 4-5. Fleet composition required to reach decarbonization targets ranging from 1 to 20 gCO₂/kWh in the Southeast, Northwest, and Texas. See Figure 4-18 for all regions.

Figure 4-5 also highlights that fusion reduces the total fleet size. As fusion penetration increases, total generation capacity is reduced. This is better understood with the context provided in Figure 4-6, which shows relative generation of each technology. Note that in all cases total generation is greater than 1, which is the value for which generation perfectly matches demand. Values greater

than 1 indicate efficiency losses or curtailment. Inefficiencies are considered in transmission as well as charging, discharging, and parasitic losses from energy storage operations.

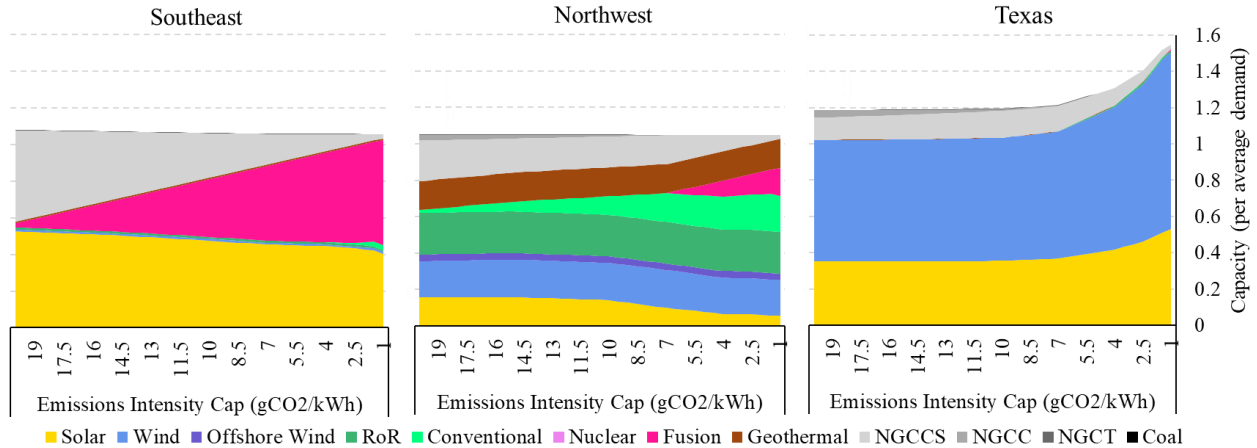


Figure 4-6. Relative generation from all technologies

Fusion supplies a large fraction of demand, compared to its buildout. This is because it operates at a higher capacity factor (CF) in comparison to other generation options. Variable renewable energy (VRE) technologies (solar, wind, offshore wind, RoR, and conventional hydro) are limited based on availabilities. Fossil fueled unit operations are limited based on decarbonization targets. Geothermal and nuclear are the only other firm, carbon-neutral generator options, which also operate at high CFs. In the Southeast, fusion supplies over 50% of electricity at carbon ceilings at or below 2.5 gCO₂/kWh, but accounts for less than 20% of fleet capacity.

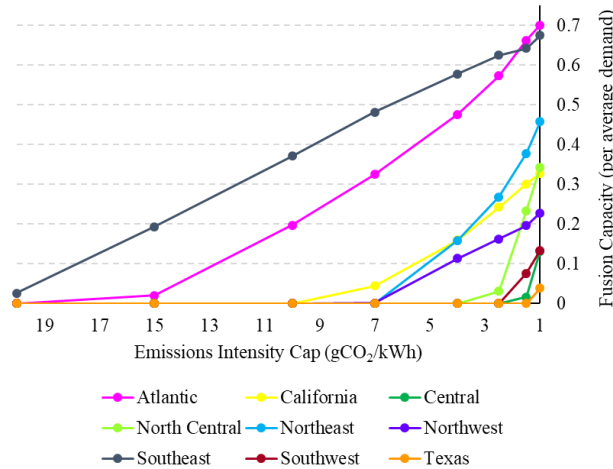


Figure 4-7. Regional fusion integration values, at decreasing carbon caps

Figure 4-7 allows regional fusion deployment to be compared at varying carbon intensities. Fusion increases monotonically in all regions as carbon ceiling decreases, but shape and magnitude of the increase integration varies significantly from region to region. The goal of this chapter is to not only to identify regions within the US that are better suited to fusion integration, but also to understand the motivation of these differences.

4.4.2 The key distinguishing factor: buildout limits

Regions differ in many characteristics, including demand shape, cost adjustment factors, CF curves, but one distinctive regional feature has been identified as most strongly dictating fusion deployment: capacity buildout limits. Below, Table 4-2 shows that buildout constraints are active in the optimization at the emissions intensity when fusion is first introduced. The light-yellow background indicates region-technology combinations which have zero buildout capacity. Also, note that solar and offshore wind limits are never active, and so not included in Table 4-2.

Table 4-2. Buildout constraints which are active when fusion is first integrated (where yellow indicates buildout limit = 0)

	Atlantic	California	Central	North Central	Northeast	Northwest	Southeast	Southwest	Texas
Wind	AT MAX	AT MAX			AT MAX		AT MAX		
RoR	AT MAX	AT MAX	AT MAX	AT MAX	AT MAX	AT MAX	AT MAX	AT MAX	
Conventional	AT MAX		AT MAX	AT MAX	AT MAX			AT MAX	
Geothermal	AT MAX	AT MAX	AT MAX	AT MAX	AT MAX	AT MAX	AT MAX	AT MAX	AT MAX
PHS				AT MAX					

First, geothermal power output is always maxed out before fusion is integrated. This is because these two resources are both dispatchable, low-carbon energy technologies, and so directly compete; and geothermal is less expensive. The regional availability of geothermal ranges from 0-20% of average demand, with exact values available in the appendix. The difference that this makes can be seen when comparing California (which has ~20% geothermal) to the Atlantic (which has no geothermal). All other technological buildout limits are similar, as is verifiable in the appendix. The California fusion integration curve in Figure 4-7 is about 0.2 capacity per demand lower than the Atlantic fusion integration curve. This is primarily due to geothermal availability. Conventional limits have a similar effect, but to a lesser extent because conventional is more expensive than geothermal and has monthly availability constraints.

The four regions which see the earliest and most significant integration of fusion (Atlantic, California, Northeast, and Southeast) have the most stringent wind constraints. In all these regions, if wind buildout is maximized and all curtailment is avoided, wind still cannot produce enough electricity to satisfy one-quarter of demand. Not surprisingly, limiting wind buildout that severely makes fusion necessary at much more lenient emissions caps. Below, Figure 4-8 shows fusion integration when wind limitations are ignored.

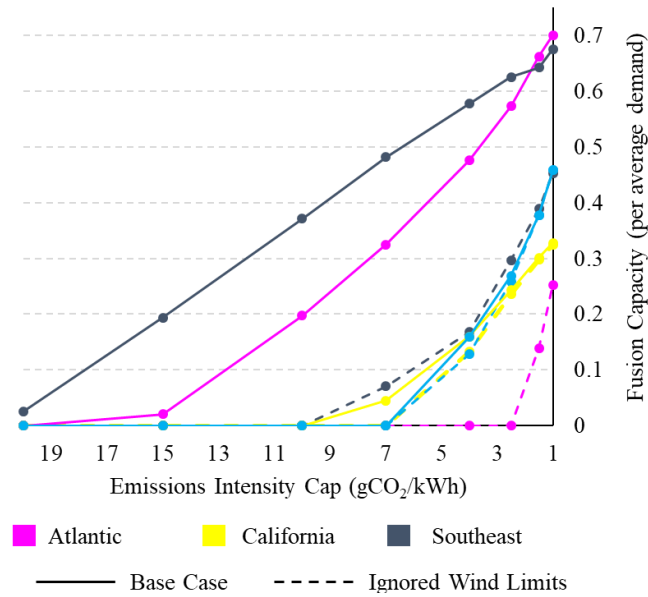


Figure 4-8. Regional fusion integration: base case (solid line), and without wind limitations (dashed lines)

4.4.3 Fusion cost sensitivity analysis

As fusion is a technology which is still under development, there is an obvious uncertainty to all presented results. To explore the potential impact of this unknown, a sensitivity analysis around fusion CAPEX is conducted. Note that since FOM is calculated as 15% of fusion annualized cost, FOM is also being adjusted with CAPEX. Assuming 85% annual CF, the LCOEs for CAPEX's of \$3,000/kW, \$6,000/kW, \$8,500/kW, and \$12,000/kW are \$52/MWh, \$81/MWh, \$110/MWh, and \$150/MWh, respectively.

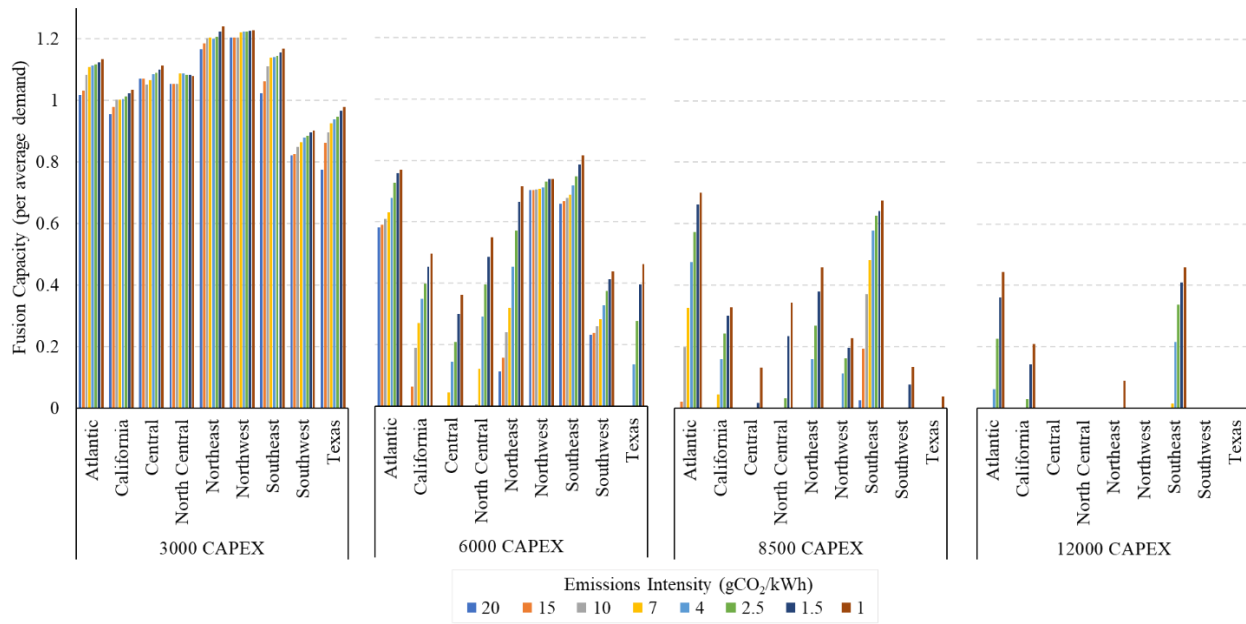


Figure 4-9. Regional fusion buildout, at varying CAPEX values

Figure 4-9 shows how the regional buildout patterns change based on CAPEX. At the lowest CAPEX, \$3,000/kW, buildout is relatively independent of carbon cap. Fusion installations vary by 2% in the most resilient region (the Northwest), and by 23% in the least resilient region (Texas). In general, fusion installations in all regions are equal to average demand +/- 20%. Fusion is supplying most of the electricity. It makes sense that Texas is most sensitive to fusion price because it is the hardest market to penetrate, as other technologies more closely compete on an economic level. In general, bars of similar heights indicate that other technologies are less competitive vs. bars of varying heights means that other technologies are more competitive with fusion.

Table 4-3. Regions with most and least fusion penetration, at varying CAPEX

	CAPEX (\$/kW)			
	3,000	6,000	8,500	12,000
Most Fusion	Northeast	Southeast	Southeast	Southeast
Second Most Fusion	Northwest	Northwest	Atlantic	Atlantic
Least Fusion	Southwest	Central	Texas	Texas, Southwest, Northwest,
Second Least Fusion	Texas	Texas	Central	Central, North Central

As detailed above, fusion adoption is largely determined by regional limitations at \$8,500/kW CAPEX. But regional behavior changes at lower CAPEX values, as is shown in Table 4-3. At lower price points, a different regional characteristic is motivating fusion adoption. Note that “most” and “least” in Table 4-3 are calculated at total fusion adoption at all carbon ceiling caps. At low CAPEX values, amount of fusion is determined, instead, by wind and solar CFs. At such low CFs, the low LCOE of wind and solar becomes less advantageous. Figure 2-5 shows the agreement between the \$3,000/kW CAPEX column in Table 4-3, and annual wind and solar CFs. The Northeast has poor solar resources and only average wind resources. Texas has above average wind and solar resources.

The \$8,500 CAPEX is the base case and therefore discussed in detail in throughout this Chapter. \$6,000/kW is a transitional CAPEX value, showing trends seen in fusion adoption at \$3,000/kW and \$8,500/kW CAPEX values. Lastly, note that Figure 4-9 at 12,000 CAPEX is similar in shape to 8,500, but shifted down by ~0.3 capacity per average demand.

This interesting shift in the determining factor of fusion buildout prompts the question: at what price point is fusion economically competitive without a carbon constraint. IG was optimized with a variety of input CAPEX values, without a carbon constraint, with results shown in Figure 4-10. Fusion must reach \$3,000-4,000/kW to be competitive with a grid of VREs supplemented with fossil-fueled generation.

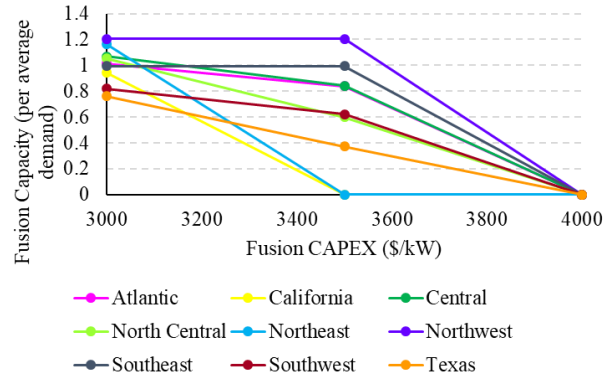


Figure 4-10. Fusion penetration, at varying CAPEX estimates, without an imposed carbon cap

4.4.4 Allow nuclear buildout

The conclusions from the analysis presented thus far in this Chapter hinge on the assumption that nuclear is not allowed in the energy generation mix. Figure 4-11 shows the importance of this assumption. With inclusion of nuclear, the need for fusion decreases drastically. In fact, zero fusion buildout is seen in California, the Northeast, and the Northwest, even at the most stringent carbon constraints. Fusion is drastically decreased in the Atlantic, Southeast, and Southwest regions. Interestingly, fusion impact is not affected in Central, North Central (at only 1.5 gCO₂/kWh), and Texas, as is explored later. The negative impact of nuclear on fusion buildout is due to the favorable CAPEX of nuclear of \$6,668/kW relative to the base case CAPEX for fusion of \$8,500/kWh.

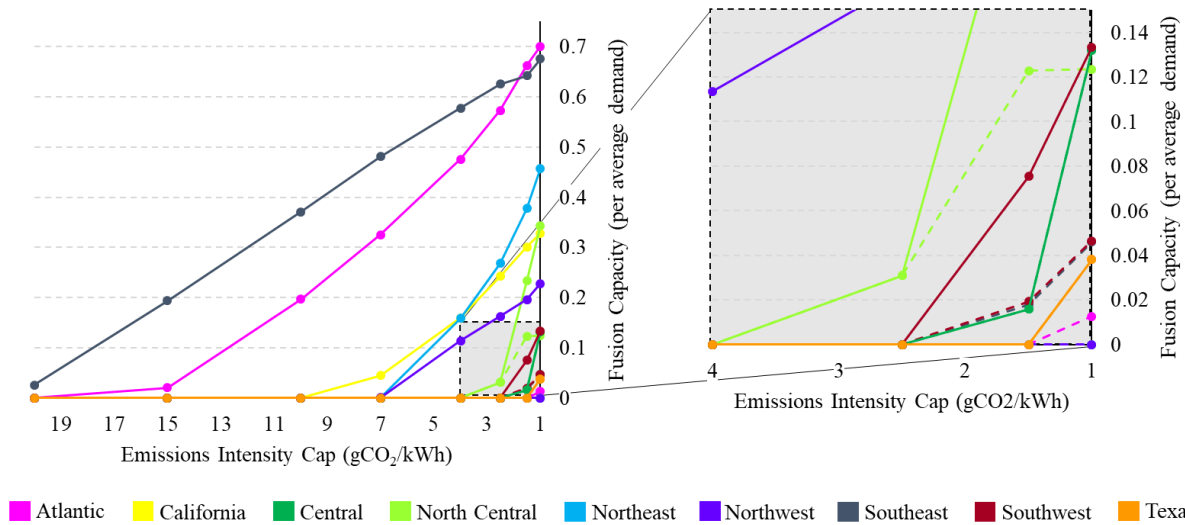


Figure 4-11. Fusion penetration base case (solid lines) vs. when nuclear buildout is allowed (dashed lines)

Nuclear buildout is shown in Figure 4-12. In most regions, nuclear has higher penetration levels than fusion, due to its lower price point, despite its inability to ramp in response to grid conditions. Note that nuclear is modeled as firm, but baseload because that is how it is currently operated in the US. Note that if this changes, results will also change.

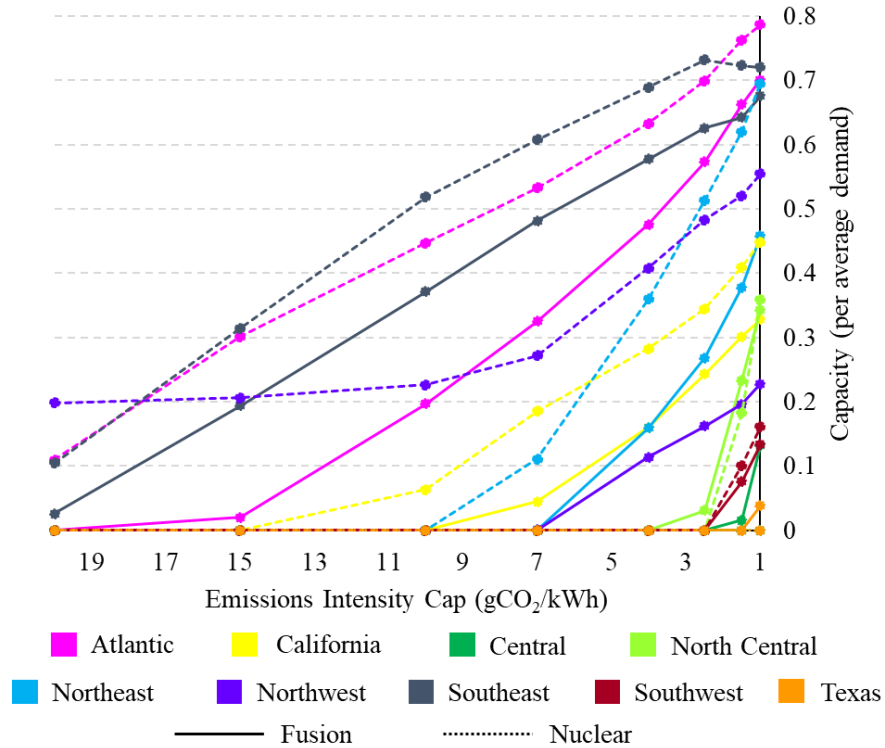


Figure 4-12. Base-case fusion buildout (solid lines) compared to nuclear buildout (dashed lines), when allowed

Regions which did not see a shift in optimization when nuclear was allowed (Central, North Central, and Texas), see no nuclear adoption. These are the three regions with the lowest annual fusion CF, as is apparent in Figure 4-13. This makes sense why nuclear, which is operated at baseload does not compete with fusion. When fusion has a low CF, its dispatchability is being leveraged significantly.

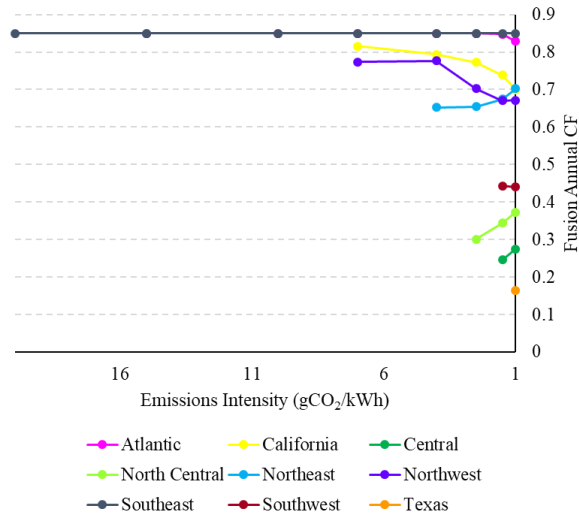


Figure 4-13. Fusion annual CFs for base-case analysis

4.4.5 Restrict fusion to baseload

The above section highlights the importance of fusion’s dispatchability. When fusion is restricted to baseload operations, penetration decreases in all regions, as seen in Figure 4-14. Fusion is not installed in Central, North Central, Southwest, and Texas. These are the regions which operate fusion at the lowest CFs, as discussed in the above subsection, and shown in Figure 4-13.

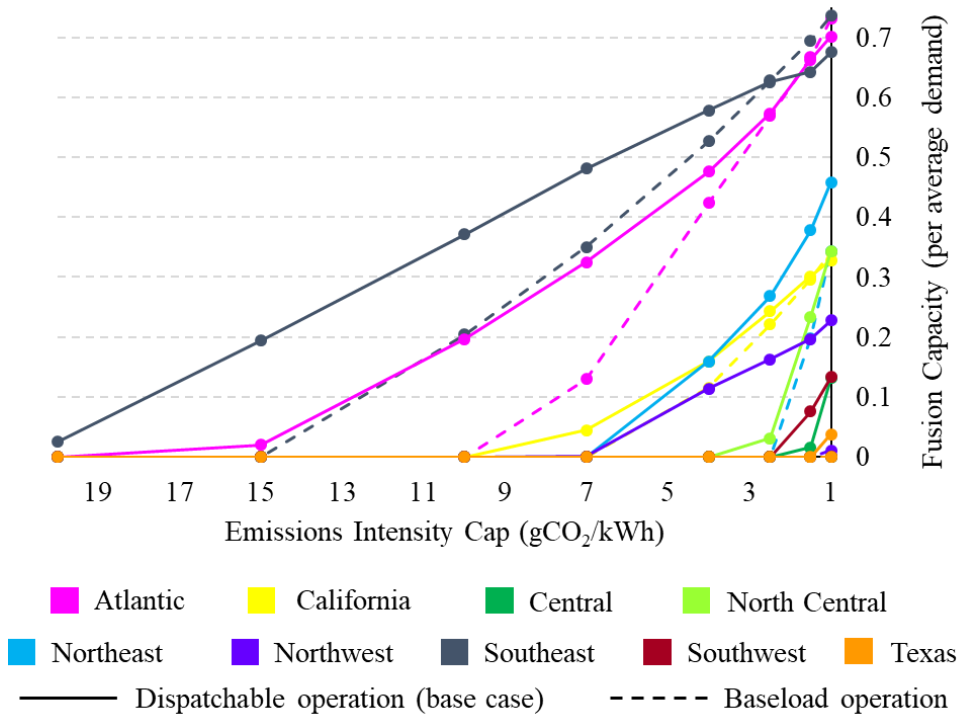


Figure 4-14. Fusion penetration when operated dispatchably (base case – solid lines) vs. restricted to baseload (dashed line)

Lastly, it should be noted that at very low decarbonization caps (1-2.5 gCO₂/kWh), fusion penetration actually increases in the Atlantic and Southeast regions. This is because fusion’s full power output is required during certain system periods with low VRE output, to limit fossil-fuel generation. This interesting behavior only occurs in regions with high fusion penetration because there is more limited buildout of other technologies.

4.4.6 Decarbonization with vs. without fusion

There is a role for fusion to play in a decarbonized grid. To further emphasize this point, the base case scenario is compared to decarbonization without fusion.

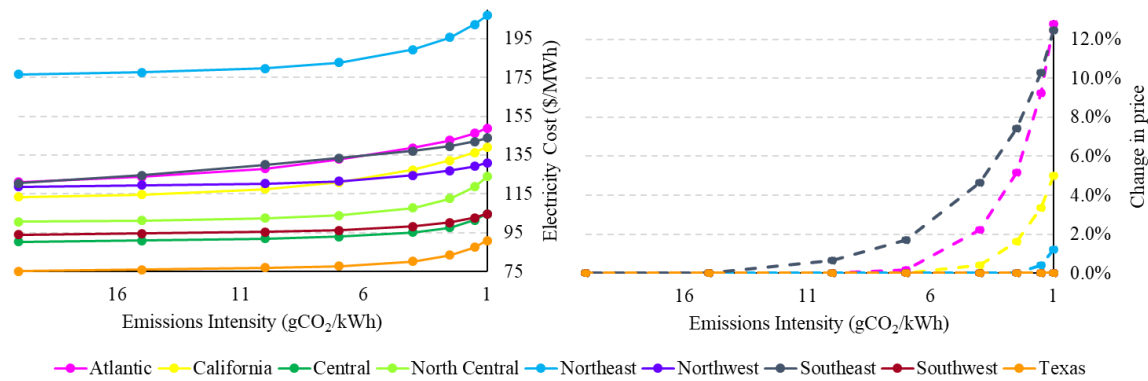


Figure 4-15. Regional electricity costs with economically optimized fusion vs. no fusion

Figure 4-15 shows that reaching deeper decarbonization targets increases electricity cost. It costs anywhere from 10-23% more to reach 1 gCO₂/kWh emissions intensity compared to 20 gCO₂/kWh, depending on region of analysis. The regions that have the highest fusion penetration (Southeast, Atlantic, California, and Northeast) have the highest electricity costs, regardless of decarbonization target. It makes sense that fusion is more competitive in already-expensive markets, making fusion more competitive.

Without fusion, regional electricity costs are even higher at deeper decarbonization targets.

Figure 4-15 shows that fusion reduces regional electricity cost by up to 13% in some regions.

One key factor contributing to this cost reduction is the fact that onshore wind limits are active in all these regions, so offshore wind buildout is required, which significantly impacts system costs.

Conversely, regions with lower fusion adoption (Northwest, North Central, Central, Southwest, and Texas) see nonzero, but negligible impact on price if fusion is not available. These regions have the ability to further build out inexpensive VRE options and are able to avoid installations of more expensive offshore wind.

4.4.7 Considering current capacities

Lastly, the impact of the greenfield assumption is explored. How important is it to consider current infrastructure? Does current infrastructure impact 2050 optimization and if so, is the impact positive or negative relative to cost? Figure 4-16 shows negligible variations in fusion adoption between greenfield analysis and a case in which current infrastructure is considered.

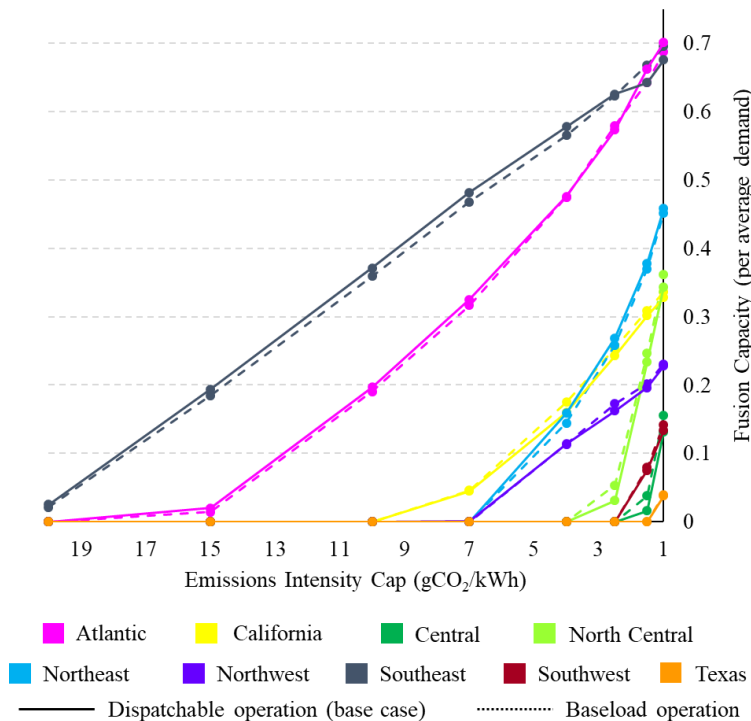


Figure 4-16. Fusion adoption assuming greenfield (base case – solid lines) compared with fusion adoption when current infrastructure is available in 2050 (dashed lines)

Figure 4-17 compares differences in fleet buildout and cost breakdowns between the base case analysis (left) vs. the case considering current infrastructure (right) for the Central region, where annual system cost is normalized by annual demand. Note that the Central region was chosen to represent these trends, but patterns identified here are consistent across all regions. Fossil fuel generation costs are the source of the significant discrepancies between these two scenarios.

Although a significant portion of fossil-fueled generators are retired, and thus do not contribute

to the fleet operations, these resources are assumed to have been financed; and the model requires continued annualized CAPEX payments until resource-specific retirement ages are met.

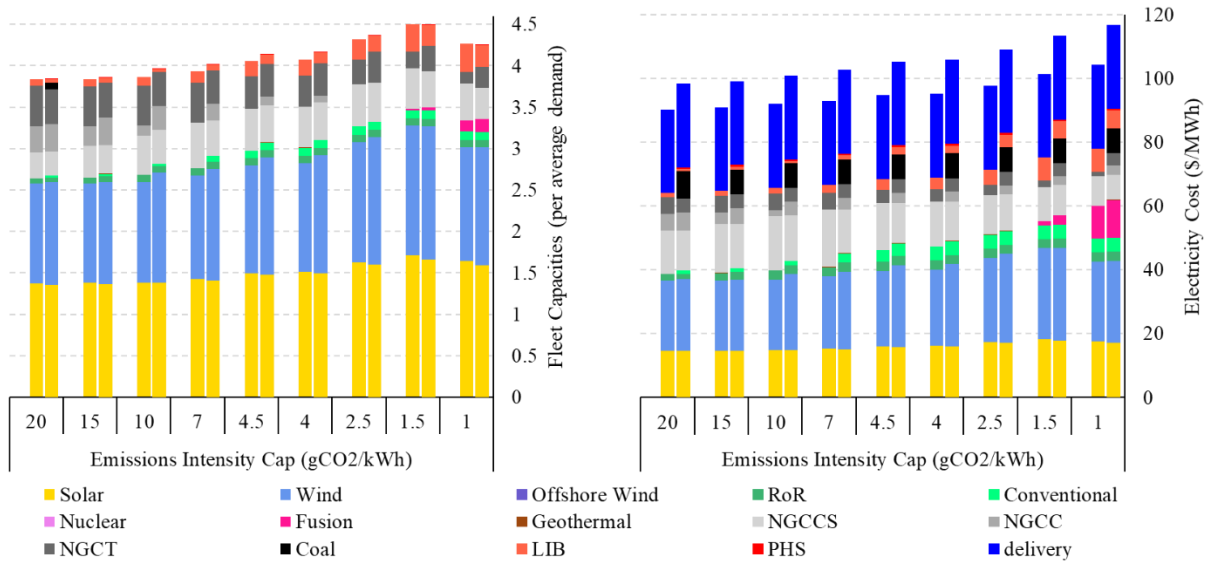


Figure 4-17. Fleet capacity (left figure) and system costs (right figure) breakdown for base case (left bars) vs. analysis which considers current infrastructure (right bars)

There is also a small difference in dispatchable clean energy penetration between these two scenarios, as is clear in Figure 4-17. Conventional and fusion are introduced into the system slightly more when current infrastructure is considered, because this allows for very minimal operations of NG without carbon capture and coal.

4.5 Conclusions

The Ideal Grid (IG) model was used to explore the potential role of fusion in each region of the US, and subsequently identify regional characteristics which make fusion especially competitive or not. There is a role for fusion in all regions, at low enough decarbonization targets, but at significantly different magnitudes. The Southeast introduces fusion even with the most lenient emissions cap imposed, (20 gCO2/kWh). Texas, on the other hand, does not leverage fusion until

the most stringent carbon cap is imposed (1 gCO₂/kWh). Although there are many differences in the represented regions, the constraint which most heavily impacts fusion adoption was identified to be buildout constraints of other generation technologies. Geothermal directly competes with fusion as it is a firm, dispatchable, carbon-free generator. Since geothermal is less expensive, it is always built to its maximum capacity before fusion is integrated into the system. Therefore, greater geothermal resources mean less fusion penetration. The second most important buildout limit is for wind. Regions with limited wind resources lead to earlier and higher fusion penetration.

This Chapter assumes a \$8,500/kW CAPEX for fusion. However, as noted previously there is a significant amount of uncertainty around this number, because fusion is still in early stages of development. A sensitivity analysis is conducted with fusion CAPEX values equal to: \$3,000/kW, \$6,000/kW, \$8,500/kW, and \$12,000/kW. At low CAPEX values, fusion penetration is dictated by annual wind and solar CFs, rather than buildout limits. This is because fusion becomes economically competitive, even without a carbon cap, at CAPEX values ranging from \$3,000-4,000/kW, depending on the region.

The majority of this analysis hinges on the assumption that no nuclear is installed. This is a very important constraint because if fusion buildout is allowed, the space for fusion shrinks significantly. The few regions which retain a small amount of fusion, even when nuclear is available are operating those fusion plants at low CF. The value of fusion over nuclear is found in fusion's dispatchability, compared to nuclear which is operated at baseload. In fact, when fusion is restricted to baseload operations, Central, North Central, Southwest, and Texas regions do not install any fusion, even in the base case where no nuclear is allowed. Operating fusion at baseload decreases penetration in all scenarios compared to the base case, except in the Atlantic

and Southeast regions at deep decarbonization level, which see a slight increase. In these cases, more fusion is installed because the full power capacity of fusion is needed in certain hours when other generating sources are unavailable.

The role of fusion in decarbonizing the power sector depends on the region of analysis. Without fusion, Southeast, Atlantic, California, and Northeast regions see an electricity increase up to 13% to reach deep decarbonization goals. In all other regions, decarbonization is achievable at similar system costs with or without fusion.

4.6 Appendix

Table 4-4. 2050 financial projections

	CAPEX	FOM	VOM	fuelcost	heatrate	Lifetime
	\$/kW	\$/kW/yr	\$/MWh	\$/MMBtu	MMBtu/MWh	years
Solar	632	13	0	0	0	30
Wind	924	23	0	0	0	30
Offwind	2,314	71	0	0	0	30
RoR	4,067	18.7	0	0	0	100
Hydro	5,317	31	0	0	0	100
Geo	5,156	104	0	0	0	30
NGCT	872	20	6.44	7.25	9.72	55
NGCC	985	24	1.61	7.25	6.196	55
NGCCS	1,611	39	3.23	7.25	7.007	55
Nuclear	6,668	152	2.47	0.66	10.45	60
Fusion	8,500	152	12.2	0	0	40

PHS	7,553	47	0	0	0	100
LIB	833	21	0	0	0	15
LIBshort	541	14	0	0	0	15
LIBlong	1,415	35	0	0	0	15
Coal	2,152	72	7.79	2.07	7.09	75

Notes:

- Solar is utility class 9, Wind is class 7, Offshore Wind is class 1, RoR is hydro class NSD 2, hydro is class NPD 5, geo is hydro/flash, NGCC and NGCCS are H-frame, nuclear is AP1000, PHS is class 13, LIB is 4-hour duration, LIBshort is 2-hour duration, and LIBlong is 8-hour duration.

Table 4-5. Regional buildout limits

	Buildout Capacity (GW)								
	Atlantic	California	Central	North Central	Northeast	Northwest	Southeast	Southwest	Texas
Solar	6063	4198	16550	17338	1832	22970	5285	12337	20626
Wind	66	34	682	1223	45	1966	2	503	1902
Offshore wind	318	588	386	620	539	342	60	0	278
RoR	6	3	6	2	4	27	1	1	1
Conventional	6	11	7	2	7	40	6	4	1
Geothermal	0	17	0	0	0	14	0	3	0
PHS	70	324	8	0	17	210	34	554	37

Sources for the values provided in Table 4-5 are included in Section 2.3.3.

Table 4-6. Scaled regional buildout limits

	Buildout Capacity (per average demand)								
	Atlantic	California	Central	North Central	Northeast	Northwest	Southeast	Southwest	Texas
Solar	37.54	51.03	240.68	256.27	31.27	295.54	83.86	306.47	248.42
Wind	0.41	0.41	9.92	18.08	0.77	25.29	0.03	12.50	22.91
Offshore wind	1.97	7.15	5.61	9.17	9.20	4.40	0.96	0.00	3.35
RoR	0.04	0.04	0.09	0.03	0.07	0.34	0.02	0.04	0.02
Conventional	0.04	0.13	0.10	0.03	0.12	0.51	0.10	0.10	0.02
Geothermal	0.00	0.21	0.00	0.00	0.00	0.18	0.00	0.07	0.00
PHS	0.43	3.94	0.12	0.00	0.29	2.70	0.53	13.77	0.45

Values in Table 4-5 were scaled by regional average 2050 demand values estimated by [37] to calculate the normalized values shown in Table 4-6.

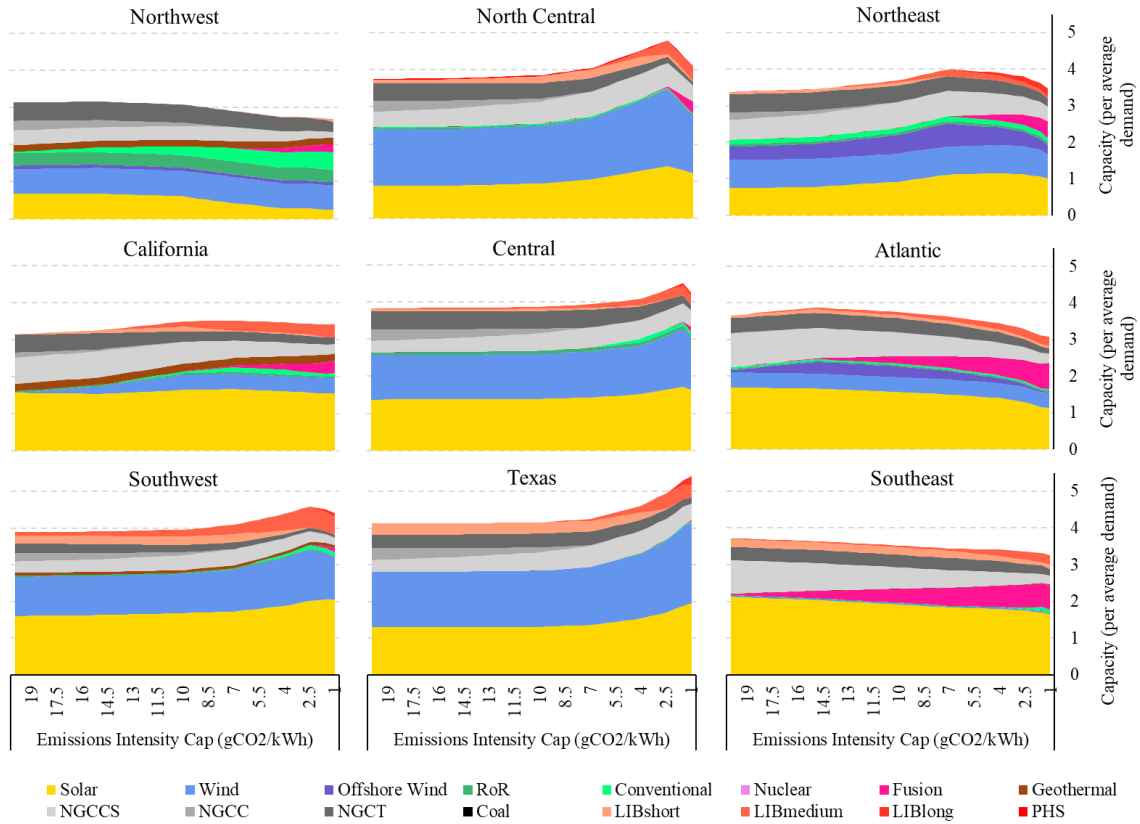


Figure 4-18. Fleet composition required to reach decarbonization targets ranging from 1 to 20 gCO₂/kWh for all nine regions

Chapter 5. Fusion Representation in a Transforming Grid

5.1 Overview

In the above Chapter, it was shown that fusion has the potential to play a nonnegligible role in decarbonizing our power sector, but determining how and when fusion should be adopted requires a new type of analysis. Here, a brownfield model is used to explore what system characteristics most highly dictate fusion adoption. Using the same assumptions, fusion adoption seen in 2050 by Evolving Grid is ~40% less than fusion deployment seen by Ideal Grid. This means that fleet optimization and evolutions before 2050 have a big impact on optimized 2050 grid composition. Many factors impact this result. Decarbonization strategy highly dictates fusion adoption. Decreasing emissions linear, rather than exponentially, decreases fusion penetration by almost 50%. Also, commercialization date impacts fusion adoption. If fusion is commercialized in 2040 rather than 2035, supply chain limitations dictate fusion buildout in 2050, also reducing deployment by almost 50%.

5.2 Introduction

Evolving Grid (EG) is a valuable addition to the currently available CEM arsenal. Its moving optimization allows the user to explore energy transitional questions. This model shows that deployment decisions made today, and over the coming year impact the grid in 2050.

5.2.1 Decarbonization motivation

Many policies and targets are set for 2050, or 2035. While these targets are important, the pathway taken to reach these targets is even more important. In fact, to limit global warming to 1.5°C by 2050, GHG emissions in 2030 must be between 25-30 GtCO₂e/year, but current national pledges target reduction to only 52-58 GtCO₂e/year in 2030 [98]. Global 2030 emissions are projected to be double what they need to be to reach 2050 NZE [98].

Decarbonization measures cannot wait. To keep the possibility of limiting global warming to

1.5°C increase within reach, drastic changes must begin today. We need to find the most cost-effective way to transition our current grid to a cleaner one by 2050, while minimizing cumulative emissions along the way.

5.2.2 Novelty of this EG analysis

This model was specifically designed to understand the potential impact of fusion, so most inputs revolve around fusion-related assumptions. This model explores the impact of a range of commercialization dates, doubling times, learning rates, and 2050 fusion CAPEX values. Note that the base case is commercialization in 2035 (since this is the timeline for most prominent companies [81]), doubling time of 2.26 (assuming that 2035 global capacity of fusion is 1 GW, and 2050 global capacity is 100), learning rate of 10% which is within the wide range seen for all technologies [99], and \$8,500 CAPEX. Also, because of the high importance of quick decarbonization, different cumulative emissions caps are applied in different scenarios.

This analysis marks the first published study which uses a brownfield capacity expansion model to evaluate the potential role of fusion in decarbonization. This section focuses on the importance of variables that limit fleet evolution, like fusion doubling time and commercialization date. Current infrastructure is also represented in the model. In this way, the complexity of the power sector transition is captured.

5.3 Modeling details

5.3.1 Nomenclature

Table 5-1. EG sets

Notation	Description	Unit
----------	-------------	------

<i>year</i>	Years of analysis, ranging from 2020 to 2050, with a 5-year step size	-
<i>N</i>	Number of years optimized per optimization timestep	years
<i>hour</i>	Incremental integer vector from 0 to 8759 * <i>N</i> with a step size of 1 that monitors the number of hours into the selected year	hour
Ψ	All generator types and energy storage types: solar, wind, offshore wind, conventional hydro, run-of-river (RoR) hydro, fusion, nuclear, geothermal (geo), natural gas (3 types), coal, pumped hydro storage (PHS), and lithium-ion battery storage (LIB, 3 durations)	-
Φ	All generator types: solar, wind, offshore wind, conventional hydro, run-of-river (RoR) hydro, fusion, nuclear, geothermal (geo), natural gas (3 types), and coal	-
Υ	Firm, but not dispatchable generating types: nuclear	-
<i>s</i>	Dispatchable, but monthly-constrained generating types: conventional	-
<i>v</i>	Dispatchable generating types: natural gas (3 types), geo, fusion, and coal	-
Ξ	Dispatchable generating types with annual CF limits: geo and fusion	-
Ω	Firm generating types: Υ , <i>s</i> , and <i>v</i>	-
Θ	VRE generating types: solar, wind, offshore wind, and RoR	-

ω	Generators using carbon capture technology: CC natural gas with 90% CCS	-
ζ	Generators technologies eligible for early retirement: NG, CC, NG CT, and coal	-
τ	Energy storage types: LIB (3 types), and PHS	-
χ	Space-limited technologies: solar, wind, offshore wind, RoR, conventional, PHS, and geo	

Table 5-2. 2-D scalar decision variables

Notation	Description	Unit
$GC_{year,Y}$	Generating capacity for each technology, Ψ , at each optimization timestep, <i>year</i>	kW
$GC_{earlyret_{year,install,z}}$	Generating capacity retired early for each eligible technology, ζ , at each optimization timestep, <i>year</i>	kW

Table 5-3. Binary decision variables

Notation	Description	Unit
$fusionexists_{year}$	1 if fusion is eligible to exist (<i>year</i> of analysis is after commercialization date), 0 if not, for each optimization timestep, <i>year</i>	-

Table 5-4. Vector decision variables

Notation	Description	Unit
$VRE2D_{year,hour}$	VRE generated energy sent to demand at every time step, <i>hour</i> , at each optimization timestep, <i>year</i>	kWh
$VRE2C_{year,hour}$	VRE generated energy curtailed at every time step, <i>hour</i> , at each optimization timestep, <i>year</i>	kWh
$VRE2storage_{year,hour,t}$	VRE generated energy sent to storage at every time step, <i>hour</i> , at each optimization timestep, <i>year</i> , for each storage technology	kWh
$firm2D_{year,hour}$	Energy generated by firm resources sent to demand at every time step, <i>hour</i> , at each optimization timestep, <i>year</i>	kWh
$firm2storage_{year,hour,t}$	Energy generated by firm resources sent to storage at every time step, <i>hour</i> , at each optimization timestep, <i>year</i>	kWh
$storage2D_{year,hour,t}$	Energy sent to demand from each storage type, τ , at every time step, <i>hour</i> , at each optimization timestep, <i>year</i>	kWh
$storagelevel_{year,hour,t}$	Energy level for each storage type, τ , at every time step, <i>hour</i> , at each optimization time step, <i>year</i>	kWh

<i>firmoutput</i> _{year, hour, W}	Energy generated by each firm generator type, Ω , at every time step, <i>hour</i> , at each optimization timestep, <i>year</i>	kWh
--	---	-----

Table 5-5. User inputs

Notation	Description	Unit
<i>hightechlearningrate</i>	Learning rate for fusion-specific costs	%
<i>learningrateappliedto</i>	Percent of total unit cost that is considered to be fusion-specific	%
<i>fusionCAPEX</i>	Fusion CAPEX in 2050	\$/kW
<i>emissionsintensitytarget</i>	Emissions intensity target for 2050	gCO ₂ /kW
<i>cumulativeconstraint</i>	Shape of emissions intensity decrease (exponential or linear)	-
<i>commercial</i>	First <i>year</i> that fusion buildout is allowed	-
<i>cfprofilestyle</i>	Selection method for VRE profiles selected (<i>all</i> , <i>high_and_low</i> , or <i>low_and_low</i>)	-
<i>doublingtime</i>	Years required to double fusion's manufacturing capacities	-

Table 5-6. EG parameters

Notation	Description	Value	Unit
-----------------	--------------------	--------------	-------------

$CF_{Q,hour}$	CF at every time step <i>hour</i> for each VRE technology, Θ	*	1
CF_Y	Hourly CF for base generators, Y	*	1
CF_X	Annual CF for base generators, Y	*	1
$CF_{month,s}$	Monthly CFs for monthly-constrained generators, s	*	1
$demand_{year,hour}$	Scaled demand at every time step <i>hour</i> , at each optimization timestep, <i>year</i>	*	kW
$TDlosses$	Fraction of generated electricity that is lost due to transmission and distribution inefficiencies	0.95 [100]	1
$CAPEX_{year,Y}$	CAPEX for each technology, Y, at each optimization timestep, <i>year</i>	*	\$/kW
$transmission_{year,Y}$	Transmission cost for each technology, Y, at each optimization timestep, <i>year</i>	*	\$/kW
$FOM_{year,Y}$	Fixed operating cost for each technology, Y, at each installation timestep, <i>year</i>	*	\$/kWh/year
$VOM_{year,Y}$	Variable operating cost for each technology (including carbon capture and storage where	*	\$/kWh

	applicable), Y, at each installation timestep, <i>year</i>		
$fuelcost_{year,Y}$	Fuel cost for each technology, Y, at each installation timestep, <i>year</i>	*	\$/MMBtu
$heatrate_{year,Y}$	Heat rate for each technology, Y, at each installation timestep, <i>year</i>	*	MMBtu/kWh
$egen_{year,Y}$	Emissions per electricity generated for each technology, Y, at each installation timestep, <i>year</i>	*	gCO ₂ -e/kWh
η_t	Efficiency of charging and discharging energy for each energy storage type	*	1
$\eta_{hourly,t}$	Hourly efficiency for each energy storage type	*	1
L_Y	Lifetime of each technology	*	Years
$stepsize$	Years between optimizations	5	years
$limit_\chi$	Maximum buildout of a region for each space-limited technology, χ	*	kW
$GCinst_{year,tech}$	Installations that already exist	*	kW
$GCret_{year,tech}$	Required retirements of already-existent infrastructure.	*	kW
$duration_\tau$	Energy capacity per power capacity of each storage technology, τ	*	kWh/kW

*variable, with more information available in the appendix

5.3.2 Building the objective function

The objective function is a linear combination of capacity-related costs and operations-related costs, as can be seen below in Equation 5.1.

$$\min \left\{ \begin{aligned} & \sum_{tech \in \Psi} \sum_{analysis \in year} \sum_{install \in year} (capital_{install,tech} + transmission_{install,tech}) * existing_{install,analysis,tech} + \\ & \sum_{tech \in \Psi} \sum_{analysis \in year} \sum_{install \in year} FOM_{install,tech} * tracking_{install,analysis,tech} + \\ & \sum_{tech \in \Omega} \sum_{analysis \in year} (VOM_{analysis,tech} + heatrate_{analysis,tech} * fuel\ cost_{analysis,tech}) * \frac{\sum_{hours \in hour} firmoutput_{analysis,hours,tech}}{N} \end{aligned} \right\} \quad (5.1)$$

The first component tracks annualized capital investments for all *existing* units. Note that existing units include generators that have been retired early because financed costs are still expected to be repaid. Capital investments are broken into two technology-specific categories: *capital* which is all infrastructure on the facility site needed to delivery electricity to the grid, and *transmission*, which is an estimate of transmission network extensions and upgrades needed to integrate a new generation unit. The second component accounts for fixed operations and maintenance costs for generation units that are function, or not retired. This exclusion of generators that are retired incentivizes early retirements of generation units that are not being used. The last component accounts for all variable operations costs. Note that carbon compression, transportation and storage costs are included in the VOM, when applicable. Also note that the fuel costs are region-specific.

Since the analysis above analysis depends on the year that infrastructure was installed, this is tracked in the tracking data frame, which is defined below, in Table 5-7.

Table 5-7. Tracking dataframe for LIB

		Install Year				
		2020	2025	2030	...	2050
Year of Analysis	2020	$GCinst_{2020,LIB}$	0	0	...	0
	2025	$GCinst_{2020,LIB}$ – $GCret_{2020:2025,LIB}$ – $GCearlyret_{2020,2025,LIB}$	$GCinst_{2025,LIB}$ + $GC_{2025,LIB}$	0	...	0
	2030	$GCinst_{2020,LIB}$ – $GCret_{2020:2030,LIB}$ – $GCearlyret_{2020,2030,LIB}$	$GCinst_{2025,LIB}$ + $GC_{2025,LIB}$ – $GCearlyret_{2025,2030,LIB}$	$GC_{2030,LIB}$...	0
	2035	$GCinst_{2020,LIB}$ – $GCret_{2020:2035,LIB}$ – $GCearlyret_{2020,2035,LIB}$	$GCinst_{2025,LIB}$ + $GC_{2025,LIB}$ – $GCearlyret_{2025,2035,LIB}$	$GC_{2030,LIB}$ – $GCearlyret_{2030,2035,LIB}$...	0
	2040	0	$GCinst_{2025,LIB}$ + $GC_{2025,LIB}$ – $GCearlyret_{2025,2040,LIB}$	$GC_{2030,LIB}$ – $GCearlyret_{2030,2040,LIB}$...	0
	2045	0	0	$GC_{2030,LIB}$ – $GCearlyret_{2030,2045,LIB}$...	0
	2050	0	0	0	...	$GC_{2050,LIB}$

$GCinst$ accounts for infrastructure already built in each region. Note that anything built after 2020 is considered to be installed in 2025, and anything built before 2020 is considered installed in 2020, but with a shortened lifetime, depending on installation year. $GCret$ is used to track the required retirements each year of current infrastructure. This system ensure that older infrastructure is forced to retire at the end of its lifetime.

Note that Table 5-7 includes many interesting patterns due to LIB’s short lifetime, such as its banded nature with large regions of scarcity. Below, Table 5-8 shows how patterns change with longer-lived technologies, such as geo.

Table 5-8. Tracking dataframe for geo

		Install Year				
		2020	2025	2030	...	2050
Year of Analysis	2020	$GCinst_{2020,geo}$	0	0	...	0
	2025	$GCinst_{2020,geo}$ – $GCret_{2020:2025,geo}$ – $GCearlyret_{2020,2025,geo}$	$GCinst_{2025,geo}$ + $GC_{2025,geo}$	0	...	0
	2030	$GCinst_{2020,geo}$ – $GCret_{2020:2030,geo}$ – $GCearlyret_{2020,2030,geo}$	$GCinst_{2025,geo}$ + $GC_{2025,geo}$ – $GCearlyret_{2025,2030,geo}$	$GC_{2030,geo}$...	0
	2035	$GCinst_{2020,geo}$ – $GCret_{2020:2035,geo}$ – $GCearlyret_{2020,2035,geo}$	$GCinst_{2025,geo}$ + $GC_{2025,geo}$ – $GCearlyret_{2025,2035,geo}$	$GC_{2030,geo}$ – $GCearlyret_{2030,2035,geo}$...	0
	2040	$GCinst_{2020,geo}$ – $GCret_{2020:2040,geo}$ – $GCearlyret_{2020,2040,geo}$	$GCinst_{2025,geo}$ + $GC_{2025,geo}$ – $GCearlyret_{2025,2040,geo}$	$GC_{2030,geo}$ – $GCearlyret_{2030,2040,geo}$...	0
	2045	$GCinst_{2020,geo}$ – $GCret_{2020:2045,geo}$ – $GCearlyret_{2020,2045,geo}$	$GCinst_{2025,geo}$ + $GC_{2025,geo}$ – $GCearlyret_{2025,2045,geo}$	$GC_{2030,geo}$ – $GCearlyret_{2030,2045,geo}$...	0
	2050	$GCinst_{2020,geo}$ – $GCret_{2020:2050,geo}$ – $GCearlyret_{2020,2050,geo}$	$GCinst_{2025,geo}$ + $GC_{2025,geo}$ – $GCearlyret_{2025,2050,geo}$	$GC_{2030,geo}$ – $GCearlyret_{2030,2045,geo}$...	$GC_{2050,geo}$

The *existing* dataframe is almost identical to the *tracking* dataframe for all technologies. The only difference is that *existing* does not record early retirements. For example, existing for geo would be Table 5-8, but without the subtractions of $GCearlyret_{installyear,yearofanalysis,geo}$ whenever applicable.

5.3.3 Hourly constraints

The imposed constraints can be categorized into two groups: hourly and annually. This section explored the hourly energy flow and behavior of the model. First, Equations 3.7 through 3.9 track the flow of energy through the available pathways, based on how the electricity is generated, and short storage options are available. Equation 3.7 ensures that demand is satisfied for every *hour* of every *year*, either directly from generation (VRE and firm) or from storage reserves. Equation 3.8 calculates all firm generation at every *hour* of every *year* and allows it to flow to demand or any of the available storage resources. Note that *TDlosses* are applied at this initial step of generation accounting, and therefore *TDlosses* do not depend on electricity pathway. Similarly, Equation 3.9 calculated VRE-generated electricity at every *hour* of every *year* and allows it to flow to demand, storage or be curtailed, with *TDlosses* applied in the same way as Equation 3.8. Notice that VRE-generated electricity can be curtailed, but firm generation cannot.

$$\begin{aligned}
 & firm2D_{years,hours} + VRE2D_{years,hours} + \sum_{tech \in \tau} storage2D_{years,hours,tech} * \eta_{years,tech} \\
 & = demand_{years,hours}
 \end{aligned} \tag{3.7}$$

$$\forall hours \in hour \wedge years \in year$$

$$\sum_{tech \in \Omega} firmoutput_{years,hours,tech} * TDlosses = firm2D_{years,hours} + firm2storage_{years,hours} \tag{3.8}$$

$$\begin{aligned}
& \forall \text{ hours} \in \text{hour} \wedge \text{ years} \in \text{year} \\
& \sum_{\text{tech} \in \Theta} CF_{\text{years}, \text{hours}, \text{tech}} * \text{tracking}_{\text{years}, \text{hour}, \text{tech}} * TDlosses = \\
& VRE2D_{\text{years}, \text{hours}} + VRE2C_{\text{years}, \text{hours}} + \sum_{\text{tech} \in \tau} VRE2storage_{\text{years}, \text{hours}, \text{tech}}
\end{aligned} \tag{3.9}$$

$$\forall \text{ hours} \in \text{hour} \wedge \text{ years} \in \text{year}$$

Equation 3.10 limits all firm output to stay below available capacity for every *hour* of every *year*. To increase generation potential, the model must size-up its resources.

$$\text{firmoutput}_{\text{years}, \text{hours}, \text{tech}} \leq \text{tracking}_{\text{years}, \text{tech}} \tag{3.10}$$

$$\forall \text{ hours} \in \text{hour} \wedge \text{ years} \in \text{year} \wedge \text{ tech} \in W$$

Equations 3.11 through 3.13 restrict energy storage operations to be within the parameters of each technology. Equation 3.11 is used to size each storage technology, ensuring that the energy level is limited to the installed energy capacity of each storage technology. Equations 3.12 and 3.13 limit the power capacity of energy storage. Note that these limits are applied before inefficiencies are accounted for. Also note that Equations 3.12 and 3.13 assume that charging and discharging power capacity is symmetric for all storage technologies. Equation 3.14 monitors that energy level of each technology. Energy level is dependent of energy level of the previous *hour* plus all electricity sent to storage in that *hour* minus any electricity sent to demand in that *hour*. Because of this historical dependence, Equation 3.14 is not applied to the first *hour*, 0.

$$\text{storagelevel}_{\text{years}, \text{hours}, \text{tech}} \leq \text{tracking}_{\text{years}, \text{hours}, \text{tech}} * \text{duration}_{\tau} \tag{3.11}$$

$$\forall \text{ hours} \in \text{hour} \wedge \text{ years} \in \text{year} \wedge \text{ tech} \in t$$

$$\text{firm2storage}_{\text{year}, \text{hours}, \text{tech}} + VRE2storage_{\text{year}, \text{hours}, \text{tech}} \leq \text{tracking}_{\text{years}, \text{tech}} \tag{3.12}$$

$$\forall \text{ hours} \in \text{hour} \wedge \text{ years} \in \text{year} \wedge \text{ tech} \in \text{t}$$

$$\text{storage2D}_{\text{years,hours,tech}} \leq \text{tracking}_{\text{years,tech}} \quad (3.13)$$

$$\forall \text{ hours} \in \text{hour} \wedge \text{ years} \in \text{year} \wedge \text{ tech} \in \text{t}$$

$$\text{storagelevel}_{\text{years,hours,tech}} = \text{storagelevel}_{\text{years,hours-1,tech}} * \eta_{\text{hourly}}_{\text{years,tech}} + (\text{VRE2storage} + \text{firm2storage}) * \eta_{\text{year,tech}} - \text{storage2D}_{\text{years,hours,tech}} \quad (3.14)$$

$$\forall \text{ hours} \in \text{hour} \setminus 0 \wedge \text{ years} \in \text{year} \wedge \text{ tech} \in \text{t}$$

Some firm generation types are limited by more than just their capacity. Equation 3.15 applies to baseload generation technologies which are restricted from any and all ramping. Equation 3.16 limits monthly CFs for relevant technologies. And Equation 3.17 limits annual CFs for relevant technologies

$$\text{firmoutput}_{\text{years,hours,tech}} = \text{CF}_{\text{tech}} \quad (3.15)$$

$$\forall \text{ hours} \in \text{hour} \wedge \text{ years} \in \text{year} \wedge \text{ tech} \in \text{Y}$$

$$\text{CF}_{\text{month,tech}} = \sum_{\text{hours=firstinmonth}}^{\text{hours=lastinmonth}} \text{firmoutput}_{\text{years,hours,tech}} \quad (3.16)$$

$$\forall \text{ month} \in \text{jan, feb ... dec} \wedge \text{ years} \in \text{year} \wedge \text{ tech} \in \text{s}$$

$$\text{CF}_{\text{tech}} \leq \frac{\sum_{\text{hours} \in \text{hour}} \text{firmoutput}_{\text{years,hours,tech}}}{\text{tracking}_{\text{years,tech}} * N * 8760} \quad (3.17)$$

$$\forall \text{ years} \in \text{year} \wedge \text{ tech} \in \text{X}$$

5.3.4 Annual constraints

The second group of constraints is applied on an annual basis. Equation 3.18 restricts model-optimized capacity buildouts in the year 2020. The capacities of each region are predefined based on historically collected data. Capacity expansion is not allowed until 2025, because this is

the first optimized year in the future. Equation 3.19 restricts nuclear buildout. Current nuclear units are operated until their retirement age, but no new nuclear can be added to the fleet.

$$GC_{2020,tech} = 0 \quad (3.18)$$

$$\forall tech \in \Phi$$

$$GC_{years,nuclear} = 0 \quad (3.19)$$

$$\forall years \in year$$

The next collection of equations constrains fusion buildout. Equation 3.20 restricts fusion buildout before it is commercially available. Equation 3.21 repackages the information in the *fusionexists* binary variable to be cleaner for the later constraints. Consequently, *turnedon* is also binary. Put simply, *turnedon* is 1 on the *year* that fusion is installed and is 0 for all other *years*. This is important because Equation 3.22 constrains the first year of fusion to be one power plant, which is assumed to be 350 MW. There are some multiplication factors because the optimization is scaled down considerably to reduce computational time. Finally, Equation 3.23 limits fusion installations based on the user-input *doublingtime*. Installations every year after the first year of fusion adoption are restricted based on the installations of the previous year.

$$GC_{years,fusion} = 0 \quad (3.20)$$

$$\forall years < commercial$$

$$turnedon_{years} = \begin{cases} 0 & \text{if } years < commercial \\ fusionexists_{years} - fusionexists_{years[-1]} & \text{if } years \geq commercial \end{cases} \quad (3.21)$$

$$350*1000 / multiplier * turnedon_{years} == GC_{years,fusion} * turnedon_{years} \quad (3.22)$$

$$\forall years \in year$$

$$GC_{years, fusion} * (1 - turnedon_{years}) \leq GC_{years, fusion} * 2^{stepsizel doublingtime} * (1 - turnedon_{years}) \quad (3.23)$$

$$\forall years \in year$$

Equation 3.24 ensures that relevant capacities remain below their regionally-specific limit.

$$tracking_{years, tech} \leq limit_{tech} \quad (3.24)$$

$$\forall years \in year \wedge tech \in c$$

And finally, Equation 3.25 limits annual emissions intensity. Note that a strict limit is applied every optimization year, without any allowance of emissions banking. This is an emissions intensity target rather than a raw emissions release limit, so allowed emissions depend on demand growth. The annual *emissionsintensity* is calculated with an extrapolation from current regional emissions intensity, included below in Figure 5-1, to user-input *emissionsintensitytarget*. This extrapolation can be done linearly (with *emissionsintensity* = *m*year+b*) or exponentially (with *emissionsintensity* = *a*b^{year}*), based on the user-selected *cumulativeconstraint* shape.

$$\sum_{hours \in hour} \sum_{tech \in v} firmoutput_{years, hours, tech} \leq emissionsintensity_{years} * \sum_{hours \in hour} demand_{hours, years} \quad (3.25)$$

$$\forall years \in year$$

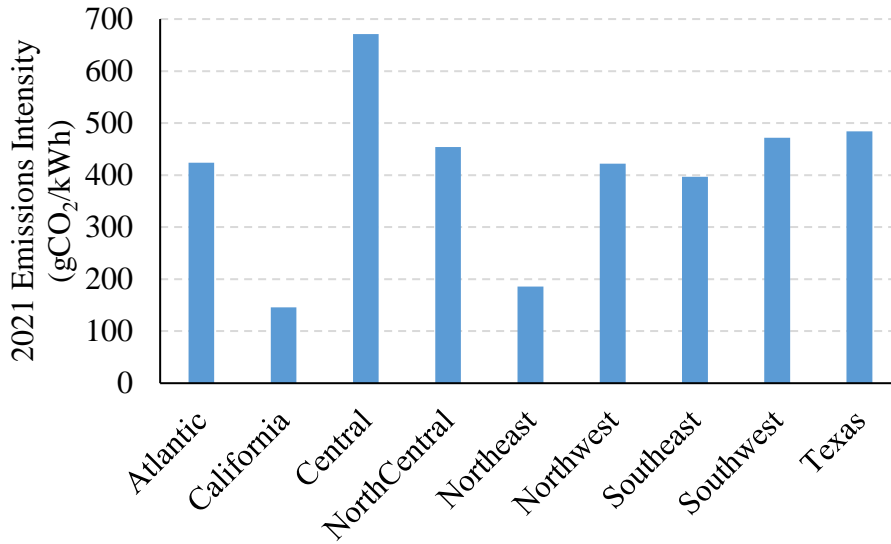


Figure 5-1. Current regional emissions intensities [101]

Figure 5-2 shows that differences in emissions reduction schemes. Note the stark discrepancies in reduction strategy based on both 1) 2021 emissions intensity per region, and 2) *cumulativeconstraint* shape. Since exponential reduction leads to much lower cumulative emissions sums, the entirety of analysis in this Chapter is imposed using an exponential *cumulativeconstraint*.

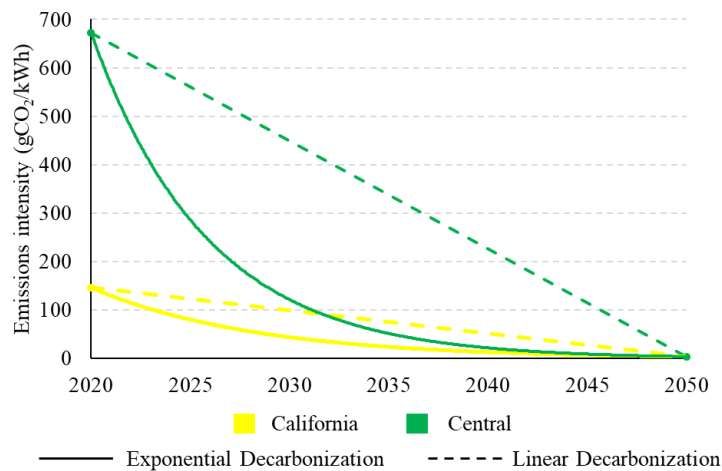


Figure 5-2. Emissions intensity constraint trend comparison between regions and reduction strategies: exponential (base case – line) and linear (dashed)

5.4 Results

5.4.1 Base case analysis

First, fusion adoption is modeled, given the aforementioned base case assumptions. Figure 5-3 shows the fleet buildout and generation results of this analysis. Note that units that are retired early are still included in the fleet capacity, but are not present in the generation graph as they are dormant. Carbon-free electricity sources steadily increase from year to year, and there are no new installations of fossil-fueled generation without carbon capture. Lastly, note that although there are 3 types of LIB being modeled, they are aggregated and displayed as one category for concision.

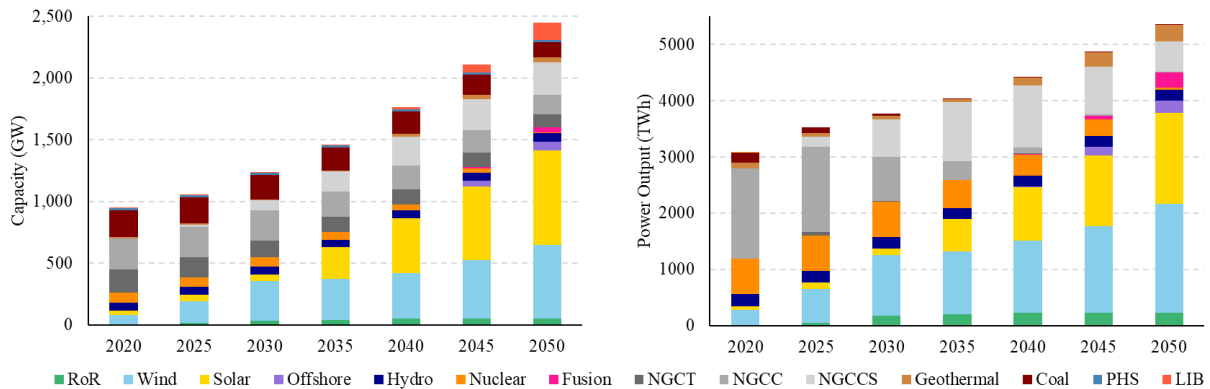


Figure 5-3. National capacities (left) and generation (right), from 2020 to 2050

In this scenario, fusion composes ~1.7% of the grid capacity by 2050, and supplies ~5.2% of demand. Note that buildout only occurs in the Atlantic and Southeast regions, as seen in Figure 5-4, which are the regions which saw the largest need for fusion in Chapter 4. Buildout begins in 2035, the year of fusion commercialization, and installments are limited by the estimated doubling rate.

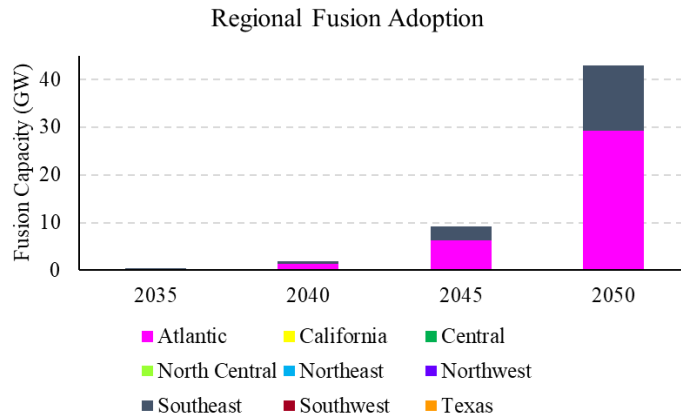


Figure 5-4. Base case regional fusion buildout

The results of this analysis are starkly different from what is presented in Chapter 4. Calculated from values shown in Figure 4-7, greenfield analysis shows that 100 GW of fusion is the optimal national buildout in 2050, given a 4 gCO₂/kWh carbon cap. This is about twice as much as seen in Figure 5-4. There are many added complexities in brownfield analysis that introduce deviations from Chapter 4’s results. The below sections explore the different constraint dimensions to best understand what evolving constraints most heavily motivate these discrepancies.

National costs and emissions values are also postprocessed and shown below. The costs associated with these high decarbonization schemes are relatively palatable, with electricity system costs rising from ~\$152/MWh in 2020 to \$175/MWh in 2050, to achieve a reduction from 212 gCO₂/kWh in 2020 to 4 gCO₂/kWh in 2050. Note that costs and emissions values for 2020 are not historical data, but rather an optimization of 2020’s infrastructure given the model’s framework and assumptions. Note that coal units still comprise a nonnegligible fraction of costs even in later years of optimization when they are retired because of inactivity. This is because their finance payments on CAPEX values must be paid until the end of their lifetime, regardless of whether the units are retired or not.

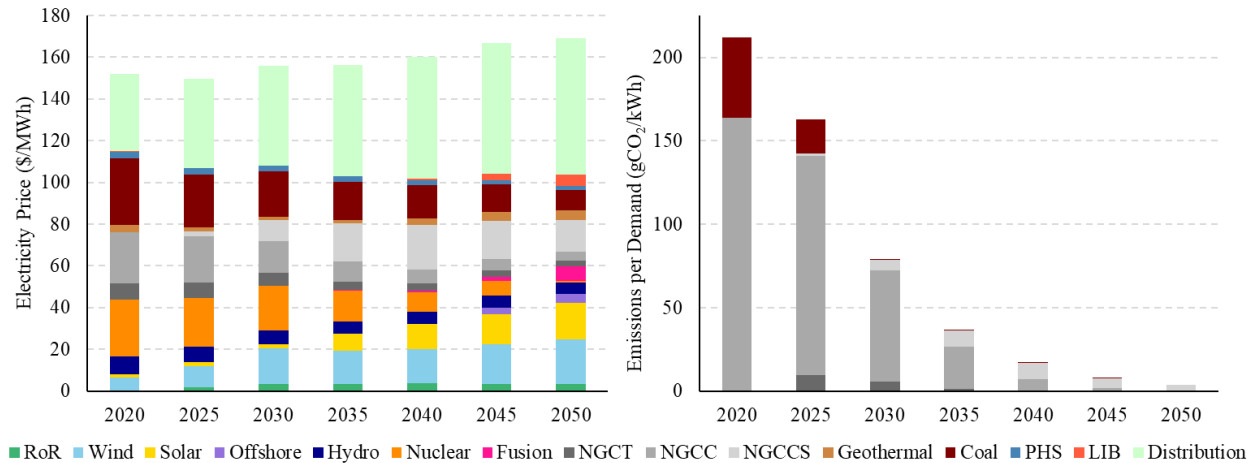


Figure 5-5. Base case national power sector costs and emissions intensity

5.4.2 Varying fusion CAPEX

As discussed in Chapter 4, fusion CAPEX is highly uncertain. And so, a sensitivity analysis is conducted in this chapter as well, with the same range of CAPEX values: \$3,000/kW, \$6,000/kW, \$8,500/kW, and \$12,000/kW. Figure 5-6 shows the impact of varying fusion CAPEX on national fleet composition. Reducing fusion CAPEX to \$6,000/kW reduces reliance on solar, wind (both land-based and offshore), natural gas with carbon capture, and energy storage, with the impact on other technologies being negligible. At this price point, fusion is installed in all regions, albeit to significantly different degrees. The Central and Northwest regions see the lowest fusion penetration, each region only installing one 350 MW plant. The Northwest has significant hydro resources which will still be in operation in 2050, which lessens the need for fusion. The Central region has a substantial nuclear fleet, most of which not retiring until 2050. Also, it has the highest initial emissions intensity so has the most lenient cap applied in 2045, when compared to the other regions, as shown in Figure 5-2. In 2045, Central allows for an emissions intensity of 9.4 gCO₂/kWh, while California is restricted to only 7.3 gCO₂/kWh.

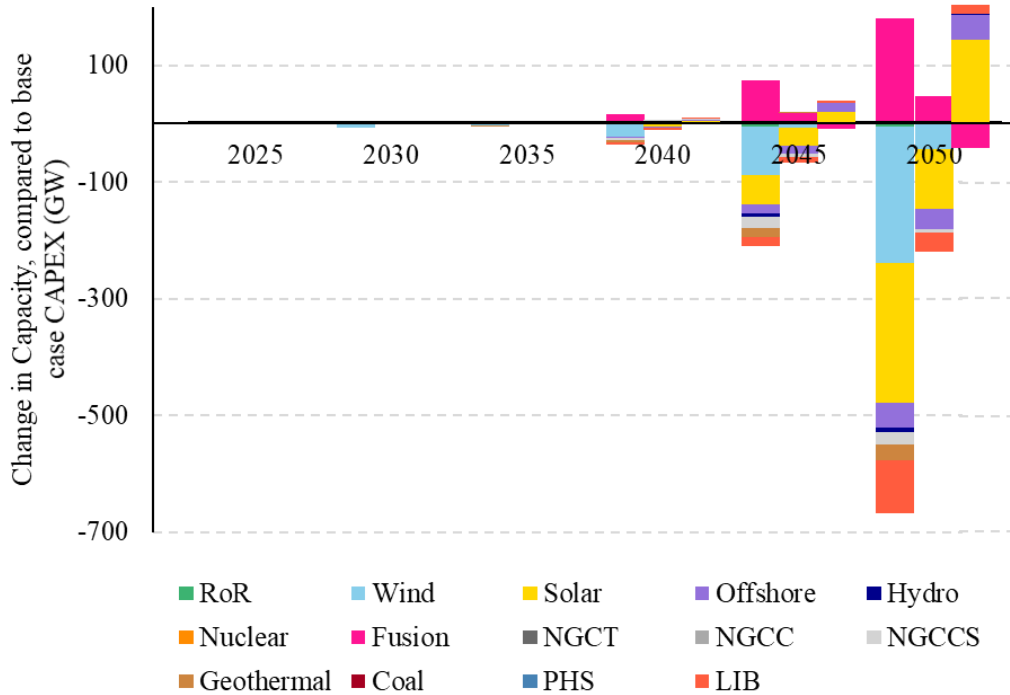


Figure 5-6. Change in capacities, as CAPEX is varied from base case: \$3,000/kW on left, \$6,000/kW on right, and \$12,000/kW on right

Once fusion is reduced to \$3,000/kW, Chapter 4 proved that it becomes competitive with wind and solar even without carbon constraints. Because of this, fusion buildout is maximized in every region from 2035-2045 (except the Southwest and Northeast in 2045). Then, fusion continues to quickly increase in 2050, but the buildout limit is high enough to no longer dictate system behavior. Lastly, note that there is still offshore wind in the national fleet, even though this is one of the first technologies that fusion normally pushes out. This is installed in the Atlantic and Southeast regions in 2045. This is needed to reach those regions respective 2045 decarbonization goals with a still developing fusion supply chain.

Lastly, at \$12,000/kW CAPEX, there is no fusion buildout. Therefore, this case can also be used to represent a scenario when fusion is not available or never commercialized. Without fusion, the

system relies more heavily on solar, offshore wind, LIBs, and a small contribution from other technologies.

5.4.3 Different learning rates

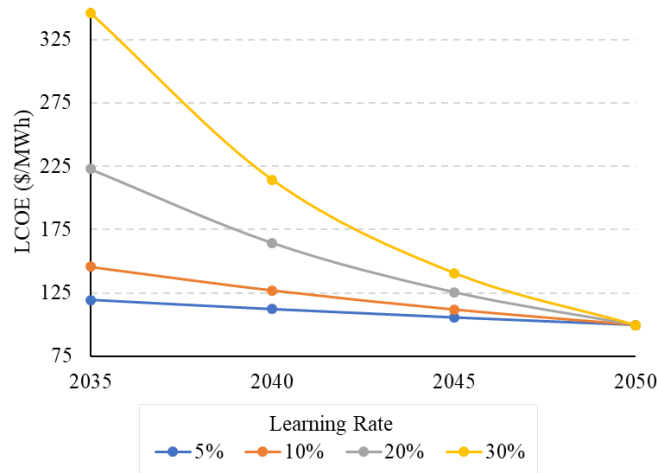


Figure 5-7. Fusion LCOE at each optimized year, depending on learning rate: 5%, 10% (base case), 20%, and 30%

Fusion’s learning rate is used to calculate fusion CAPEX at year of analysis, extrapolated out from the assumed 2050 value. Since the final cost is fixed, rather than the initial, a higher learning rate leads to a higher cost of fusion in 2035, and therefore lesser adoption. This is unintuitive, and so figures are labeled with “initial cost” rather than learning rate, for clarity. Learning rates tested are: 10% (base case), 20% (high 2035 cost), 30% (very high 2035 cost), and 5% (low 2035 cost). Note that the learning rate is always only applied to 60% of CAPEX, because this is the estimated fraction of the cost that is fusion-specific. Other costs, such as balance-of-plant costs are used to not have any learning rate because they will be very similar-, if not identical-to current technologies. Figure 5-7 shows the evolution of fusion’s CAPEX, at the different learning rates. Given a 5% learning rate, LCOE reduces by 17% over 15 years, compared to at a learning rate of 30%, LCOE reduces by 71% over 15 years.

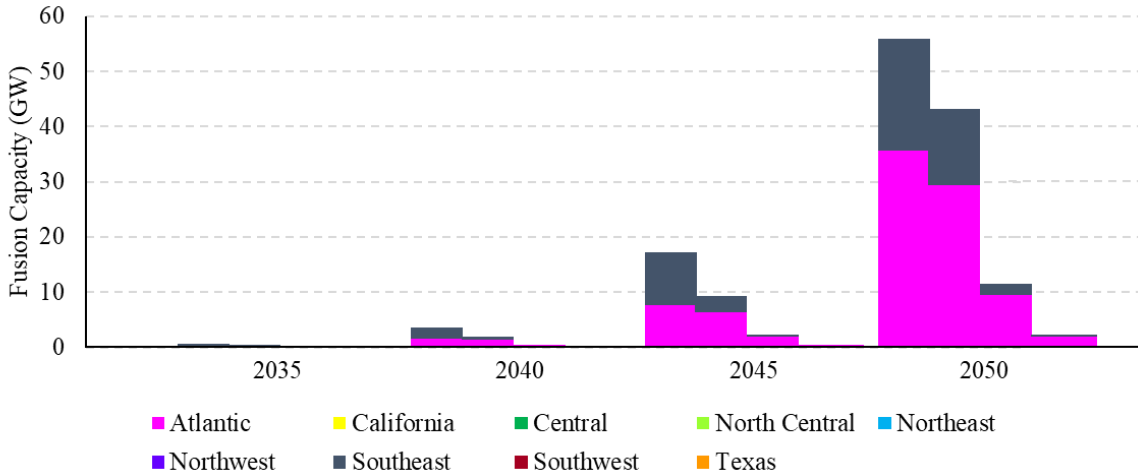


Figure 5-8. Fusion penetration, depending on learning rate: 5% left, 10% center left (base case), 20% center right, and 30% right

Learning rate has a high impact not only on early years of adoption, but also national total sum of fusion by 2050. This is because of the doubling limit. In fact, installations occurring in years before 2050 are often at their limit. Table 5-9 shows that fusion’s buildout limit is active, meaning that installations in earlier years are necessary to reach the optimal fusion capacities in 2050. As fusion’s learning rate increases, fusion installations are delayed and reduced to avoid the heightened costs of new technology.

Table 5-9. Years when fusion buildout is limited by learning rate

	5% learning		10% learning		20% learning		30% learning	
	Atlantic	Southeast	Atlantic	Southeast	Atlantic	Southeast	Atlantic	Southeast
2035		MAX						
2040	MAX	MAX	MAX	MAX	MAX			
2045	MAX	MAX	MAX	MAX	MAX	MAX	MAX	
2050	MAX		MAX	MAX	MAX	MAX	MAX	MAX

5.4.4 Varying fusion commercialization

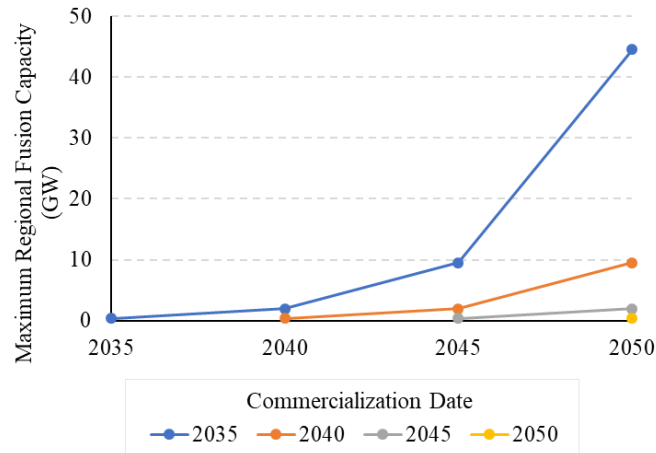


Figure 5-9. Maximum regional fusion capacity, based on commercialization date: 2035 (base case), 2040, 2045, and 2050

Fusion commercialization also affects buildout. Figure 5-9 shows the maximum fusion capacity that can be reached in a region, based on commercialization date. These values are calculated based on the base case doubling time. Note that all other variables are considered to be the same as the base case, including fusion costs, learning rate, and size of fusion plant.

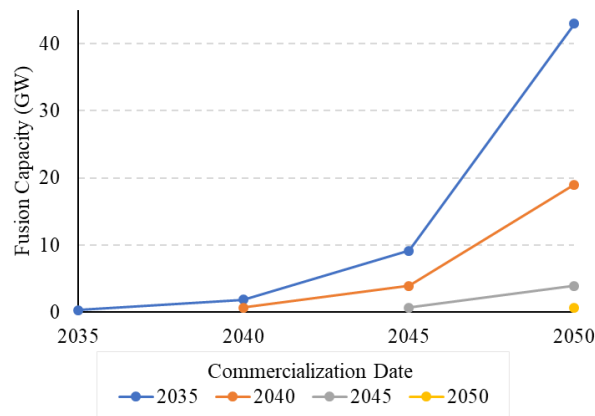


Figure 5-10. Commercialization date's impact on regional maximum fusion buildout

Figure 5-10 shows national fusion capacity, given a range of commercialization dates. The trends present in Figure 5-10 are similar to those in Figure 5-9. This is because for any

commercialization date after 2035, fusion buildout is limited every year based on the assumed doubling time. Note that analysis was conducted for 2030 commercialization of fusion, but that no regions adopted fusion before 2035, so this analysis is not pictured for concision.

5.4.5 Varying doubling time

Doubling time impacts both LCOE and maximum allowed fusion buildout. Note that maximum installations are calculated assuming that the previous year also reached its supply chain limit. If a year does not build all possible units, the following year will have a lesser maximum buildout capacity. This is often the case as seen in the other sections of analysis. Also, note that LCOE is not dependent on regional installations. This is because utility costs will be determined by the national and global demand for fusion, not regional. Lastly, the doubling times of 2.7 years, 2.3 years, and 2.0 years are calculated based on 1 GW global fusion in 2035, and 50 GW, 100 GW, and 200 GW of global fusion in 2050, respectively.

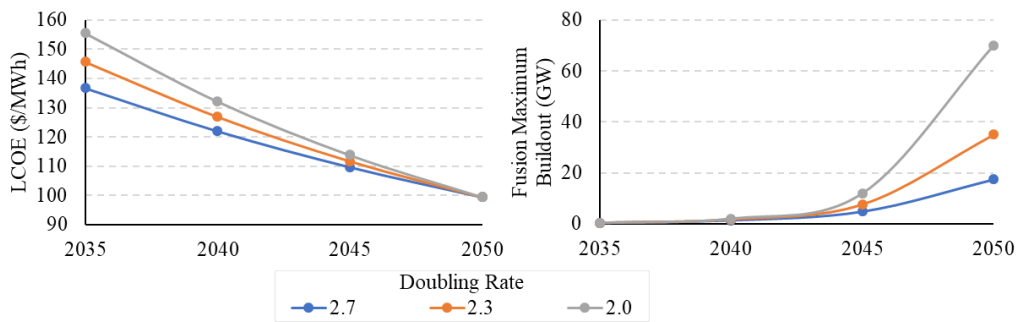


Figure 5-11. LCOE and maximum allowed buildout, based on variable doubling time: 2.7 years, 2.3 years (base case), and 2.0 years

The contrasting adjustment to parameters leads to interesting behavior, shown in Figure 5-12. In the Southeast, increased doubling time, with lower fusion costs leads to increased fusion buildout for all years. At these lower costs, the buildout limit is active from 2040-2050. Since buildout is slower than in the base case, which is also maximized over this timeframe, the relative difference

in installations decreases, although the actual difference increases. The system behavior is simply opposite what is seen with an increased doubling time.

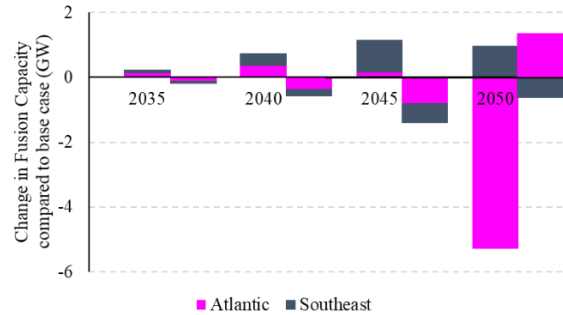


Figure 5-12. Impact of doubling rate on fusion buildout, compared to base case (2.3 years doubling time): 2.7 years on left and 2.0 years on right

In the Atlantic, when doubling time increases, fusion capacity is maxed out in every year. Fusion capacity starts higher, but is surpassed by the base case in 2050. The increased early installations are to build up the supply chain. When doubling time is decreased, the opposite behavior is true. Fusion installations start lower, but surpass base case capacities by 2050.

5.4.6 Varying carbon cap

Chapter 4 shows how more ambitious decarbonization goals integrate more fusion into the optimal greenfield buildout. The shape of this trend, under brownfield assumptions, is shown in Figure 5-13. At a 2.5 gCO₂/kWh carbon cap, not only do Atlantic and Southeast fusion installations increase, but California, North Central, and the Northeast all install a single 350 MW plant in 2050. Conversely, with a 15 gCO₂/kWh carbon cap, the only fusion installation is a single 350 MW unit in the Southeast. The brownfield installations compared to greenfield are 43% at 2.5 gCO₂/kWh, 40% at 4 gCO₂/kWh, and 3% at 15 gCO₂/kWh.

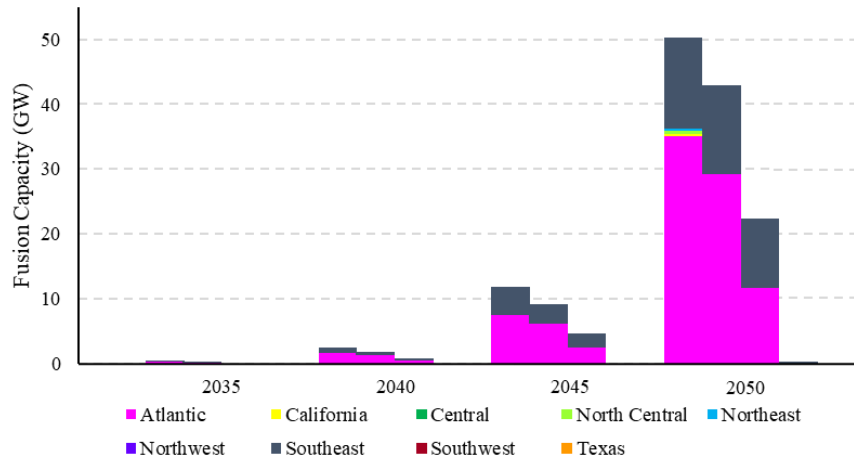


Figure 5-13. Fusion penetration at varying carbon caps: 2.5 gCO₂/kWh (left), 4 gCO₂/kWh (base case – center cleft), linear 4 gCO₂/kWh (center right), and 15 gCO₂/kWh (right)

When a linear carbon constraint is allowed, fusion reliance decreases. There is less need for fusion in the earlier years, but equal need in 2050. This shows how important intermediary decarbonization targets are, as they will shape our 2050 grid composition. Figure 5-14 shows the tradeoff between linear and exponential decarbonization schemes in terms of costs and emissions. Linear decarbonization is cheaper during years 2025-2045 because the system opts for a dirtier, less-expensive buildout. Linear decarbonization is cheaper in 2050 because clean resources were installed later, when their costs are projected to be lower. Given a linear decarbonization strategy, the Atlantic and Southeast grid emissions intensities are still around 70 by 2045. And ultimately, linear decarbonization allows for more than double the cumulative emissions from 2020 to 2050.

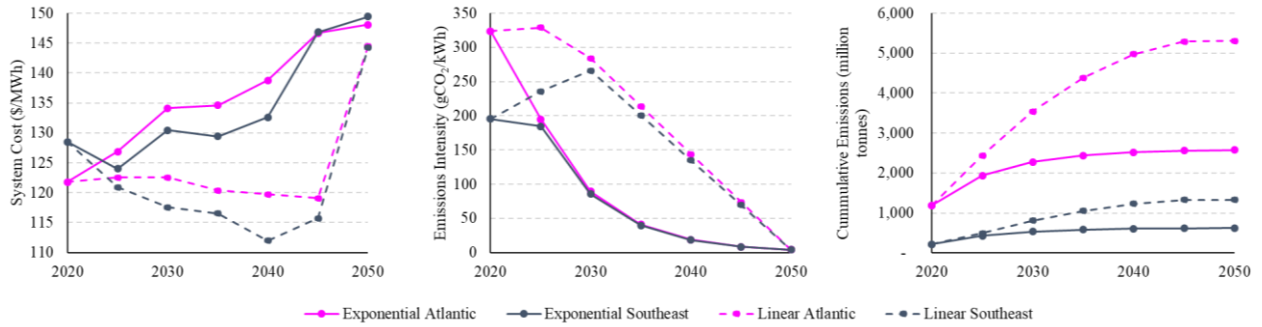


Figure 5-14. System cost, emission intensity, and cumulative emissions given an exponential (base case – line) vs. linear (dashed) decarbonization strategy

5.4.7 Comparison of constraint impacts

This Chapter reviews the impact of many different variables: fusion CAPEX, fusion learning rate, fusion doubling rate, date of commercialization, and carbon constraint. It was shown that all these parameters affect fusion buildout, albeit to varying degrees. Figure 5-15 compares the impact of each input, to highlight which constraints hold the highest impact on the future of fusion. Note that the ranges explored for each parameter are not analogous, so a direct comparison, although interesting, is not fair. Note that Figure 5-16 in the Appendix shows the same information, in percent format.

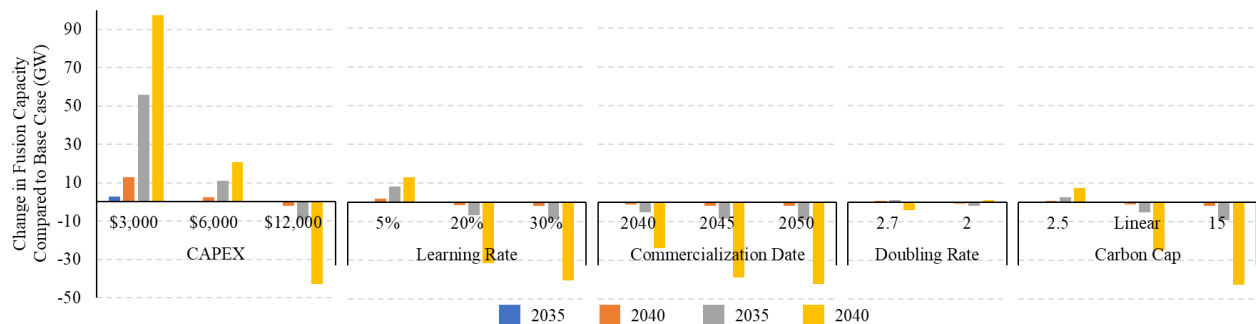


Figure 5-15. Comparison of parameter impact on fusion capacity

5.5 Conclusions

The range of CAPEX values have the greatest potential to influence fusion adoption.

Commercialization date can only negatively impact fusion adoption. An earlier commercialization date serves no benefit to the system, and a later date constricts fusion buildout. Learning rate has a significant impact on fusion buildout. Less expensive costs encourage buildout, which increases the supply change capacity. The supply chain is limiting from 2040-2050 in the base case, so early adoption is key to allow large installations in 2050. Doubling rate has a nonhomogeneous impact on regions. A shorter doubling time allows some regions to wait until later years to install larger amounts of fusion. In other regions, different behavior is observed.

Also, it was shown that the imposed carbon cap highly dictates fusion adoption. Imposing a tighter carbon cap (2.5 gCO₂/kWh) incentivizes a 17% increase in fusion installations by 2050 compared to the base case, while imposing a more lenient carbon cap (15 gCO₂/kWh) reduces fusion adoption by 99%. Lastly, linear decarbonization is compared to exponential. Linear reduction reduces fusion penetration by 58%. It allows for a 2-3% cheaper regional grid, but at the cost of over double the cumulative emissions. It has been shown that there are many uncertain factors which will influence the role that fusion will play in a decarbonized power sector.

5.6 Appendix

Table 5-10. Scalar financial values for all technologies

	Overnight Capital Cost (\$/kW)	Fixed Operation Cost (\$/kW/yr)	Variable Operational Cost (\$/MWh)	Fuel cost (\$/MMBtu)	Heat Rate (MMBtu/MWh)	Lifetime (yr)
Abbreviation	CAPEX	FOM	VOM			L
Solar ₂₀₂₁	1291	23	0	0	0	30
Solar ₂₀₂₅	1248	20	0	0	0	30
Solar ₂₀₃₀	1038	18	0	0	0	30
Solar ₂₀₃₅	829	16	0	0	0	30
Solar ₂₀₄₀	764	15	0	0	0	30
Solar ₂₀₄₅	698	14	0	0	0	30
Solar ₂₀₅₀	632	13	0	0	0	30
Solar ₂₀₂₁₋₂₀₅₀ source	2023 ATB Publication [71]					
Wind ₂₀₂₁	1363	30	0	0	0	30
Wind ₂₀₂₅	1268	29	0	0	0	30
Wind ₂₀₃₀	1150	27	0	0	0	30
Wind ₂₀₃₅	1093	26	0	0	0	30
Wind ₂₀₄₀	1037	25	0	0	0	30
Wind ₂₀₄₅	980	24	0	0	0	30

Wind ₂₀₅₀	924	23	0	0	0	30
Wind ₂₀₂₁₋₂₀₅₀ source	2023 ATB Publication [71] – Class 7					
Offw ₂₀₂₁	3396	107	0	0	0	30
Offw ₂₀₂₅	2962	95	0	0	0	30
Offw ₂₀₃₀	2723	87	0	0	0	30
Offw ₂₀₃₅	2575	81	0	0	0	30
Offw ₂₀₄₀	2468	77	0	0	0	30
Offw ₂₀₄₅	2383	74	0	0	0	30
Offw ₂₀₅₀	2314	71	0	0	0	30
Offw ₂₀₂₁₋₂₀₅₀ source	2023 ATB Publication [71] – Class 1; CAPEX includes grid connection costs					
RoR ₂₀₂₁	4067	19	0	0	0	100
RoR ₂₀₂₅	4067	19	0	0	0	100
RoR ₂₀₃₀	4067	19	0	0	0	100
RoR ₂₀₃₅	4067	19	0	0	0	100
RoR ₂₀₄₀	4067	19	0	0	0	100
RoR ₂₀₄₅	4067	19	0	0	0	100
RoR ₂₀₅₀	4067	19	0	0	0	100
RoR ₂₀₂₁₋₂₀₅₀ source	2023 ATB Publication [71] – Average of Class NSD 2					
Hydro ₂₀₂₁	4843	32	0	0	0	100
Hydro ₂₀₂₅	4843	32	0	0	0	100
Hydro ₂₀₃₀	5159	32	0	0	0	100
Hydro ₂₀₃₅	5539	32	0	0	0	100
Hydro ₂₀₄₀	5317	31	0	0	0	100

Hydro ₂₀₄₅	5317	31	0	0	0	100
Hydro ₂₀₅₀	5317	31	0	0	0	100
Hydro ₂₀₂₁₋₂₀₅₀ source	2023 ATB Publication [71] – Average of Class NPD 5					
Geo ₂₀₂₁	6750	114	0	0	0	30
Geo ₂₀₂₅	6469	111	0	0	0	30
Geo ₂₀₃₀	5926	107	0	0	0	30
Geo ₂₀₃₅	5559	104	0	0	0	30
Geo ₂₀₄₀	5421	104	0	0	0	30
Geo ₂₀₄₅	5287	104	0	0	0	30
Geo ₂₀₅₀	5156	104	0	0	0	30
Geo ₂₀₂₁₋₂₀₅₀ source	2023 ATB Publication [71] – Hydro/Flash					
NGCT ₂₀₂₁	1120	24	6.44	2.99	9.72	55
NGCT ₂₀₂₅	1094	24	6.44	3.51	9.72	55
NGCT ₂₀₃₀	1050	23	6.44	3.85	9.72	55
NGCT ₂₀₃₅	1005	22	6.44	3.96	9.72	55
NGCT ₂₀₄₀	961	22	6.44	4.04	9.72	55
NGCT ₂₀₄₅	917	21	6.44	4.08	9.72	55
NGCT ₂₀₅₀	872	20	6.44	4.31	9.72	55
NGCT ₂₀₂₁₋₂₀₅₀ source	[102] for fuel cost & 2023 ATB Publication [71] all else					
NGCC ₂₀₂₁	1283	31	1.96	2.99	6.2	55
NGCC ₂₀₂₅	1246	30	1.91	3.51	6.17	55
NGCC ₂₀₃₀	1185	28	1.84	3.85	6.12	55
NGCC ₂₀₃₅	1124	27	1.77	3.96	6.08	55

NGCC ₂₀₄₀	1078	26	1.72	4.04	6.08	55
NGCC ₂₀₄₅	1031	25	1.66	4.08	6.08	55
NGCC ₂₀₅₀	985	24	1.61	4.31	6.08	55
NGCC ₂₀₂₁₋₂₀₅₀ source	[102] for fuel cost & 2023 ATB Publication [71] all else – H-Frame					
NGCCS ₂₀₂₁	2531	59	4.4	2.99	7.01	55
NGCCS ₂₀₂₅	2396	56	4.22	3.51	6.95	55
NGCCS ₂₀₃₀	2170	51	3.91	3.85	6.84	55
NGCCS ₂₀₃₅	1944	46	3.61	3.96	6.74	55
NGCCS ₂₀₄₀	1833	44	3.48	4.04	6.74	55
NGCCS ₂₀₄₅	1722	41	3.353	4.08	6.74	55
NGCCS ₂₀₅₀	1611	39	3.23	4.31	6.74	55
NGCCS ₂₀₂₁₋₂₀₅₀ source	[102] for fuel cost & 2023 ATB Publication [71] all else – H-Frame; 95% CCS					
Nuclear ₂₀₂₁	9440	152	2.47	0.66	10.45	60
Nuclear ₂₀₂₅	8106	152	2.47	0.66	10.45	60
Nuclear ₂₀₃₀	7730	152	2.47	0.66	10.45	60
Nuclear ₂₀₃₅	7473	152	2.47	0.66	10.45	60
Nuclear ₂₀₄₀	7209	152	2.47	0.66	10.45	60
Nuclear ₂₀₄₅	6961	152	2.47	0.66	10.45	60
Nuclear ₂₀₅₀	6668	152	2.47	0.66	10.45	60
Nuclear ₂₀₂₁₋₂₀₅₀ source	2023 ATB Publication [71]					
Fusion ₂₀₂₁	8500	152	2.47	0	0	40

Fusion ₂₀₂₅	8500	152	2.47	0	0	40
Fusion ₂₀₃₀	8500	152	2.47	0	0	40
Fusion ₂₀₃₅	8500	152	2.47	0	0	40
Fusion ₂₀₄₀	8500	152	2.47	0	0	40
Fusion ₂₀₄₅	8500	152	2.47	0	0	40
Fusion ₂₀₅₀	8500	152	2.47	0	0	40
Fusion ₂₀₂₁₋₂₀₅₀ source	2023 ATB Publication [71] – nuclear, except OCC, heat rate, fuel cost, L, and ITC which are explained below					
PHS ₂₀₂₁	7082	47	0	0	0	100
PHS ₂₀₂₅	7082	47	0	0	0	100
PHS ₂₀₃₀	7082	47	0	0	0	100
PHS ₂₀₃₅	7082	47	0	0	0	100
PHS ₂₀₄₀	7082	47	0	0	0	100
PHS ₂₀₄₅	7082	47	0	0	0	100
PHS ₂₀₅₀	7082	47	0	0	0	100
PHS ₂₀₂₁₋₂₀₅₀ source	2023 ATB Publication [71] – Class 13					
LIB ₂₀₂₁	1587	40	0	0	0	15
LIB ₂₀₂₅	1436	36	0	0	0	15
LIB ₂₀₃₀	1204	30	0	0	0	15
LIB ₂₀₃₅	111	28	0	0	0	15
LIB ₂₀₄₀	1018	25	0	0	0	15
LIB ₂₀₄₅	925	23	0	0	0	15
LIB ₂₀₅₀	833	21	0	0	0	15

LIB ₂₀₂₁₋₂₀₅₀ source	2023 ATB Publication [71] – 4Hr for CAPEX, FOM, LIB, L, and PTC and ITC; Utility PV Plus Battery for all else					
LIBshort ₂₀₂₁	943	24	0	0	0	15
LIBshort ₂₀₂₅	862	22	0	0	0	15
LIBshort ₂₀₃₀	749	19	0	0	0	15
LIBshort ₂₀₃₅	697	17	0	0	0	15
LIBshort ₂₀₄₀	646	16	0	0	0	15
LIBshort ₂₀₄₅	594	15	0	0	0	15
LIBshort ₂₀₅₀	541	14	0	0	0	15
LIBshort ₂₀₂₁₋₂₀₅₀ source	2023 ATB Publication [71] – 2Hr for CAPEX, FOM, LIB, L, and PTC and ITC; Utility PV Plus Battery for all else					
LIBlong ₂₀₂₁	2875	72	0	0	0	15
LIBlong ₂₀₂₅	2584	65	0	0	0	15
LIBlong ₂₀₃₀	2114	53	0	0	0	15
LIBlong ₂₀₃₅	1938	48	0	0	0	15
LIBlong ₂₀₄₀	1763	44	0	0	0	15
LIBlong ₂₀₄₅	1589	40	0	0	0	15
LIBlong ₂₀₅₀	1415	35	0	0	0	15
LIBlong ₂₀₂₁₋₂₀₅₀ source	2023 ATB Publication [71] – 8Hr for CAPEX, FOM, LIB, L, and PTC and ITC; Utility PV Plus Battery for all else					
Coal ₂₀₂₁	2746	76	8.33	2.15	8.47	75
Coal ₂₀₂₅	2704	76	8.27	2.07	8.47	75
Coal ₂₀₃₀	2554	74	7.97	2.07	7.61	75
Coal ₂₀₃₅	2423	72	7.79	2.07	7.09	75

Coal ₂₀₄₀	2339	72	7.79	2.06	7.09	75
Coal ₂₀₄₅	2259	72	7.79	2.07	7.09	75
Coal ₂₀₅₀	2152	72	7.79	2.07	7.09	75
Coal ₂₀₂₁₋₂₀₅₀ source	2020 ATB Publication [102] for fuel cost and lifetime, 2023 ATB Publication [71] for CFF & 2021 ATB Publication [103] all else – new-AvgCF					

- Converting to 2021 dollars [71]:
 - 2018\$ to 2019\$ multiplier = 1.0181
 - 2019\$ to 2020\$ multiplier = 1.0123
 - 2020\$ to 2021\$ multiplier = 1.047

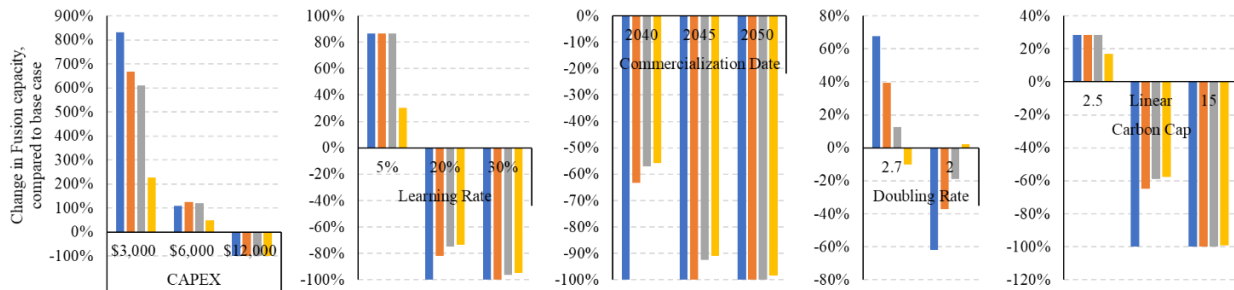


Figure 5-16. Change in fusion capacity, with varying parameter values (%)

Chapter 6. Summary of contributions and future directions

6.1 Novel and impactful contributions

The analyses in this thesis explore decarbonization of the power sector from multiple angles. Chapters 2 and 5 introduce two novel CEMs, Ideal Grid and Evolving Grid, which are unique and valuable to the field due to their combination of three main characteristics: 1) they are open source, 2) they allow for extensive individual and comparative analysis of nine regions of the US, and most importantly, 3) they consider emissions from all stages of the life cycle. These models can be used to answer a broad range of questions, illustrated by the 4 main case studies presented above, each in a different Chapter.

Chapter 2 shows how bespoke decarbonization strategies are needed because there is significant diversity and nuance in optimized transitional decision making just within the US. For example, annual wind CF has a high correlation with a region's low emissions intensity LCOE. Chapter 2 also shows that decarbonization is cheaper in regions with available hydro resources.

Chapter 3 shows the importance of LCA. The US power sector requires major transitions to reach national decarbonization goals, meaning we have the opportunity, and responsibility, to redesign and rebuild a large portion of current infrastructure. It is important to redesign in ways which will minimize costs, and yet result in a robust and reliable grid. The industry standard for current policy and analysis is to optimize the reduction of power-plant tailpipe emissions.

Chapter 3 shows that this inaccurate approximation leads to a dirtier grid and neglects up to 50% of emissions, when the target emissions intensity is 20 gCO₂/kWh. To actually reach net-zero requires negative-emissions technologies and will be more expensive than most models are currently predicting. But to be serious about our goals, we must consider these embodied emissions.

Chapter 4 explores the potential role of a developing technology, fusion. Fusion is a low-carbon, dispatchable generating option. In this analysis, fusion is assumed to have a CAPEX of \$8,500/kW. Fusion penetration was found to be highest in regions which had severely limited onshore wind buildout options. Fusion allows these systems to decarbonize with significantly less reliance on offshore wind. A sensitivity was conducted on fusion costs and it was found that fusion becomes economically viable in regions at a CAPEX of \$3,000-4,000/kW, without carbon caps. However, if nuclear buildout is allowed, the space for fusion penetration decreases significantly. In fact, California, the Northeast, and the Northwest see no fusion adoption at all in these scenarios. Fusion has the potential to play a role in decarbonization, but to strikingly different degrees, depending on regional characteristics and costs.

Chapter 5 shows that grid inertia has a great impact on the role of new technologies. National fusion adoption is tracked from commercialization to 2050, assuming an exponential decrease in emissions intensity, targeting 4 gCO₂/kWh in 2050. Fusion adoption begins in 2035 and reaches ~43 GW of total capacity by 2050. This base case brownfield analysis sees only ~40% as much fusion penetration as greenfield analysis. The impacts of varying CAPEX, learning rate, commercialization date, doubling rate, and carbon cap are all discussed. The range of CAPEX values explored showed the largest impact on buildout, which aligns with conclusions from Chapter 4. Other than carbon cap, initial commercialization date was shown to pose the largest threat to fusion adoption. Maximum buildout rate constrains the base case from 2040-2050. Delaying commercialization date further constricts this time period. The complexities of brownfield analysis reveal that decarbonization strategy, fusion commercialization date, and fusion CAPEX strongly dictate fusion adoption.

The below sections present ongoing research leveraging IG and EG as examples of the broader impact of the work in this thesis. These two case studies are introduced and have their methodology described. The first demonstrates the coupling of sectors and discusses the challenges and opportunities around this occurrence in the transportation sector. The second is showcases IG's range with a discussion around subsidies and their optimization. Note that these examples are demonstrations of IG and EG extensions, rather than completed, comprehensive analysis.

6.2 Enabling electric vehicle-to-grid interactions

6.2.1 Introduction

In 2021, the transportation sector was the largest emitter in the US, responsible for 29% of annual emissions [104]. We know that converting to electric vehicles (EVs) is the main strategy for decarbonization of this sector. Since transportation is responsible for such a large portion of our national energy demand (36%), we understand that electrification will pose a nonnegligible change to our electric load [105]. However, with a little imagination, one can actually think of EVs not only as drain on the power sector, but also a resource. In fact, within the confines of grid-discussions, EV batteries can be considered intermittent electricity sources and sinks on wheels, used to power transportation as well as supply other grid services. Similar to how current LIBs are operated, EVs have the potential to inject electricity back into the grid. The undeniable value of this type of operation is outlined in Owens et al.'s paper [106].

The most flexible *type* of analysis is vehicle to grid (V2G); this allows the aggregate resource of EV batteries to be used as an energy storage resource for the grid. Electricity can be sent to EV batteries from the grid and can also be sent from EV batteries to the grid. Bidirectional electricity

flow is allowed. It is constrained as described a complex series of equations below. *Smart* and *uncontrolled* charging schemes only allow for monodirectional electricity flow from the grid to EV batteries. *Uncontrolled* assumes a charging schedule based on charger and vehicle availability. *Smart* charging allows the model to optimize the aggregated EV battery charging scheme to minimize overall system costs. This will encourage charging to occur in periods where there is low demand and/or excess generated electricity available.

Owens' analysis focuses on the impact of electrifying New England's light-duty fleet. The study suggested here integrates IG to explore the difference in impact of medium-duty *V2G* capabilities. It explores the regional difference in the vehicle fleet, power sector fleet, and the intersection of these discrepancies to better understand *V2G* nuances. Note that the analysis suggested here is different from the above Chapters because capacities are predefined based on projections. Instead of build-out-related questions, this case study is better suited for economic dispatch questions: given a defined future scenario, what is the value of *smart* charging or *V2G*? This analysis is targeted at two future dates (2035 and 2050), which will answer the question: how will the role and importance of *V2G* capabilities change over time? Lastly, a tax is imposed to see explore how *V2G* amplifies the impact of a carbon tax, as it enlarges the optimization space.

6.2.2 Methodology

This project is built upon the Ideal Grid model, with important added nomenclature and constraints presented below. All other values, set, equations, constraints, etc. that were presented in Chapter 2 apply to this analysis, except when noted otherwise.

6.2.2.1 Nomenclature

Table 6-1. Sets specific to V2G analysis

Notation	Description	Unit
τ	Energy storage types: LIB (3 types), PHS, and EV	-

Table 6-2. Vector decision variables specific to V2G

Notation	Description	Unit
EV_{level}_{hour}	EV battery energy level at every time step <i>hour</i>	kWh
$VRE2EV_{hour}$	VRE generated energy sent to EV batteries at every time step <i>hour</i>	kWh
$G2EV_{hour}$	Dispatchable generated energy sent to EV batteries at every time step <i>hour</i>	kWh
$EV2D_{hour}$	Energy leaving EV batteries at every time step <i>hour</i>	kWh

Table 6-3. User inputs specific to V2G

Notation	Description	Unit
<i>type</i>	Describes the type of interaction between the grid and EVs (<i>uncontrolled, smart, or V2G</i>)	kWh

Table 6-4. EV parameters

Notation	Description	Unit
$driving_{hour}$	Discharge from the EV energy storage technology due to driving, at every time step <i>hour</i>	kWh

$Pcap_{hour}$	Power capacity of EV energy storage technology available for charging and charging, at every time step $hour$	kW
$Ecap$	Maximum energy capacity of the EV fleet	kWh
$minSOC_{hour}$	Minimum state of charge for the EV energy storage technology, at every time step $hour$	kWh
$fraction$	The fraction of the fleet which is approximated to be at a charger, at every time step $hour$	1
$dischargecost$	Penalty of EV battery technology discharge to the grid (valued at \$0.00948/kWh)	\$/kWh

6.2.2.2 Objective function

The IG objective function presented in Chapter 2 is adjusted based on the model's new capabilities.

$$yearlycost = \min \left\{ \begin{array}{l} \sum_{j \in hour} EV2D_j * dischargecost + \\ \sum_{i \in \psi} (VOM_i + fuelcost_i * heatrate_i) * total_i + \\ \sum_{i \in \psi} e_{tax} * (eGC_i * GC_i + e_i * total_i) + \\ \sum_{i \in \omega} ecaptured_i * cCCS \end{array} \right\} \quad (6.1)$$

The optimization of capacity expansion is removed because sizing of technologies are set based on *Cambium* projections discussed below. The first component in Equation 6.1 is the addition of a discharge penalty. This is to penalize vehicle discharges to the grid which are cause additional battery degradation.

6.2.2.3 Hourly constraints

Electricity flow is tracked very similarly to Equations 2.11 through 2.13 presented in Chapter 2.

The adjusted versions are shown below. Notice that VRE and dispatchable generated electricity has the added flexibility to flow to EV battery energy storage, as seen in Equations 6.2 and 6.3.

When *uncontrolled* type analysis is being conducted, generation to EV is predefined, not optimized. Equation 6.4 shows that demand can be satisfied by injecting electricity back into the grid. Note that the addition to equation 6.4 is only valid when V2G is user-selected.

$$G2D_j + G2LIB_j + G2PHS_j + G2EV_j = \sum_{i \in \Omega} GC_i * CF_{i,j} * (1 - TDlosses) \quad (6.2)$$

$$VRE2D_j + VRE2LIB_j + VRE2PHS_j + VRE2C_j + VRE2EV_j = \sum_{i \in \Theta} GC_i * CF_{i,j} * (1 - TDlosses) \quad (6.3)$$

$$G2D_j + VRE2D_j + LIB2D_j * \eta_{LIB} + PHS2D_j * \eta_{PHS} + EV2D_j * \eta_{LIB} = \underline{D}underlined_j \quad (6.4)$$

$$\forall j \in hour$$

The hourly energy level of EV batteries is tracked with equation 6.5. This is very similar to the LIBs modeled in chapter 2, but with the added discharge of powering the EV.

$$EVlevel_j = EVlevel_{j-1} * \eta_{hourly_{LIB}} + (G2EV_j + VRE2EV_j) * \eta_{LIB} - EV2D_j - driving_j \quad (6.5)$$

$$\forall j \in hour/0$$

The next group of hourly constraints restricts EV battery level and operations. Equation 6.6 restricts energy in EV batteries to remain below their energy capacity limit. Equations 6.7 and 6.8 enforce charging and discharging limitations, respectively.

$$EVlevel_j \leq Ecap \quad (6.6)$$

$$VRE2EV_j + G2EV_j \leq (Ecap - EVlevel_j) * fraction_j \quad (6.7)$$

$$EV2D_j \leq EVlevel_j * fraction_j \quad (6.8)$$

$$\forall j \in hour$$

The last hourly constraint is unique to this Chapter of analysis. Equation 6.9 ensures that the EV battery state of charge remains above a specified range, which varies temporally.

$$\min SOC_j \leq EVlevel_j \quad (6.9)$$

$$\forall j \in hour$$

6.2.2.4 Annual constraints

The last EV-specific constraint is included below. The state of charge at the first hour is constrained to equal the state of charge in the last hour so that the battery is not used as an annual energy sink or source.

$$EVlevel_0 = EVlevel_{j[-1]} \quad (6.10)$$

6.2.3 Data sources

6.2.3.1 Capacity projections

Capacity projections are sourced from NREL's Cambium resource [37]. Cambium's Mid-Case projection has biennial state-level capacity projections based on current policies and subsidies. These values can be aggregated to reflect buildout in each of the nine regions of analysis. Figure 6-1 shows how regional fleets are projected to grow and evolve. It is important to note that although there is significant VRE buildout, these resources are still supplemented by a nonnegligible number of fossil-fueled generators.

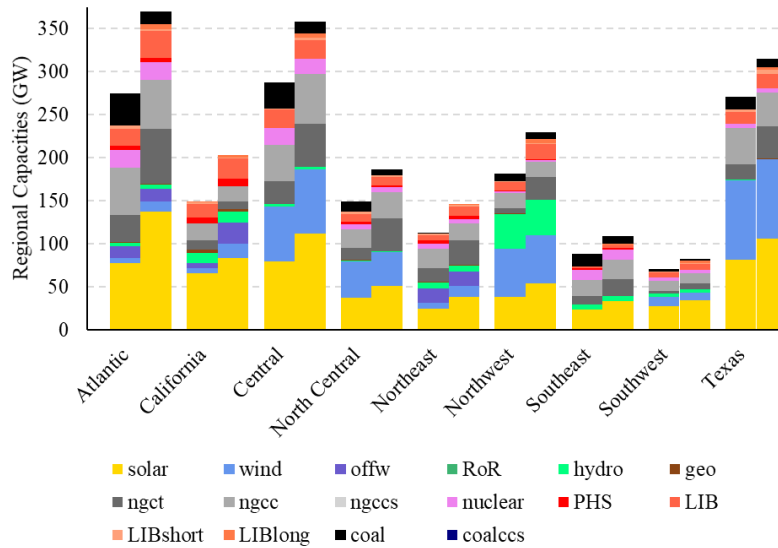


Figure 6-1. Cambium's mid-case projected regional capacities in 2035 (left) and 2050 (right)

6.2.3.2 Demand projections

Demand projections are sourced by multiplying 2022 demand shapes from EIA’s “Real-Time Operating Grid” [107] by region-specific power projections from EIA’s “Annual Energy Outlook” [9]. Figure 6-2 shows that there are starkly different projected changes in demand in each region. Note that the added load of electrified transportation is not included in the below values; only increases in residential, commercial, and industrial electric demand are represented in Figure 6-2.

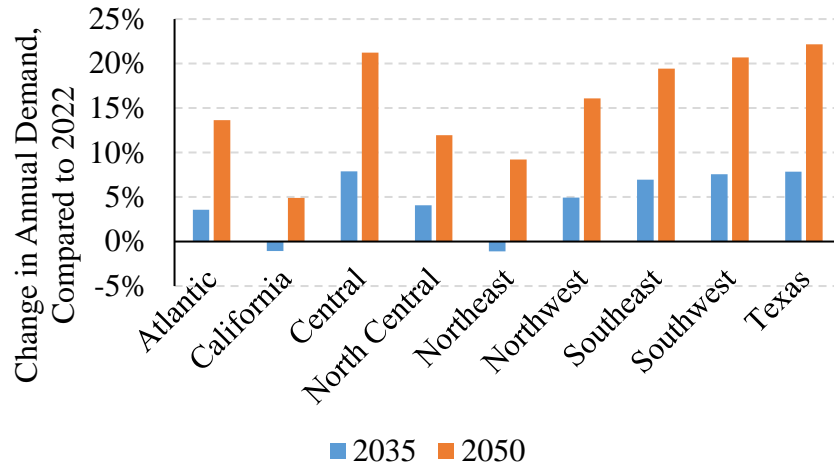


Figure 6-2. Projections of change of regional annual demand sum, excluding transportation demand

6.2.3.3 Vehicle demand and parameter calculations

The vehicle fleet represented in this model is made of class 3-6 trucks, more colloquially known as medium-duty trucks, including delivery trucks, buses, ambulances, etc. By using 2019 state-level registration data from Oak Ridge National Lab’s Transportation Energy Data Book (TEDB) [108] and the National Truck Equipment Association (NTEA) [109], current fleet sizes can be calculated for each region. Next, the Argonne National Lab’s VISION model [110] is used to extrapolate from current fleet sizes to 2035 and 2050 sizes, assuming that future regional sales are proportional to current stock size. This gives regional *Ecap* values.

Fleet operations are estimated using NREL’s Fleet DNA travel data [111]. Fleet DNA has 974 days of driving data for 94 class 3-6 vehicles. Each vehicle has a daily departure time and return time. From this information, *fraction* and $Pcap_{hour}$ are calculated. The remaining V2G-specific variables ($driving_{hour}$ and $minSOC_{hour}$) are calculated with the following assumptions: 1) vehicles travel 52 miles per day (based on aggregated fleet DNA data), 2) vehicles have an efficiency of 1.5 mi/kWh, and 3) EV batteries have 100 kWh energy capacity. Lastly, note that when

uncontrolled analysis is being conducted, it is assumed that vehicles are recharged starting the *hour* after they return from use.

6.2.4 Planned analysis and hypotheses

Since only economic dispatch is optimized in this analysis, system operations rather than recommended buildout are the focus of this case study. The base-case to which more flexible analysis is compared is *uncontrolled*, which represents a future scenario in which EV batteries are not leveraged in any way. The largest improvements will be seen in the *V2G* analysis because there is the most optimization allowed. *Smart* charging is still expected to see measurable improvements from the *uncontrolled* analysis.

The objective function is a cost minimization, so there will be a reduction in system cost as we unlock *V2G* capabilities, but the larger improvement will be seen in emissions intensity levels. This is because the only way for the system to reduce costs is by reducing VOM and fuel costs, because capital and FOM costs are fixed. Since VOM and fuel costs are only nonnegligible in thermal generating units, these power output from these units will reduce. While operational costs are a relatively small fraction of the overall lifetime costs of thermal generating units, operational emissions are the main source of greenhouse gasses. Reduction of fossil-fueled generation has a significantly higher impact on emissions intensity than on system cost. Having said that, it is still important to note the cost reductions because they can motivate *V2G* adoption.

6.3 Subsidy analysis

6.3.1 Introduction

As mentioned in the above Chapters, significant power-system reform is required to reach targeted emissions reduction levels. To encourage this transition, there is a collection of national subsidies that have been enacted; most notably is the Inflation Reduction Act (IRA) [112].

The IRA is recognized as the most significant climate legislation ever passed. Bistline et al's review of the IRA's impact using a variety of US energy sector models shows that the IRA is projected to motivate 38-80% reduction in emissions compared to 2005 level, by 2030, and stimulate 66-87% reductions by 2035 [113]. This draws the US's Paris agreement target of reaching 50-52% reduction by 2030 into range [114]. But, even with this promising enactment, there remains serious need to further decarbonize the power sector to halt the damage of climate change.

There are two types of subsidies: investment tax credits (ITCs) are calculated based on system cost and applied the year of installation, and production tax credits (PTCs) are calculated based on power generated and are applied for the first 10 years of system operation. Both these calculated tax credits reduce federal income tax liability [115].

The research suggested here explores the best way to decarbonize without subsidies vs with current subsidies. In general, we want to make decarbonization cheaper, but we don't want to accidentally favor one technology over another. This analysis will look at how subsidies encourage decarbonization as well as whether they are optimal or not. Furthermore, there will be a comparison between regions to understand if region-specific subsidy designs can more

effectively incentivize decarbonization. Alternative subsidy schemes are explored to see how the IRA can be built upon and its momentum can be furthered.

6.3.2 Methodology

This analysis uses the equations, constraints and parameters presented in Chapter 5. The only difference is the change in calculation of capital cost. The annual calculation of capital cost is defined in Equations 2-20 through 2-26 of Chapter 2’s appendix, where both PTC and ITC are considered. In the base-case of this analysis, both PTC and ITC are considered to be 0, regardless of installation year. The difference in LCOE of each technology is shown below in Figure 6-3. Fossil-fuel powered generators are not included because they are not eligible for subsidy. It is clear that government programs subsidize different percentages of technology’s costs. For example, in 2035, wind LCOE is reduced by ~72% while nuclear LCOE is reduced by ~20%. The percent reduction difference is because nuclear is more expensive than solar, but the same price reduction is applied.

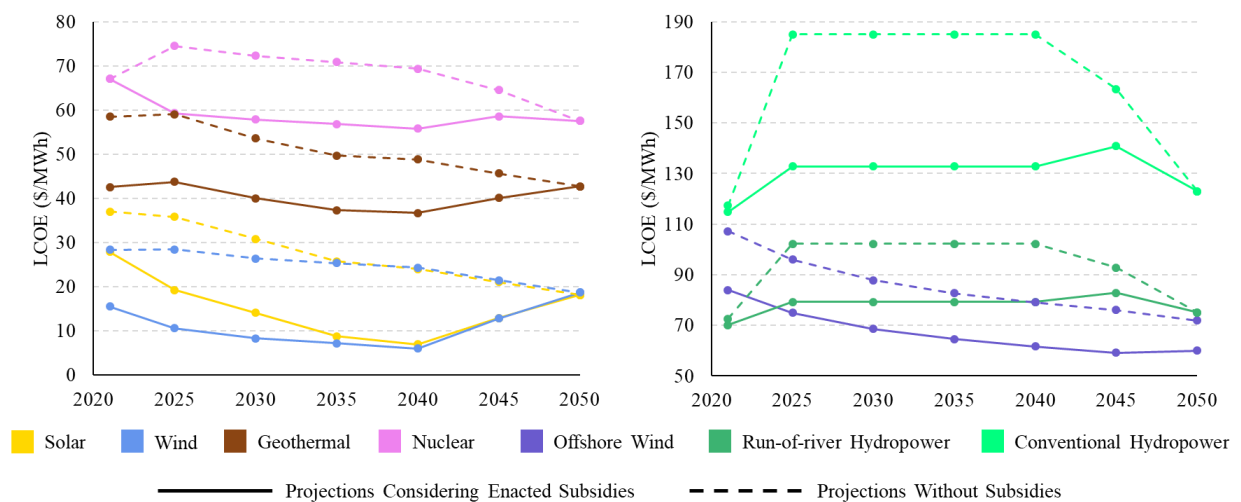


Figure 6-3. LCOE projections based on enacted subsidies vs. ignoring subsidies

6.3.3 Planned analysis and hypotheses

Decarbonization buildout strategies will be compared when subsidies are applied vs are not applied. Based on Figure 6-3, one can hypothesize that subsidies encourage the adoption of the less expensive technologies (solar and wind) over more expensive technologies (offshore wind and hydro). By assuming that the costs of subsidies are indirectly being passed onto the consumer via increased taxes, the total cost to the consumer can be recalculated. Ideally, increased decarbonization is encouraged with little overall system cost increase. The danger of flat subsidies across all technologies is that they impact technologies differently, and therefore may lead to overbuilding of certain technologies.

Out of this research, a series of alternative subsidy schemes can be proposed. Of special note is the investigation into region-specific designs. Also, the combination of carbon taxes in conjunction with subsidies will be investigated. What level and type of carbon taxes achieve the same decarbonization results as are projected with the IRA?

6.4 Connecting back to the big picture

This thesis motivates the quick and strategic reduction of all global emissions. This work is based on US emissions and targets because of its current and historically high contributions to total global emissions. The power sector is the focus of analysis as it is expected to be integrated into other sectors of the energy economy. Two tools were presented, and numerous valuable conclusions were identified. But, as described in the introduction, power sector decarbonization must be paired with significant transformation in the other sectors as well. The above V2G analysis provides a prime example of the transition of other sectors and how these evolutions will impact the power sector and vice versa. Similar V2G analysis shows that with only 14% fleet participation in V2G services in 2050, the need for stationary storage is completely

displaced [106]. The production of green electrolytic hydrogen is another example of tight coupling between the power sector and others. In fact, a novel study shows how economical hydrogen production can be achieved with a collection of renewables [116]. Johnson's work optimizing decarbonization of India's steel sector shows how similar techniques can be used in other industries to effectively strategize transitions [117]. All of these areas of analyses are instrumental in achieving an economical and robust clean energy economy. Also, economic tools may be linked to this work. To achieve our goals, accurate and comprehensive investigations of climate change must be conducted, as well as extensive exploration of all potential mitigation strategies. The power sector is vital to our national and global decarbonization strategies, but swift and significant efforts must be made to decarbonize all sectors and stages of the energy economy.

Chapter 7. References

- [1] P. Friedlingstein *et al.*, “Global Carbon Budget 2021,” *Earth Syst. Sci. Data*, vol. 14, no. 4, pp. 1917–2005, Apr. 2022, doi: 10.5194/essd-14-1917-2022.
- [2] IPCC, *Global Warming of 1.5°C*. Cambridge University Press, 2022.
- [3] I. Energy Agency, “Net Zero Roadmap: A Global Pathway to Keep the 1.5 °C Goal in Reach - 2023 Update,” 2023.
- [4] K. L. Ebi *et al.*, “Extreme Weather and Climate Change: Population Health and Health System Implications,” *Annu. Rev. Public Heal.*, vol. 42, pp. 293–315, 2021, doi: 10.1146/annurev-publhealth.
- [5] T. Hasegawa, G. Sakurai, S. Fujimori, K. Takahashi, Y. Hijioaka, and T. Masui, “Extreme climate events increase risk of global food insecurity and adaptation needs,” *Nat. Food*, vol. 2, 2021, doi: 10.1038/s43016-021-00335-4.
- [6] T. Carleton *et al.*, “Valuing the Global Mortality Consequences of Climate Change Accounting for Adaptation Costs and Benefits,” *Q. J. Econ.*, vol. 137, no. 4, pp. 2037–2105, Sep. 2022, doi: 10.1093/qje/qjac020.
- [7] D. J. Frame *et al.*, “Climate change attribution and the economic costs of extreme weather events: a study on damages from extreme rainfall and drought,” *Clim. Change*, vol. 162, pp. 781–797, 2020, doi: 10.1007/s10584-020-02729-y.
- [8] H. Ritchie and M. Roser, “CO2 and Greenhouse Gas Emissions,” *Our World in Data*, 2020. [Online]. Available: <https://ourworldindata.org/co2-and-greenhouse-gas-emissions>.
- [9] J. DeCarolis and A. LaRose, “Annual Energy Outlook 2023,” 2023.
- [10] J. W. Busby *et al.*, “Cascading risks: Understanding the 2021 winter blackout in Texas,” *Energy Research and Social Science*, vol. 77. Elsevier Ltd, 01-Jul-2021, doi: 10.1016/j.erss.2021.102106.
- [11] M. Weiss and M. Weiss, “An assessment of threats to the American power grid,” *Energy, Sustainability and Society*, vol. 9, no. 1. BioMed Central Ltd., p. 18, 29-May-2019, doi: 10.1186/s13705-019-0199-y.
- [12] J. D. Jenkins and N. A. Sepulveda, “Enhanced Decision Support for a Changing Electricity Landscape: The GenX Configurable Electricity Resource Capacity Expansion Model,” 2017.
- [13] J. Johnston, R. Henriquez-Auba, B. Maluenda, and M. Fripp, “Switch 2.0: A modern platform for planning high-renewable power systems,” *SoftwareX*, vol. 10, p. 100251, Jul. 2019, doi: 10.1016/j.softx.2019.100251.
- [14] M. Contaldi, F. Gracceva, and G. Tosato, “Evaluation of green-certificates policies using the MARKAL-MACRO-Italy model,” *Energy Policy*, vol. 35, no. 2, pp. 797–808, Feb. 2007, doi: 10.1016/j.enpol.2006.03.011.
- [15] R. Loulou, G. Goldstein, and K. Noble, “Energy Technology Systems Analysis

- Programme Documentation for the MARKAL Family of Models,” 2004.
- [16] W. Short *et al.*, “Regional Energy Deployment System (ReEDS),” 2011.
- [17] H.-C. Gils and T. Fitcher, “Energy system model REMix,” 2016.
- [18] “RESOLVE Capacity Expansion Model,” 2019.
- [19] S. Osorio, R. Pietzcker, A. Levesque, and J. Sitarz, “Documentation of LIMES-EU,” 2021.
- [20] C. Gaete-Morales, M. Kittel, A. Roth, and W. P. Schill, “DIETERpy: A Python framework for the Dispatch and Investment Evaluation Tool with Endogenous Renewables,” *SoftwareX*, vol. 15, Jul. 2021, doi: 10.1016/j.softx.2021.100784.
- [21] A. Farnsworth and E. Gençer, “Highlighting regional decarbonization challenges with novel capacity expansion model,” *Clean. Energy Syst.*, vol. 5, p. 100078, Aug. 2023, doi: 10.1016/j.cles.2023.100078.
- [22] E. Gençer, S. Torkamani, I. Miller, T. W. Wu, and F. O’Sullivan, “Sustainable energy system analysis modeling environment: Analyzing life cycle emissions of the energy transition,” *Appl. Energy*, vol. 277, Nov. 2020, doi: 10.1016/j.apenergy.2020.115550.
- [23] I. Miller, E. Gençer, H. S. Vogelbaum, P. R. Brown, S. Torkamani, and F. M. O’Sullivan, “Parametric modeling of life cycle greenhouse gas emissions from photovoltaic power,” *Appl. Energy*, vol. 238, pp. 760–774, 2019, doi: 10.1016/j.apenergy.2019.01.012.
- [24] “Frequently Asked Questions,” *US Energy Information Administration*, 2021. [Online]. Available: <https://www.eia.gov/tools/faqs/faq.php?id=74&t=11>. [Accessed: 06-Jun-2022].
- [25] D. S. Mallapragada, N. A. Sepulveda, and J. D. Jenkins, “Long-run system value of battery energy storage in future grids with increasing wind and solar generation,” *Appl. Energy*, vol. 275, Oct. 2020, doi: 10.1016/j.apenergy.2020.115390.
- [26] D. S. Mallapragada, N. A. Sepulveda, and J. D. Jenkins, “Long-run system value of battery energy storage in future grids with increasing wind and solar generation,” *Appl. Energy*, vol. 275, p. 115390, Oct. 2020, doi: 10.1016/j.apenergy.2020.115390.
- [27] R. O. Amber Mahone, Zachary Subin, M. C. Mackay Miller, Lauren Regan, and B. Marcelo Saenz, “On the Path to Decarbonization,” *IEEE Power Energy Mag.*, 2018.
- [28] J. E. T. Bistline and G. J. Blanford, “Value of technology in the U.S. electric power sector: Impacts of full portfolios and technological change on the costs of meeting decarbonization goals,” in *Energy Economics*, 2020, vol. 86, p. 104694, doi: 10.1016/j.eneco.2020.104694.
- [29] S. Carley, “Decarbonization of the U.S. electricity sector: Are state energy policy portfolios the solution?,” *Energy Econ.*, 2011.
- [30] F. Ueckerdt, R. Pietzcker, Y. Scholz, D. Stetter, A. Giannousakis, and G. Luderer, “Decarbonizing global power supply under region-specific consideration of challenges and options of integrating variable renewables in the REMIND model,” *Energy Econ.*, vol. 64, pp. 665–684, May 2017, doi: 10.1016/j.eneco.2016.05.012.

- [31] R. S. Rocío Uría-Martínez, Megan M. Johnson, “U.S. Hydropower Market Report,” 2021.
- [32] E. G. Dimanchev, J. L. Hodge, and J. E. Parsons, “The role of hydropower reservoirs in deep decarbonization policy,” *Energy Policy*, vol. 155, p. 112369, Aug. 2021, doi: 10.1016/j.enpol.2021.112369.
- [33] D. M. Bain and T. L. Acker, “Hydropower Impacts on Electrical System Production Costs in the Southwest United States,” doi: 10.3390/en11020368.
- [34] J. M. Williams, “The hydropower myth,” *Environ. Sci. Pollut. Res.*, vol. 27, no. 12, pp. 12882–12888, Apr. 2020, doi: 10.1007/s11356-019-04657-6.
- [35] E. F. Moran, M. C. Lopez, N. Moore, N. Müller, and D. W. Hyndman, “Sustainable hydropower in the 21st century,” *Proc. Natl. Acad. Sci. U. S. A.*, vol. 115, no. 47, pp. 11891–11898, Nov. 2018, doi: 10.1073/pnas.1809426115.
- [36] “Meeting the Dual Challenge,” 2019.
- [37] P. Gagnon, B. Cowiestoll, and M. Schwarz, “Cambium 2022 Scenario Descriptions and Documentation,” 2022.
- [38] J. Zayas, “Hydropower Vision Report,” *US Department of Energy*, 2016. [Online]. Available: <https://www.energy.gov/eere/water/downloads/hydropower-vision-report-full-report>. [Accessed: 28-Nov-2022].
- [39] B. Hadjerioua, Y. Wei, and S.-C. Kao, “An Assessment of Energy Potential at Non-Powered Dams in the United States,” 2012.
- [40] “Electric Power Annual 2012,” *EIA*, 2013. [Online]. Available: <https://www.eia.gov/electricity/annual/>. [Accessed: 28-Nov-2022].
- [41] S.-C. Kao *et al.*, “New Stream-reach Development: A Comprehensive Assessment of Hydropower Energy Potential in the United States,” Oak Ridge, TN (United States), Apr. 2014.
- [42] E. Rosenlieb, D. Heimiller, and S. Cohen, “Closed-Loop Pumped Storage Hydropower Resource Assessment for the United States,” 2022.
- [43] A. Farnsworth and E. Gençer, *Accurately Modeling Hydropower in the USA*. 33rd European Symposium on Computer Aided Process Engineering, 2023.
- [44] P. R. Brown and A. Botterud, “The Value of Inter-Regional Coordination and Transmission in Decarbonizing the US Electricity System,” *Joule*, vol. 5, no. 1, pp. 115–134, Jan. 2021, doi: 10.1016/j.joule.2020.11.013.
- [45] C. Draxl, A. Clifton, B. M. Hodge, and J. McCaa, “The Wind Integration National Dataset (WIND) Toolkit,” *Appl. Energy*, vol. 151, pp. 355–366, Aug. 2015, doi: 10.1016/j.apenergy.2015.03.121.
- [46] “NSRDB: National Solar Radiation Database,” *NREL*, 2022. [Online]. Available: <https://nsrdb.nrel.gov/>. [Accessed: 06-Jun-2022].
- [47] J. M. Atri Bera, Nga Nguyen, Saad Alzahrani, Khalil Sinjari, “Variability Reduction of

- Wind Power using Aggregation and Energy Storage,” *IEEE*, 2020.
- [48] B. E. Ellis, N. Pearre, and L. Swan, “Power ramp rates and variability of individual and aggregate photovoltaic systems using measured production data at the municipal scale,” *Sol. Energy*, vol. 220, pp. 363–370, May 2021, doi: 10.1016/j.solener.2021.03.042.
- [49] J.-P. Sasse and E. Trutnevvyte, “Distributional trade-offs between regionally equitable and cost-efficient allocation of renewable electricity generation,” 2019, doi: 10.1016/j.apenergy.2019.113724.
- [50] P. Maloney, “How market forces are pushing utilities to operate nuclear plants more flexibly,” *Utility Dive*, 2016. [Online]. Available: <https://www.utilitydive.com/news/how-market-forces-are-pushing-utilities-to-operate-nuclear-plants-more-flex/427496/>. [Accessed: 06-Jun-2022].
- [51] C. Budischak, D. Sewell, H. Thomson, L. MacH, D. E. Veron, and W. Kempton, “Cost-minimized combinations of wind power, solar power and electrochemical storage, powering the grid up to 99.9% of the time,” *J. Power Sources*, vol. 225, pp. 60–74, Mar. 2013, doi: 10.1016/j.jpowsour.2012.09.054.
- [52] L. Liu *et al.*, “Optimizing wind/solar combinations at finer scales to mitigate renewable energy variability in China,” *Renew. Sustain. Energy Rev.*, vol. 132, p. 110151, Oct. 2020, doi: 10.1016/j.rser.2020.110151.
- [53] M. A. Brown and Y. Li, “Carbon pricing and energy efficiency: pathways to deep decarbonization of the US electric sector,” *Energy Effic.*, 2018, doi: 10.1007/s12053-018-9686-9.
- [54] X. Liu *et al.*, “Low-carbon technology diffusion in the decarbonization of the power sector: Policy implications,” *Energy Policy*, vol. 116, pp. 344–356, May 2018, doi: 10.1016/j.enpol.2018.02.001.
- [55] H. Kamala and D. Harris, “The California Nuclear Waste Act,” 2015.
- [56] S. Carrara, “Reactor ageing and phase-out policies: global and regional prospects for nuclear power generation,” *Energy Policy*, vol. 147, Dec. 2020, doi: 10.1016/j.enpol.2020.111834.
- [57] J. Kelly and A. Elgowainy, “Updating Transmission and Distribution Losses in the GREET® Model,” no. September, 2018.
- [58] “2022 Annual Technology Baseline,” *NREL*, 2022. [Online]. Available: <https://atb.nrel.gov/>.
- [59] “SESAME,” *MITEI*, 2022. [Online]. Available: <https://sesame.mit.edu/app/profile>. [Accessed: 28-Jul-2022].
- [60] H. L. Raadal, L. Gagnon, I. S. Modahl, and O. J. Hanssen, “Life cycle greenhouse gas (GHG) emissions from the generation of wind and hydro power,” *Renewable and Sustainable Energy Reviews*, vol. 15, no. 7. Pergamon, pp. 3417–3422, 01-Sep-2011, doi: 10.1016/j.rser.2011.05.001.

- [61] Z. Guo, S. Ge, X. Yao, H. Li, and X. Li, “Life cycle sustainability assessment of pumped hydro energy storage,” *Int. J. Energy Res.*, vol. 44, no. 1, pp. 192–204, Jan. 2020, doi: 10.1002/er.4890.
- [62] K. Ralon, P., Taylor, M., Ilas, A., Diaz-Bone, H., & Kairies, *Electricity storage and renewables: Costs and markets to 2030*, no. October. 2017.
- [63] “2020 Annual Technology Baseline,” *NREL*, 2020. .
- [64] “Prices and Outlook,” *U.S. Energy Information Administration*, 2020. [Online]. Available: <https://www.eia.gov/todayinenergy/detail.php?id=34172>. [Accessed: 03-Jun-2022].
- [65] “FACT SHEET: President Biden Sets 2030 Greenhouse Gas Pollution Reduction Target Aimed at Creating Good-Paying Union Jobs and Securing U.S. Leadership on Clean Energy Technologies,” *The White House*, 2021. [Online]. Available: <https://www.whitehouse.gov/briefing-room/statements-releases/2021/04/22/fact-sheet-president-biden-sets-2030-greenhouse-gas-pollution-reduction-target-aimed-at-creating-good-paying-union-jobs-and-securing-u-s-leadership-on-clean-energy-technologies/>. [Accessed: 27-Jul-2023].
- [66] D. Byles and S. Mohagheghi, “Sustainable Power Grid Expansion: Life Cycle Assessment, Modeling Approaches, Challenges, and Opportunities,” 2023, doi: 10.3390/su15118788.
- [67] S. Rauner and M. Budzinski, “Holistic energy system modeling combining multi-objective optimization and life cycle assessment,” *Environ. Res. Lett.*, 2017, doi: 10.1088/1748-9326/aa914d.
- [68] D.-J. Van De Ven *et al.*, “The potential land requirements and related land use change emissions of solar energy,” *Sci. Rep.*, vol. 11, p. 2021, 2021, doi: 10.1038/s41598-021-82042-5.
- [69] M. Pehl, A. Arvesen, F. Humpenöder, A. Popp, E. G. Hertwich, and G. Luderer, “Understanding future emissions from low-carbon power systems by integration of life-cycle assessment and integrated energy modelling,” *Technology*, no. 3, 2017, doi: 10.1038/s41560-017-0032-9.
- [70] J. Fernández-González, M. Rumayor, A. Domínguez-Ramos, A. Irabien, and I. Ortiz, “The Relevance of Life Cycle Assessment Tools in the Development of Emerging Decarbonization Technologies,” *JACS Au*, Sep. 2023, doi: 10.1021/jacsau.3c00276.
- [71] National Renewable Energy Laboratory, “2023 Annual Technology Baseline (ATB) Cost and Performance Data for Electricity Generation Technologies,” 2023.
- [72] M. Schwartz, D. Heimiller, S. Haymes, and W. Musial, “Assessment of Offshore Wind Energy Resources for the United States,” 2010.
- [73] A. Lopez, B. Roberts, D. Heimiller, N. Blair, and G. Porro, “U.S. Renewable Energy Technical Potentials: A GIS-Based Analysis,” 2012.
- [74] A. Reuther *et al.*, “Interactive Supercomputing on 40,000 Cores for Machine Learning and Data Analytics,” *IEEE*, 2018. [Online]. Available:

- <https://ieeexplore.ieee.org/stamp/stamp.jsp?tp=&arnumber=8547629>. [Accessed: 26-Jul-2023].
- [75] “Greenhouse Gas Emissions from a Typical Passenger Vehicle | US EPA.” [Online]. Available: <https://www.epa.gov/greenvehicles/greenhouse-gas-emissions-typical-passenger-vehicle>. [Accessed: 02-Nov-2023].
- [76] “Going carbon negative: What are the technology options? – Analysis - IEA.” [Online]. Available: <https://www.iea.org/commentaries/going-carbon-negative-what-are-the-technology-options>. [Accessed: 02-Nov-2023].
- [77] L. Desport *et al.*, “Deploying direct air capture at scale: How close to reality?,” *Energy Econ.*, vol. 129, p. 107244, Jan. 2024, doi: 10.1016/j.eneco.2023.107244.
- [78] L. Rosa, D. L. Sanchez, and M. Mazzotti, “Assessment of carbon dioxide removal potential via BECCS in a carbon-neutral Europe †,” *This J. is Cite this Energy Environ. Sci.*, vol. 14, p. 3086, 2021, doi: 10.1039/d1ee00642h.
- [79] E. Baik *et al.*, “What is different about different net-zero carbon electricity systems?,” *Energy Clim. Chang.*, vol. 2, Dec. 2021, doi: 10.1016/j.egycc.2021.100046.
- [80] M. A. Madsen, M. Gaspar, and R. Kenn, “Fusion Energy,” 2021.
- [81] A. Holland, “The global fusion industry in 2022,” 2021.
- [82] J. Schwartz, W. Ricks, E. Kolemen, and J. Jenkins, “The value of fusion energy to a decarbonized United States electric grid,” 2022.
- [83] K. Gi, F. Sano, K. Akimoto, R. Hiwatari, and K. Tobita, “Potential contribution of fusion power generation to low-carbon development under the Paris Agreement and associated uncertainties,” *Energy Strateg. Rev.*, vol. 27, Jan. 2020, doi: 10.1016/j.esr.2019.100432.
- [84] T. E. G. Nicholas *et al.*, “Re-examining the role of nuclear fusion in a renewables-based energy mix,” *Energy Policy*, vol. 149, no. June 2020, p. 112043, 2021, doi: 10.1016/j.enpol.2020.112043.
- [85] K. Tokimatsu *et al.*, “Studies of Nuclear Fusion Energy Potential Based on a Long-term World Energy and Environment Model,” 2003.
- [86] N. A. Sepulveda, J. D. Jenkins, F. J. de Sisternes, and R. K. Lester, “The Role of Firm Low-Carbon Electricity Resources in Deep Decarbonization of Power Generation,” *Joule*, vol. 2, no. 11, pp. 2403–2420, Nov. 2018, doi: 10.1016/j.joule.2018.08.006.
- [87] C. Bustreo, U. Giuliani, D. Maggio, and G. Zollino, “How fusion power can contribute to a fully decarbonized European power mix after 2050,” *Fusion Eng. Des.*, vol. 146, no. April, pp. 2189–2193, 2019, doi: 10.1016/j.fusengdes.2019.03.150.
- [88] D. Turnbull, A. Glaser, and R. J. Goldston, “Investigating the value of fusion energy using the Global Change Assessment Model,” *Energy Econ.*, vol. 51, pp. 346–353, Sep. 2015, doi: 10.1016/j.eneco.2015.08.001.
- [89] M. C. Handley, D. Slesinski, • Scott, and C. Hsu, “Potential Early Markets for Fusion Energy,” *J. Fusion Energy*, vol. 40, 2021, doi: 10.1007/s10894-021-00306-4.

- [90] L. Guazzotto and J. Freidberg, “A steady state vs pulsed fusion neutron science facility,” *Nucl. Fusion*, vol. 62, no. 12, Dec. 2022, doi: 10.1088/1741-4326/ac9e09.
- [91] “THE EMISSIONS & GENERATION RESOURCE INTEGRATED DATABASE eGRID Technical Guide with Year 2021 Data Clean Air Markets Division.”
- [92] J. M. Kemp, J. Seel, W. Gorman, J. Rand, and R. Wisler, “Interconnection Cost Analysis in ISO-New England Interconnection costs have risen, especially among projects that withdraw from the queue,” 2023.
- [93] J. Seel *et al.*, “Generator Interconnection Cost Analysis in the Southwest Power Pool (SPP) Territory Network upgrade costs have risen, especially among projects that withdraw from the queue,” 2023.
- [94] J. M. Kemp *et al.*, “Interconnection Cost Analysis in the NYISO Territory,” 2023.
- [95] J. Seel *et al.*, “Interconnection Cost Analysis in the PJM Territory Interconnection costs have escalated as interconnection requests have grown,” 2023.
- [96] J. Seel, J. Rand, W. Gorman, D. Millstein, and R. Wisler, “Interconnection Cost Analysis in the Midcontinent Independent System Operator (MISO) Territory,” 2022.
- [97] U. Energy Information Administration, “Capital Cost and Performance Characteristic Estimates for Utility Scale Electric Power Generating Technologies,” 2020.
- [98] T. Gasser and G. Luderer, “Mitigation Pathways Compatible with 1.5°C in the Context of Sustainable Development,” in *Global Warming of 1.5°C*, Cambridge University Press, 2022, pp. 93–174.
- [99] E. S. Rubin, M. L. Azevedo, P. Jaramillo, and S. Yeh, “A review of learning rates for electricity supply technologies,” 2015, doi: 10.1016/j.enpol.2015.06.011.
- [100] “Frequently Asked Questions (FAQs) - U.S. Energy Information Administration (EIA).” [Online]. Available: <https://www.eia.gov/tools/faqs/faq.php?id=105&t=3>. [Accessed: 22-Dec-2023].
- [101] “State Carbon Dioxide Emissions Data - U.S. Energy Information Administration (EIA).” [Online]. Available: <https://www.eia.gov/environment/emissions/state/>. [Accessed: 26-Dec-2023].
- [102] “2020 Annual Technology Baseline,” *NREL*. [Online]. Available: <https://atb-archive.nrel.gov/electricity/2020/data.php>.
- [103] “2021-ATB.” .
- [104] U. Epa and C. Change Division, “Inventory of U.S. Greenhouse Gas Emissions and Sinks: 1990-2021 – Main Report,” 1990.
- [105] “U.S. energy facts explained - consumption and production - U.S. Energy Information Administration (EIA).” [Online]. Available: <https://www.eia.gov/energyexplained/us-energy-facts/>. [Accessed: 27-Dec-2023].
- [106] J. Owens, I. Miller, and E. Gençer, “Can vehicle-to-grid facilitate the transition to low

- carbon energy systems?,” *Energy Adv.*, no. 12, pp. 984–998, Dec. 2022, doi: 10.1039/d2ya00204c.
- [107] “Real-time Operating Grid,” *US Energy Information Administration*, 2022. [Online]. Available: https://www.eia.gov/electricity/gridmonitor/dashboard/electric_overview/US48/US48. [Accessed: 06-Jun-2022].
- [108] S. Davis and R. Boundy, *Transportation Energy Data Book*. Oak Ridge National Laboratory, 2022.
- [109] “NTEA – The Work Truck Association™.” [Online]. Available: <https://www.ntea.com/>. [Accessed: 27-Dec-2023].
- [110] “VISION Model | Argonne National Laboratory.” [Online]. Available: <https://www.anl.gov/esia/vision-model>. [Accessed: 27-Dec-2023].
- [111] “Fleet DNA: Commercial Fleet Vehicle Operating Data | Transportation and Mobility Research | NREL.” [Online]. Available: <https://www.nrel.gov/transportation/fleetest-fleet-dna.html>. [Accessed: 27-Dec-2023].
- [112] “By The Numbers: The Inflation Reduction Act.” The White House, Washington DC, 2022.
- [113] J. Bistline *et al.*, “Emissions and energy impacts of the Inflation Reduction Act,” *Science* (80-.), vol. 380, no. 6652, pp. 1324–1327, Jun. 2023, doi: 10.1126/science.adg3781.
- [114] “The Paris Agreement,” *UNFCCC*, 2022. [Online]. Available: <https://unfccc.int/process-and-meetings/the-paris-agreement/the-paris-agreement>. [Accessed: 18-Nov-2020].
- [115] “Federal Solar Tax Credits for Businesses | Department of Energy.” [Online]. Available: <https://www.energy.gov/eere/solar/federal-solar-tax-credits-businesses>. [Accessed: 27-Dec-2023].
- [116] P. Sizaire, “Evaluating the Infrastructure Requirements of a Low- Carbon Hydrogen Supply Chain in Germany and the Gulf Coast,” 2023.
- [117] S. Johnson, L. Deng, and E. Gençer, “Environmental and economic evaluation of decarbonization strategies for the Indian steel industry,” *Energy Convers. Manag.*, vol. 293, p. 117511, Oct. 2023, doi: 10.1016/j.enconman.2023.117511.